AD-A073 853 VISIDYNE INC BURLINGTON MASS F/G 20/6
ROCKETBORNE LASER BACKSCATTER EXPERIMENT.(U)
MAR 79 O SHEPHERD, A G HURD, W H SHEEHAN F19628-76-C-0253
UNCLASSIFIED VI-475 AFGL-TR-79-0081 NL

1 OF 2
AD A073853

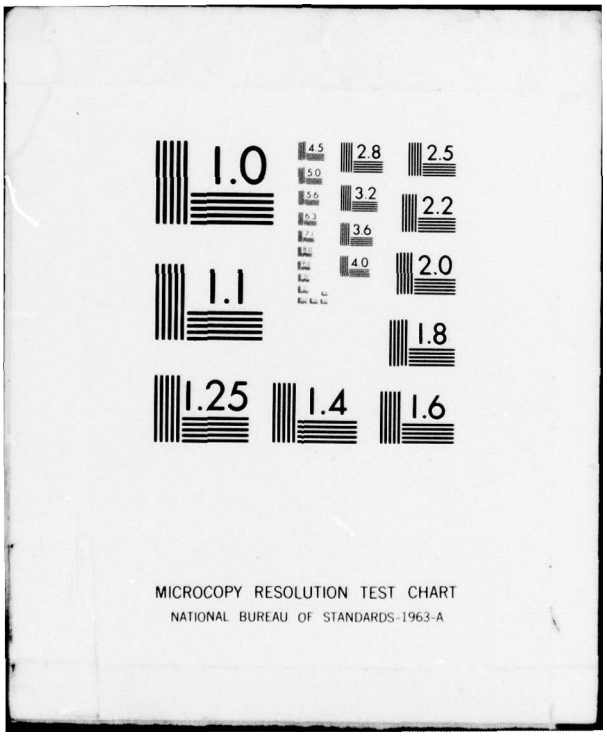
1.0
1.1
1.25
1.4
1.6
1.8
2.0
2.2
2.5
2.8
3.2
3.6
4.0
4.5
5.0
5.6
6.3
7.1
MICROCOPY RESOLUTION TEST CHART
NATIONAL BUREAU OF STANDARDS-1963-A

AFGL-TR-79-0081

LEVEL

VI-475

ROCKETBORNE LASER BACKSCATTER EXPERIMENT

O. Shepherd
A. G. Hurd
W. H. Sheehan
R. D. Bucknam

Visidyne, Inc.
19 Third Avenue
Northwest Industrial Park
Burlington, Massachusetts 01803

15 March 1979

Final Report: 6 May 1976 – 15 February 1979

AIR FORCE GEOPHYSICS LABORATORY
AIR FORCE SYSTEMS COMMAND
UNITED STATES AIR FORCE
HANSCOM AFB, MASSACHUSETTS 01731

UNCLASSIFIED

SECURITY CLASSIFICATION OF THIS PAGE (When Data Entered)

(19) REPORT DOCUMENTATION PAGE	READ INSTRUCTIONS BEFORE COMPLETING FORM
1. REPORT NUMBER (18) AFGL-TR-79-0081	2. GOVT ACCESSION NO. / 3. RECIPIENT'S CATALOG NUMBER
4. TITLE (and Subtitle) (6) ROCKETBORNE LASER BACKSCATTER EXPERIMENT	5. TYPE OF REPORT & PERIOD COVERED (9) Final Report, 6 May 1976-15 February 1979
	6. PERFORMING ORG. REPORT NUMBER (14) VI-475
7. AUTHOR(s) O. Shepherd, A. G. Hurd, R. D. Bucknam	8. CONTRACT OR GRANT NUMBER(s) (15) F19628-76-C-0253
9. PERFORMING ORGANIZATION NAME AND ADDRESS Visidyne, Inc. 19 Third Avenue, Northwest Industrial Park Burlington, Massachusetts 01803 (16)	10. PROGRAM ELEMENT, PROJECT, TASK AREA & WORK UNIT NUMBERS 62101F 66901A0 (17) 20 01
11. CONTROLLING OFFICE NAME AND ADDRESS Air Force Geophysics Laboratory (LKB) (11) Hanscom AFB, Massachusetts 01731 Contract Monitor: Joseph P. McIsaac	12. REPORT DATE 15 March 1979
	13. NUMBER OF PAGES 180
14. MONITORING AGENCY NAME & ADDRESS (if different from Controlling Office) (12) 180p.	15. SECURITY CLASS. (of this report) Unclassified
	15a. DECLASSIFICATION/DOWNGRADING SCHEDULE

16. DISTRIBUTION STATEMENT (of this Report)

Approved for public release; distribution unlimited

17. DISTRIBUTION STATEMENT (of the abstract entered in Block 20, if different from Report)

(10) O. /Shepherd, A. G. /Hurd, W. H. /Sheehan R. D. /Bucknam

18. SUPPLEMENTARY NOTES

19. KEY WORDS (Continue on reverse side if necessary and identify by block number)

Atmospheric Density
Thermosphere
Rayleigh Scattering
Dye Laser
Rocketborne Payload

20. ABSTRACT (Continue on reverse side if necessary and identify by block number)

A previously flown rocket payload designed to measure atmospheric density in the thermosphere through Rayleigh, backscatter of a dye laser signal, was modified and refurbished ~~by Visidyne, Inc.~~ In its earlier field test ~~by another contractor,~~ the payload failed to provide any data, apparently because of a timing problem. Relaunched 24 July 1978 from White Sands Missile Range, the laser failed to operate because of a minor component failure. However, measured

DD FORM 1 JAN 73 1473 EDITION OF 1 NOV 65 IS OBSOLETE

UNCLASSIFIED

SECURITY CLASSIFICATION OF THIS PAGE (When Data Entered)

390862

background intensities were orders of magnitude higher than anticipated. The source of the background signals has not been positively identified since the rocket aspect data have not been finalized. The most likely source appears to be scattering from the earth's atmosphere illuminated by the below horizon sun.

PREFACE

The authors wish to acknowledge the extensive corporative support provided to this program by Visidyne, Inc., in particular J. W. Carpenter, H. S. Richardson, Jr., and W. P. Reidy. For their earlier work in this experiment, the authors are indebted to L. Weeks and C. Doiron, previously with AFGL.

Others who contributed to the completion of this effort were: G. Aurilio, M. Conley, S. A. Rappaport, J. W. Reed, and T. F. Zehnpfennig of Visidyne, Inc.; L. Smart of Wentworth Institute of Technology; and D. Bedo, W. Donnell, J. Geary, and J. McIsaac of AFGL.

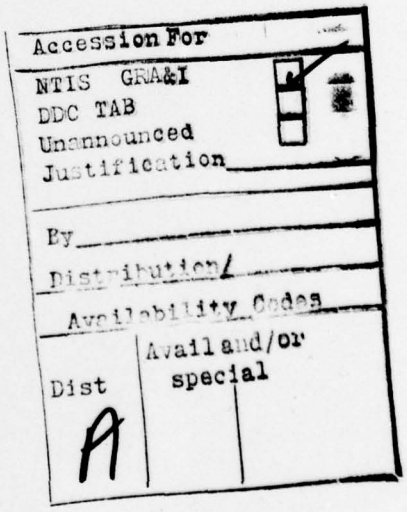

TABLE OF CONTENTS

LIST OF FIGURES

1.0 INTRODUCTION

The rocket-borne Laser Background Experiment was originally designed, fabricated, and flight tested by another contractor[1,2]. Its purpose was to measure atmospheric density as a function of altitude by monitoring the atmospheric Rayleigh scattering of a dye laser operating at 4580Å. No data on atmospheric density were obtained from the initial launch of the instrumentation. The objective of this contract was to refurbish and/or redesign the instrumentation to perform the intended measurements.

The engineering task required for this program was significantly greater than originally anticipated. As proposed, an existing operational Laser Backscatter Experiment payload was to be refurbished and selected subsystems redesigned so as to improve operation and/or increase system reliability. After the GFE payload and support equipment had been received and inspected, it became apparent that much more extensive modifications were required. The following existing subsystems were totally redesigned:

a. The laser dye and coolant circulation system including reservoirs, pumps, tubing and fittings, filters, and control electronics flow monitors.
b. The laser high voltage (25 kv) power supply and its control electronics.
c. The laser firing spark gap high voltage (40 kv) trigger circuitry.
d. The laser firing timing circuitry.
e. The entire laser section mechanical mounting structure and all electronic packaging.
f. The laser 28 vdc battery, the supporting electronics' 28 vdc battery, and their respective power distribution systems.
g. The laser section telemetry interface.
h. The laser section electrical cabling.
i. The laser boresight pointing optics.

j. The backscatter sensor electronics.
k. The laser output power monitor electronics.
l. The system timing electronics.
m. The sensor electronic packaging.
n. The sensor cabling.
o. The payload ground support equipment and all test cabling.

The GFE components considered qualified to be reflown with minor refurbishment required were:

a. The main optics casting.
b. The collecting optics, primary and secondary, and optical structure.
c. The laser high voltage capacitor and spark gap.
d. The laser high voltage step-up transformer.
e. The laser flash lamp assembly.
f. The sensor photomultiplier.

However, items c through f failed to perform during testing and were repaired or replaced.

At 2205 hours, 24 July 1978, the Laser Backscatter Experiment Payload was again launched from White Sands Missile Range using an Aerobee 150 vehicle. All vehicle and payload support systems performed to specifications. The payload attained an apogee of 150 km approximately 205 seconds after launch and the payload was recovered successfully the following day. No laser backscatter data were obtained during the flight because of a component failure within the laser high voltage power supply which prevented laser firing. Sky background signals were detected by the backscatter sensor. A subsequent analysis of the component failure is given in Appendix L.

2.0 SCIENTIFIC OBJECTIVES AND ANTICIPATED SIGNAL LEVELS

The purpose of this experiment was to determine the total atmospheric density in the thermosphere in the 60 to 140 km altitude range. The measurement technique utilized backscattering of a pulsed laser signal at 4580Å generated and collected by a rocket-borne payload. Visidyne's effort was to modify, refurbish, and provide field support for a rocket payload previously unsuccessfully flown to make the above measurements. The previous field test by another contractor[1,2] failed to obtain any data, apparently because of timing problems.

The technical approach followed by Visidyne in this contract emphasized checkout and calibration of the complete system as well as individual components. The calibration and test simulated as closely as possible the flight operation. It included a precise measurement of the detector system response along the laser path and an accurate calibration of the detector response. Of particular importance to the experiment was the detector/laser timing accuracy.

In general, in the wavelength spectral range of the laser source, the nighttime continuum is of the order of 2×10^6 photons sec^{-1}-cm^{-2}-$Å^{-1}$ (Figure 2.1)[3]. The night sky background photon flux collected by the detector optics and incident on the photomultiplier is:

$$N_{night\ sky} = 2 \times 10^6 \frac{A\Omega\Delta\lambda}{4\pi} \text{ (photons sec}^{-1}\text{)}$$

where A is the effective collecting area of the detector (700 cm^2)

Ω is the solid angle viewed by the detector system (4×10^{-3} sr)

$\Delta\lambda$ is the bandwidth of the detector (100 Å)

Hence,

$$N_{night\ sky} = 4 \times 10^7 \text{ (photons sec}^{-1}\text{)}$$

By comparison, the anticipated rayleigh scattered laser signal flux is given by

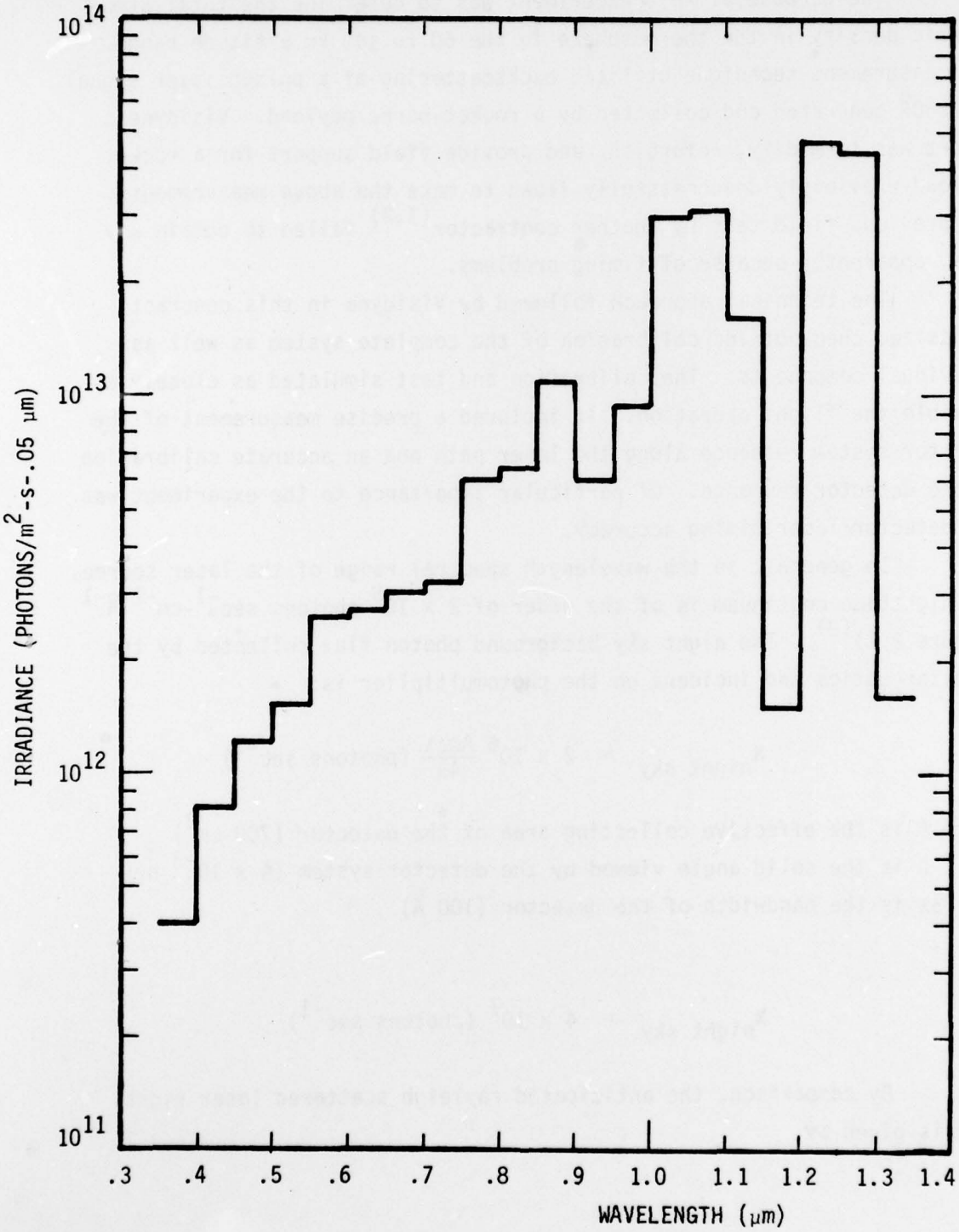

FIGURE 2.1 NATURAL NIGHT SKY SPECTRAL IRRADIANCE ON HORIZONTAL EARTH'S SURFACE

$$N_{rayleigh} = \frac{P_{laser}\ \sigma_{rayleigh}\ \rho A}{\Delta t \quad 2\pi} \left\{\frac{1}{R_1} - \frac{1}{R_2}\right\} \text{ (photons sec}^{-1}\text{)}$$

where P_{laser} is the number of laser produced photons per pulse (2.2×10^{18} for 1 joule pulse and photon energy 2.7 eV)

$\sigma_{rayleigh}$ is the rayleigh scattering cross section (9.6×10^{-27} cm^2 @ 4580Å)

ρ is the particle density (6.4×10^{15} cm^{-3} at 60 km and 9.3×10^{10} cm^{-3} at 140 km, U.S. Standard Atmosphere, 1976, NOAA-S/T76-1562)

A is the detector effective collecting area (700 cm^2)

Δt is the integration time (6.8×10^{-6} sec)

R_1, R_2 are the near and far distances to the portion of the laser beam that contributes to the return signal and are assumed to be to the half power points of the laser response curve in Section 4 (R_1 = 140 cm, R_2 = 340 cm).

Thus,

$$N_{rayleigh} = 1.5 \times 10^{-3}\ \rho$$

We can compare the night sky background and anticipated rayleigh scattering signals by taking the ratio

$$\text{Ratio} = \frac{N_{rayleigh\ scattering}}{N_{night\ sky}} = \frac{1.5 \times 10^{-3}}{4 \times 10^{7}}\ \rho$$

so that the ratio as a function of altitude is as follows:

ALTITUDE (km)	RATIO
60	2.4×10^5
80	1.4×10^4
100	4.5×10^2
120	1.9×10^1
140	3.5×10^0

Therefore, the night sky background signal contribution is negligible except when the rocket payload was near apogee.

It should be noted that the experimental data requirements were revised during the program. The original altitude region of interest, 90 km to 160 km, was revised to be 60 km to 140 km.

3.0 PAYLOAD DESIGN, FABRICATION, AND PREINTEGRATION TESTS

3.1 Vehicle

The GFE payload was designed to mate with an Aerobee 150 rocket[1]. Figure 3.1 shows the payload configuration. Location of the principal components within the payload was relatively unchanged by the Visidyne modifications with the exception that the dye and coolant reservoirs were mounted in the forward part of the ogive and the ogive skin divides into two parts. An extension of the ogive length was required to accommodate the reservoirs. The redesigned payload is shown in Figure 3.2.

The payload electrical interface is given in Appendix A and the experiment telemetry assignments are in Appendix B.

3.2 Transmitter

The transmitter was located in the section of the payload forward of the optics casting. A block diagram of the transmitter is shown in Figure 3.3. The transmitter optics were in the optics casting.

3.2.1 Laser

The flashlamp-pumped dye laser was part of the GFE (Government Furnished Equipment). It was designed and manufactured by Candela Corporation, Needham Heights, MA. and is of coaxial flashlamp design described by Furumoto and Ceccon[4].

The dye used was Coumarin 2 (4,6-Dimethyl-7-ethylamino-Coumarin). All dye concentrate was from the same lot number manufactured by Eastman Kodak Co., Rochester, N.Y. It was mixed with methanol (Certified A.C.S.) and distilled water to make a 1.5×10^{-4} M solution. Complete mixing instructions are given in Appendix C. The tuning range for Coumarin 2 lasing is from 4300-4800Å. Spectral measurements made at AFGL with a variety of dye mixes showing that all Kodak mixes had peak lasing wavelengths of 4569 ± 20Å[5] were confirmed at Visidyne by using a narrow band transmission filter.

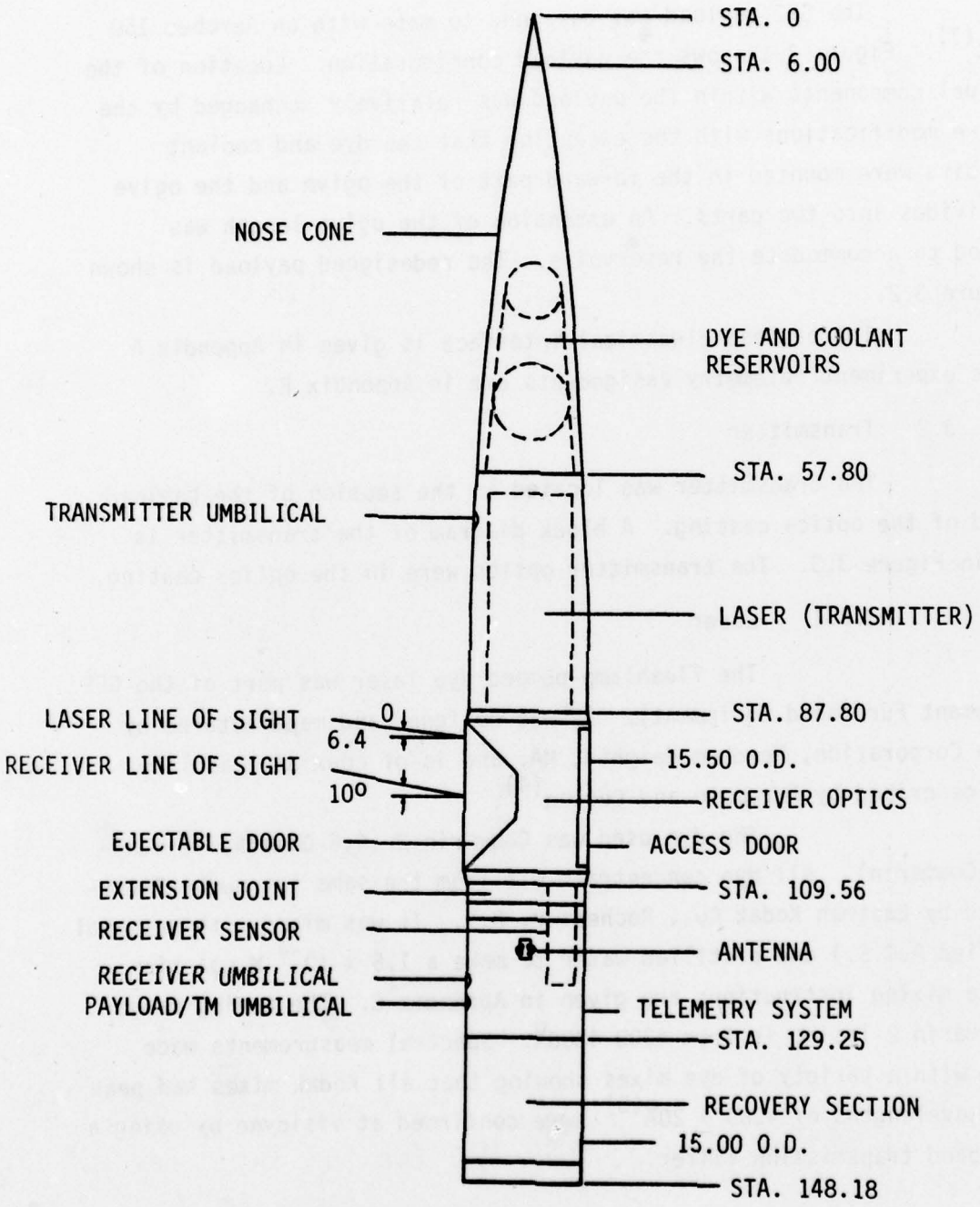

FIGURE 3.1 PAYLOAD CONFIGURATION (DIMENSIONS IN INCHES - TOTAL WEIGHT: 376.75 LBS.)

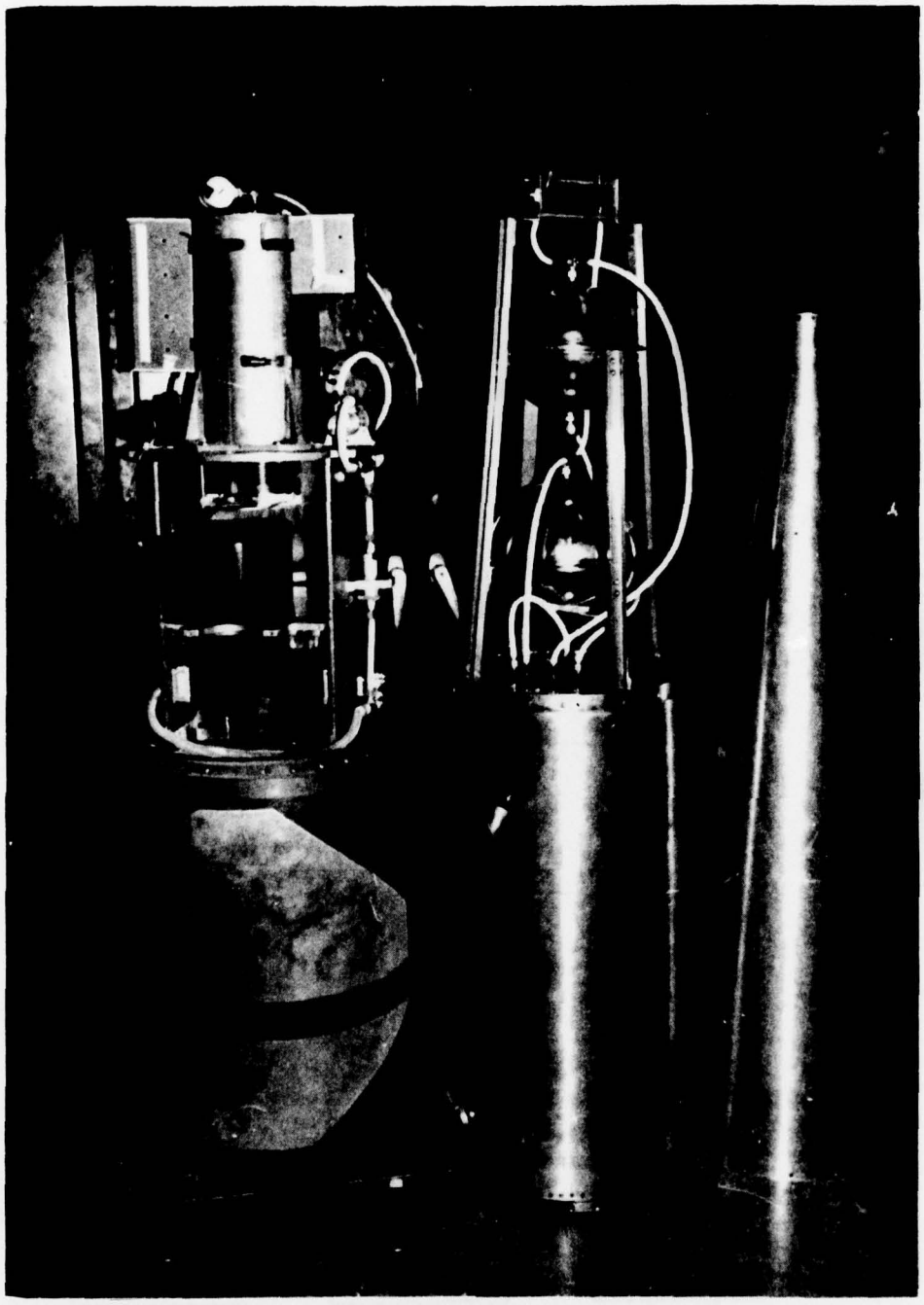

FIGURE 3.2 PAYLOAD, FORWARD SECTION, DISASSEMBLED

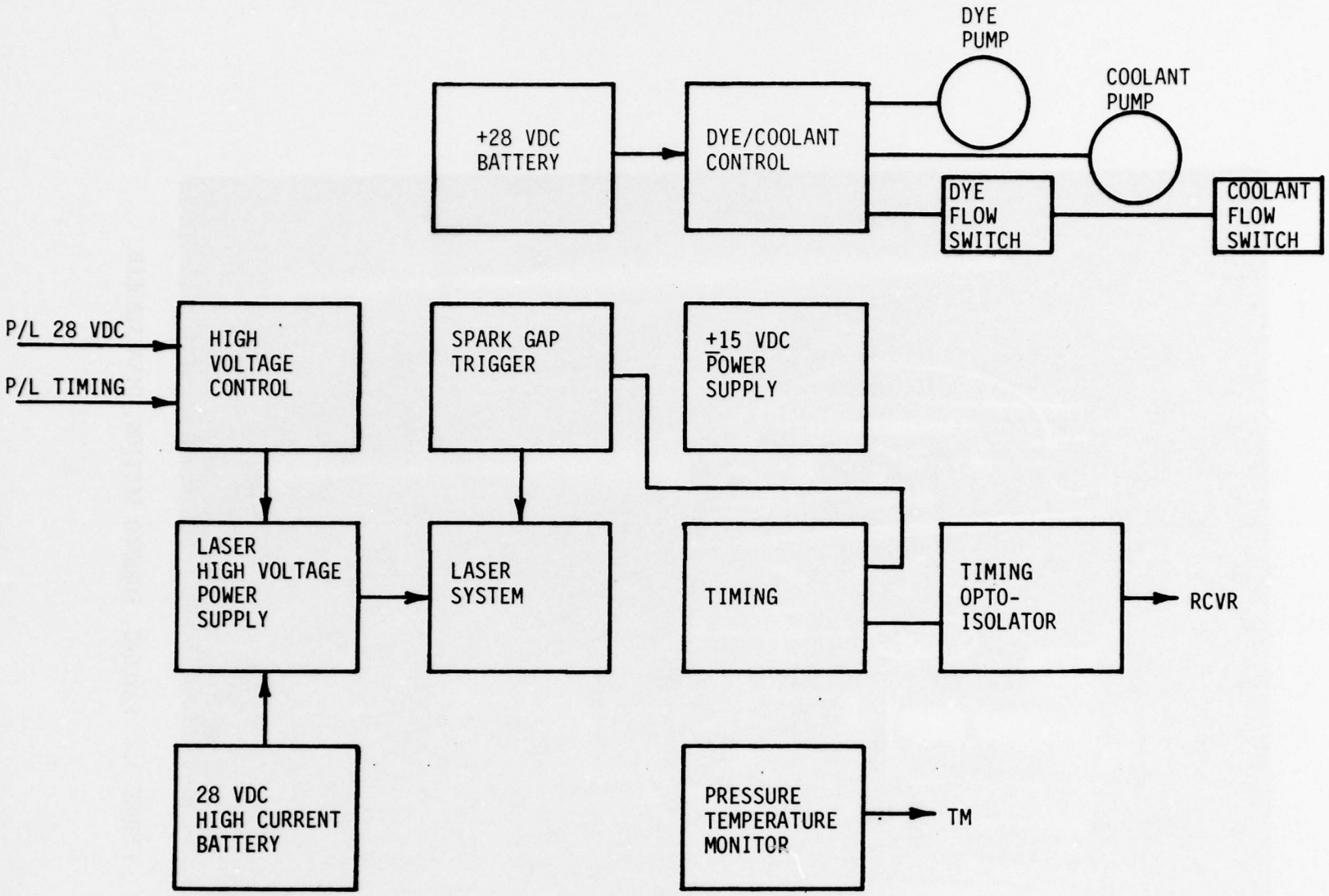

FIGURE 3.3 TRANSMITTER BLOCK DIAGRAM

The rear laser mirror has a 99.9% reflecting coating while the front, or output, laser mirror has a coating which has a transmission of about 85% at 4500Å as shown in Appendix D.

Appendices E and F consist of detailed instructions for the initial and final laser alignment procedures and safety procedures.

A spare dye laser was also part of the GFE. Both lasers were beset with problems. Although the flashlamps were guaranteed for 5000 flashes and rated for 30,000, failure occurred in each after totals of only hundreds of flashes. The seals between the body of the laser and the dye and coolant fittings were prone to leak, even after checking by the manufacturer. The O-ring groove for the front end mirror on one was too deep, causing the mirror to crack during alignment and/or dye leakage. These problems were the cause of extended delays. Nevertheless, the cooperation of Dick Herron of Candela in rectifying many of them was most appreciated.

3.2.2 Optics

The transmitter optics are shown as part of Figure 3.4. Although relatively simple, they were considerably modified from those of the GFE. The latter consisted of an anti-reflection coated window to maintain the pressure in the laser compartment of the payload and a plane dielectric mirror on a two dimensional adjustment mount to permit folding of the laser beam out at the desired elevation angle. These two optical components were replaced with a single constant deviation pentaprism, which acted as both a pressure seal and a folding mirror. Characteristics of the pentaprism are as follows:

Material: Suprasil 1 Fused Silica
Deviation Angle: $96.4^{o} \pm 10$ arc seconds
Polish: Laser Quality 10/5
Flatness: 1/4 wave or better at 4600Å

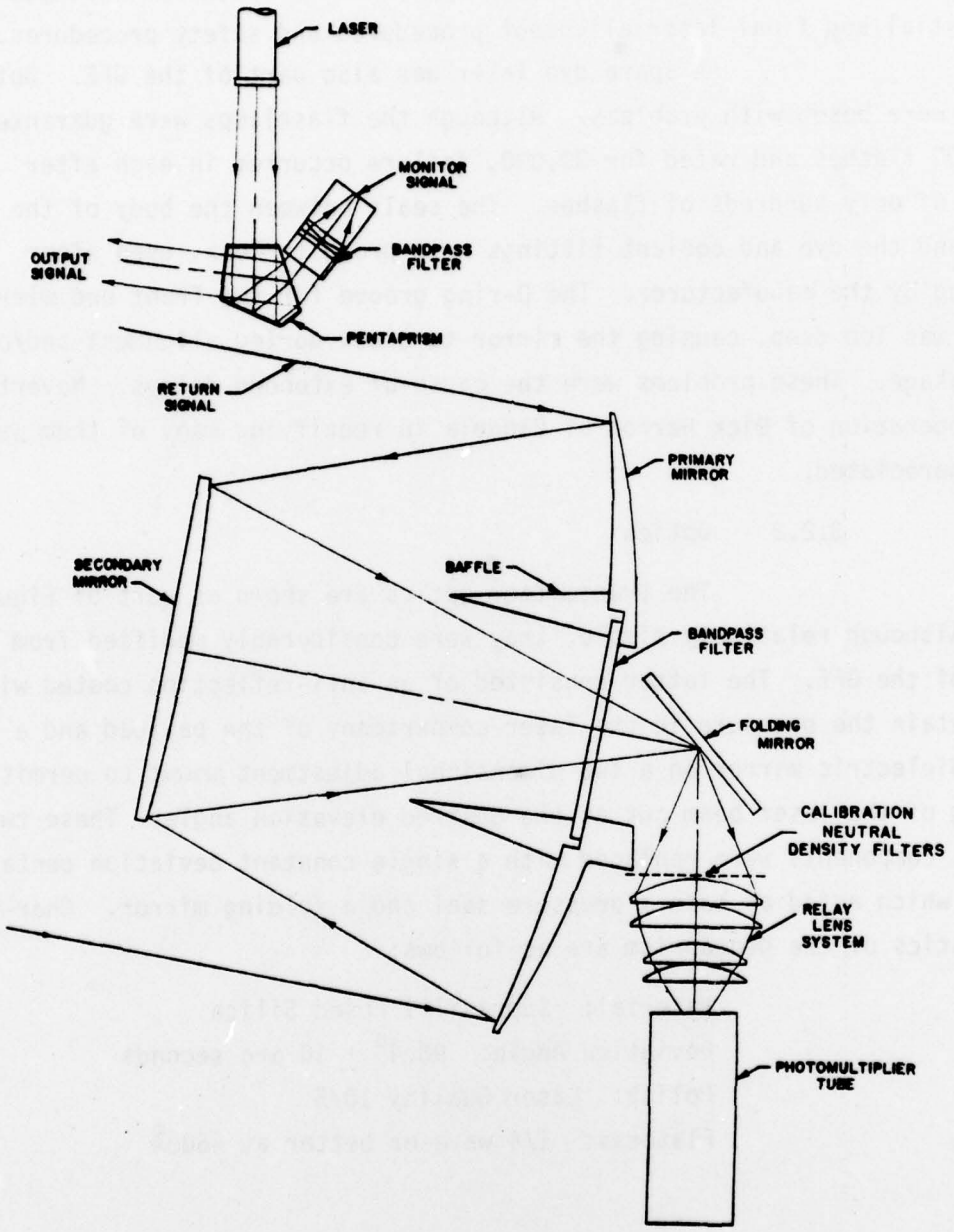

FIGURE 3.4 PAYLOAD OPTICS DESIGN

The entrance and exit surfaces have a "V" coating for less than 0.1% reflectance at 4600Å. A representative curve is given in Appendix D. The first internal reflection surface has a high reflectance multilayer dielectric coating for 4600Å with a black lacquer overcoat. The second internal reflection surface has a similar coating but one that transmits about 2% at 4600Å as shown in Appendix D. This small fraction of the laser output signal is transmitted through a narrow bandpass filter (Appendix D) and focused by a lens onto a fiber optics bundle which is bifurcated on the other end to provide signals for a laser power monitor and a timing pulse.

Suprasil 1 was chosen as the material for the penta-prism for the following reasons:

1. It has a very low absorption at 4600Å.
2. It has high radiation resistance.
3. It is fluorescence free.
4. It has a very high optical homogeneity.

Apertures in the transmitter section were re-dimensioned. It appeared that as previously designed, they were all equal to the nominal diameter at the face of the laser. However, since the beam is slightly divergent and because some decentering of the apertures with respect to the beam axis is inevitable, a portion of the beam was being obstructed.

3.2.3 Dye and Coolant Systems

A schematic of the laser dye and coolant circulation system is shown in Figure 3.5. The plumbing system, as received as part of the GFE, was not suitable for reflight. Consequently, Visidyne made extensive modifications to the system, including replacing the two square reservoir tanks with two spherical stainless steel ones, the dye tank having a capacity of 6.0 liters and the coolant tank a capacity of 2.5 liters. The spherical shape minimized the possibility of trapped air. These tanks can be clearly seen in Figure 3.2. Repositioning of the tanks into the nose cone also improved the filling operation.

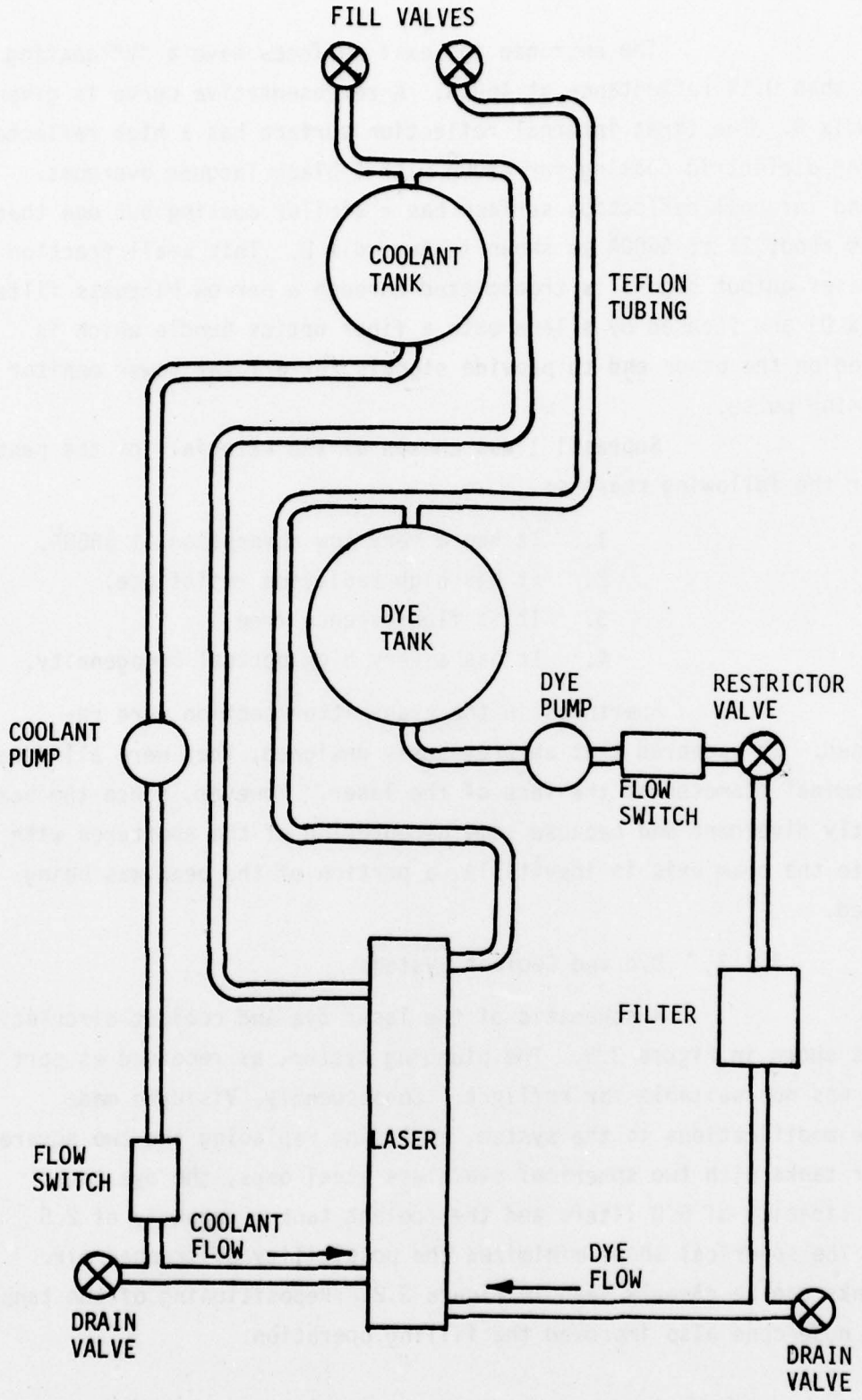

FIGURE 3.5 DYE AND COOLANT CIRCULATION SYSTEM

The dye system contains a 1/2 micron filter at the dye input side of the laser, and a micrometer restrictor valve is mounted at the dye input side of the laser. Flow monitors are included in both the coolant and dye lines. Each line also has a Micropump Model 12A-31-303 which is a stainless steel, magnetically coupled, leak-proof gear pump running at 7000 rpm at 28 vdc. Contamination-free operation is assured since there is no shaft seal to wear, leak, or generate heat. These gear-rotor pumps replaced the centrifugal-type pumps, thus eliminating the need for priming. In addition, materials in the dye pumping system that come in contact with the dye are limited to stainless steel and teflon.

Two locations of trapped bubbles in the dye system of the GFE laser could not be eliminated. They were the top end of the laser, from which bubbles could be released only by tipping the laser horizontally, and the bellows of the teflon tubing, from which bubbles could be released by tapping with the pump operating. Both of these methods became standard operating procedures.

3.2.4 High Voltage Power Supply

The GFE laser high voltage power supply is described in Reference 1. Upon receipt of the power supply, the unit was inspected and the following conclusions were reached:

1. The power supply was susceptible to failure if the driver-multivibrator circuit output waveform was not symmetrical under all operating conditions. Since the driver circuit waveform did not have any dead-band, simultaneous conduction of both sets of output transistors was virtually assured. The result of such simultaneous conduction would have been a greatly increased transistor collector current which would in turn have caused greatly increased power

dissipation or transistor destruction.

2. The inverter circuit output transistors were operated in a parallel configuration. This is inherently unreliable because these transistors must be matched for both switching times and emitter resistance.

3. The thermal heat sink of the inverter transistors consisted of a solid copper block. This had the disadvantage of limiting the duration of power supply operation by the thermal capacity of the heat sink and the maximum operating temperature of the transistor. Based upon reliability and qualification testing requirements, it is desirable to have a power supply rated to as near to continuous duty as possible.

4. The packaging and wiring of the high voltage and low voltage sections of the power supply were found to be unacceptable.

5. The high voltage power supply step-up transformer was tested and found acceptable for using in the new power supply. Later, this unit was to fail during test and it was replaced with a new unit purchased from another manufacturer.

6. The laser high voltage power supply Ag-Zn batteries were found to be inadequate to provide the currents required by the power supply.

7. The switching relay used to turn on the high voltage power supply was not rated for the required carry current (100 amps).

On the basis of the above conclusions, a new high voltage power supply design was required.

The schematic diagrams for the circuits comprising the laser high voltage power supply are shown in Figure 3.6: High Voltage Battery Wiring Diagram; Figure 3.7: High Voltage Control Circuit; and Figure 3.8: Laser Power Supply.

The primary function of the high voltage control circuit is to generate and control the high voltage power supply inverter drive waveform. The drive waveform was generated using a regulating pulse width modulator integrated circuit, A3(SG3524). This circuit contains a voltage reference, an oscillator, a current limiting control, and a pair of output drive transistors.

This circuit was set up to provide a 1.5 kHz inverter drive waveform with a potentiometer-adjustable dead band. The regulator was set up so that the drive waveform was disabled if the energy storage capacitor high voltage exceeded a preset value (~23 kv), or the transistor emitter current exceeded a specified maximum value. This feature was found useful during testing of the supply at full power as it prevented transistor destruction due to excessive collector current. This feature was disabled after the power supply circuit component values had been finalized.

Other functions of this circuit are as follows:

1. Provide external and internal power switching control for the high voltage power relay (K1).
2. Provide H/V ENABLE-SAFE switching (K2) from the GSE.
3. The laser capacitor high voltage monitor signal current (H/V monitor signal) was inputted into A2/4-1 for current to voltage conversion.

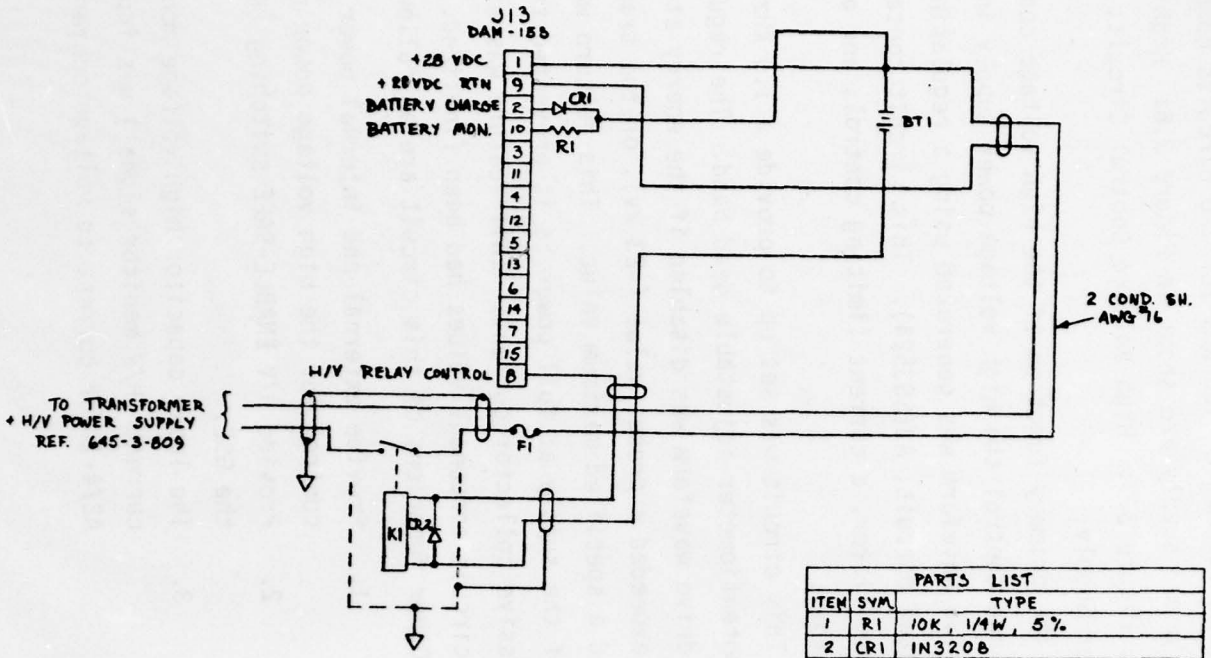

PARTS LIST		
ITEM	SYM.	TYPE
1	R1	10K, 1/4W, 5%
2	CR1	IN3208
3	CR2	UTR 2B10
4	F1	AGU40
5	BT1	28 VDC(AG-ZN, 18=PML15, YARDNEY)
6	K1	CH9565H13A

FIGURE 3-6 HIGH VOLTAGE BATTERY WIRING DIAGRAM

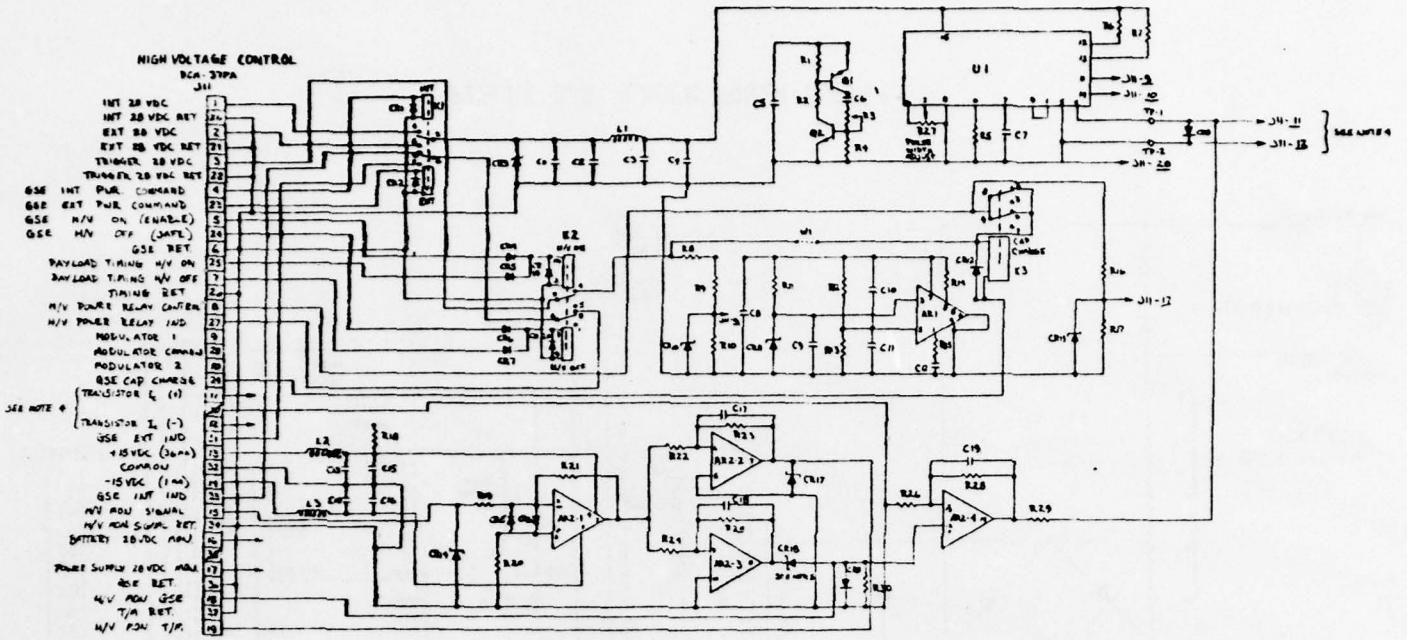

PARTS LIST

J11	DCHA-37PA
L1, L2, L3	SYFRONICS SRS-100
R1, R2	MCMB-24V, PB
R3	MCMB-24V, PB
Q2	2N2222
U1	56-3849
AR1	RCA 3094 DT
AR2	[illegible]
CR1, CR2, CR4, CR5, CR6, CR7, CR9, CR12, CR19, CR20	[illegible]
CR3, CR14,	TRW TRANSIENT SUPPRESSOR
CR10, CR13, CR17, CR18	6A25A
CR8, CR15, CR16	[illegible]
CR11	1N759A
C1, C9, C5, C7, C8, C10	CROSS-[illegible]
C11, C15, C16, C17, C19	
C2, C3	47 mfd 35 WVDC CSR13
C4	CROSS BARRIER
C9, C13, C14	[illegible] 20 WVDC CSR13
C12	CROSS BARRIER
C18	CROSS BARRIER
Q1	2N2907

R1, R2, R4	12 K
R3	20 K POTENTIOMETER, BOURNS 3382
R5	2.2 K
R6, R7	470 Ω, 2W, 5%
R8, R15	1K
R9, R16	33 K
R10, R17	9.1 K
R11	15 K
R12, R19	47 K
R14	100 K
R18	25 K
R20	8.2 K
R21	22 K
R22	20 K
R23, R23	3.3 K
R24	51 K
R25	11 K
R26	60 Ω
R27	100 K POTENTIOMETER, BOURNS 3382
R28, R29	1K
R30	10 K

ALL RESISTORS ARE 1/4 WATT, 5% UNLESS NOTED

NOTES:

1. THE FOLLOWING COMPONENTS COMPRISED PULSE WIDTH ADJUST CIRCUIT 1

   R1, R2, R3, R4
   Q1, Q2
   C5, C6

   THIS CIRCUIT WAS REPLACED WITH R27 AND THUS THE ABOVE LISTED COMPONENTS, ALTHOUGH MOUNTED ON THE CIRCUIT BOARD, ARE NOT FUNCTIONAL.

2. THE FOLLOWING COMPONENTS COMPRISED A CIRCUIT WHOSE FUNCTION WAS TO SHUT OFF THE GFE HIGH VOLTAGE POWER SUPPLY WHEN THE 28 VDC NOMINAL DROPPED BELOW A PRESET VALUE. THIS PROTECTION CIRCUIT WAS NOT REQUIRED FOR THE NEW HIGH VOLTAGE POWER SUPPLY

   R11, R12, R13, R14, R15
   C8, C9, C10, C11, C12
   D11
   AR1

   THESE COMPONENTS ARE MOUNTED ON THE BOARD BUT ARE NOT FUNCTIONAL.

3. R18 WAS TO BE PART OF A TEMPERATURE MONITOR CIRCUIT BUT WAS DELETED.
4. THIS CONNECTION REMOVED PRIOR TO FINAL TEST.
5. CR18 FAILED PRIOR TO OR DURING 7/24/78 FLIGHT

FIGURE 3.7 HIGH VOLTAGE CONTROL CIRCUIT

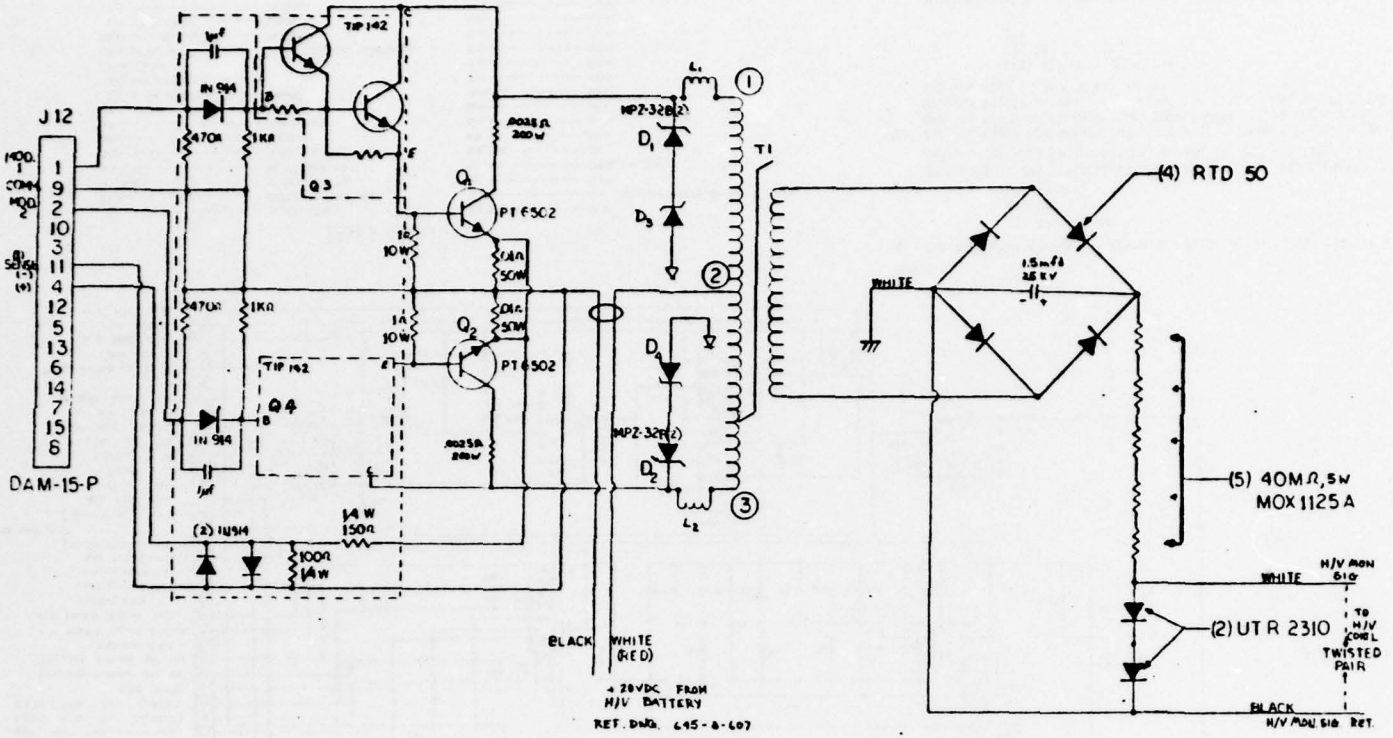

FIGURE 3.8 LASER POWER SUPPLY

4. A1 is a power comparator whose function is to shut down the high voltage power supply inverter if the battery voltage decreased to less than a predetermined value. This had been a requirement of the old power supply but it was not required for the new design. Thus, it was disabled.

The schematic of the laser power supply is shown in Figure 3.7. The inverter drive waveforms from the high voltage control circuit (MOD1, MOD2) are applied to their respective Darlingtons. The drive waveforms are generated by the output transistors of a switching regulator integrated circuit. In order to achieve high switching speeds, these transistors are not switched completely off. The function of the PI network in the power supply is to clamp the Darlington drive current to zero when the regulator drive is off.

To replace the parallel transistor configuration of the GFE supply, a single pair of ultra-high power transistors were used (PT6502).

Typical transistor characteristics are:

V_{CEO}	80 Volts
I_{cMAX}	200 A
I_c	100 A
$P_D(T=25^oC)$	350 W
$V_{CE(SAT)}$	0.75 Volts
t_r	2.0 μsec

Thus, a single pair of unmatched transistors could be used to drive the step-up transformer primary winding.

Inductances L1 and L2 are in the circuit to limit the transformer primary current to a 120 amp maximum in a transistor 330 μsec on - time (1.5 kHz). A pair of .0025 ohm resistors are also in the primary circuit. Their function is to provide a drive voltage across

Q3,Q4 when Q1,Q2 are conducting high collector current. Without the resistors, Q1,Q2 will drop out of saturation and very high power dissipations will result.

The function of the zener diodes, CR1-CR4, is to suppress inductive switching transients appearing across the transistors.

The high voltage step-up transformer (Mag-Cap 6483) had the following specifications:

Frequency	1.5 kHz
Primary	Bifilar Winding (Inverter)
Secondary	50 kv Stand-Off Voltage
Step-up Ratio	~800
Voltage (Center Tap)	28 VDC
Current (avg.)	50 amp
Duty Cycle	100 percent
Core Material	Permalloy

The high voltage rectifier circuit was mounted on the top surface of the transformer. High voltage integrity was maintained within this circuit by the judicious use of insulation and encapsulation. The assembly procedures were as follows:

1. The high voltage rectifier assembly was laid out so that the distance between high potentials was maximized. In addition, the distance from high potentials to outside walls or surface was maximized.
2. All interconnections were solder-balled and any residual flux removed.
3. All sharp edges on points were removed.
4. G-10 epoxy board 1/16" thick was used as the outside wall material.
5. High voltage leads were 50 Kv rated with silicone rubber insulation.

6. Low voltage leads were PVC insulated. No teflon insulated wires were used because adhesion of the encapsulating RTV to wire insulation was required.
7. All components and surfaces were degreased and cleaned using Freon TF.
8. After cleaning, all components were handled using white gloves.
9. All components and surfaces were fully immersed in RTV primer (Dow Corning 1201).
10. All wires and leads connecting the outside of the power supply were mechanically strain relieved.
11. After mixing, the uncured Dow Corning 3110 with catalyst S was pumped down in a vacuum bell jar to remove trapped gas bubbles.
12. The high voltage assembly was encapsulated by pouring. Care was taken to remove all bubbles and voids.
13. After the encapsulation had cured, the assembly was high potential tested to 50 kv.

The high voltage rectifier is a full-wave bridge made up of four EDI-RTD-50, fast recovery, 50 kv diodes. The high voltage dc output is connected to the energy storage capacitor (High Voltage Components, Inc., 5L500.25, 1.5 mfd, 25 kv). The capacitor is of a coaxial configuration such that the output pulse width of the xenon flash lamp is approximately one microsecond. A schematic drawing of the laser energy storage circuit is shown in Figure 3.9.

The high voltage power supply applies high voltage to the inner plate of the capacitor. The outer plate is grounded through the 1 kΩ resistor. When a 40 kV trigger pulse is applied to the pressurized spark gap electrode, a very low impedance path is created between the inner plate and ground. Thus, the outer plate is rapidly switched from ground

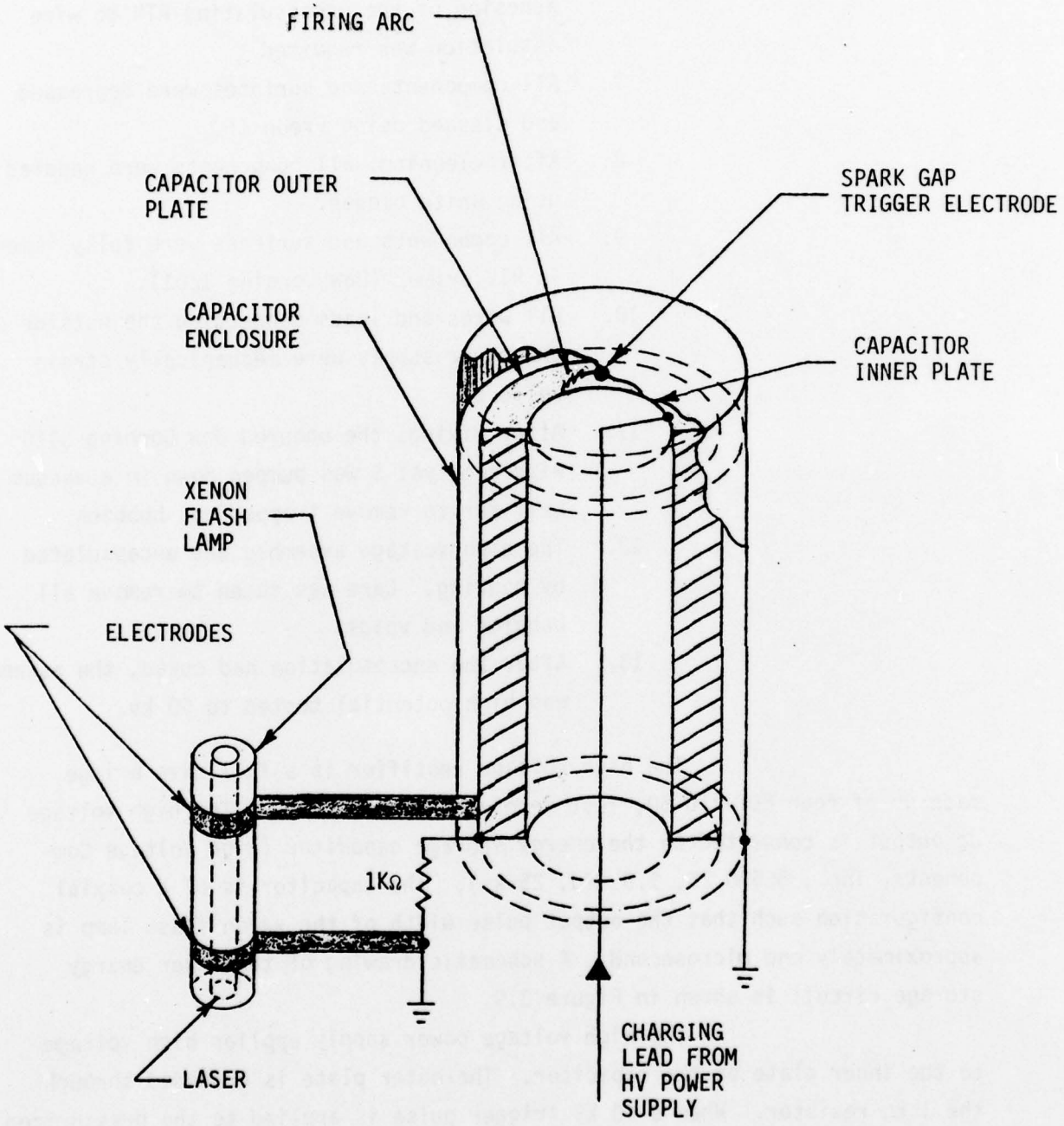

FIGURE 3.9 ENERGY STORAGE CIRCUIT SCHEMATIC

potential to that of the charge voltage. At this point, the laser pump xenon lamp fires and the capacitor discharges through the lamp. In the case of a failed lamp, the capacitor will discharge through the resistor.

The step-up high voltage transformer initially used was the GFE unit. This unit performed until payload integration when the unit failed due to high voltage breakdown from within the transformer to the payload structure. The breakdown path was dug out to remove carbon and then the void filled with epoxy. The unit was then installed in the payload and retested. Another similar breakdown failure occurred at another part of the transformer. After the second failure, the transformer was considered to be unsuitable for flight. The cause of this failure appeared to be improper encapsulation techniques during the original manufacture.

A new high voltage transformer was designed, fabricated, and tested. This unit was made by Mag Cap Engineering, Inc. Since the new transformer was of a different size than the GFE unit, the high voltage rectifier assembly packaging had to be redesigned. The new unit was hi-pot tested and then installed in the payload for an operational capacitor charging test. Upon successful completion of this test, the unit was brought to AFGL where it was subjected to a subassembly level vibration test (Appendix G).

A photograph of the high voltage battery is given in Figure 3.10. The battery consists of 18 series-connected Ag-Zn cells to provide a nominal voltage of 28 VDC. An investigation disclosed that the smallest cell which the manufacturer would recommend for this high peak current application was the PML-15. This is a primary Ag-Zn 15 amp-hr cell capable of reliably delivering peak currents up to 200 amps. These cells are stored in a dry-charge state and become charged to full capacity 72 hours after being filled with electrolyte. Full capacity is retained for approximately 30 days, after which a gradual capacity reduction occurs.

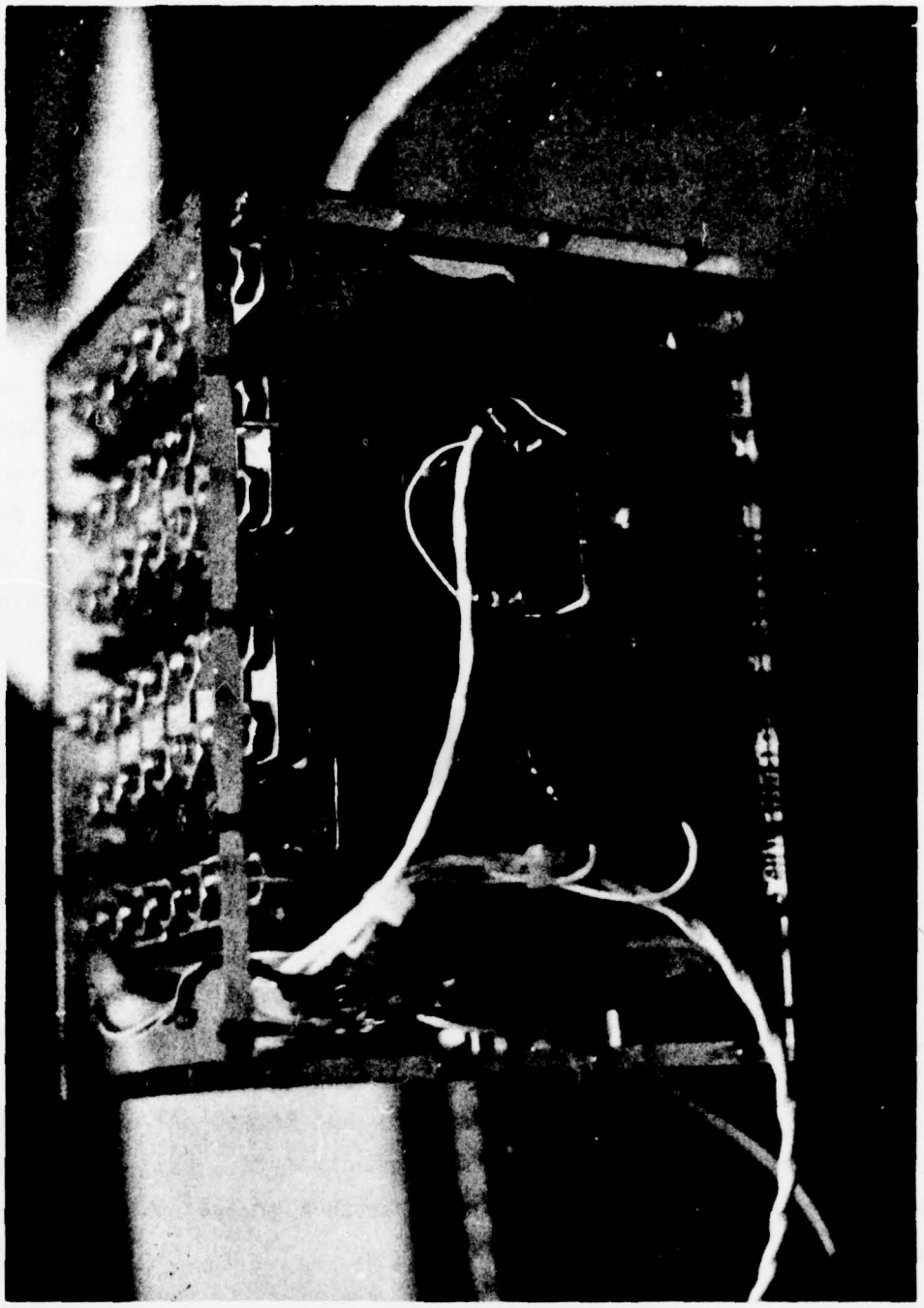

FIGURE 3.10 HIGH VOLTAGE BATTERY

The capacity of the PML-15 cells greatly exceeds that which was required by the laser power supply during flight. Typical average power supply current is 45 amps. Thus, a nominal 20 minute operation time is provided for.

Included in the battery package, shown in Figure 3.10, were the following:

1. A charging diode and monitor resistor to permit battery charging through the umbilical.
2. A 40 amp fuse, F1, to protect the high voltage power supply wiring in the event of a switching transistor short circuit. This fuse was replaced by a brass shorting plug for flight.
3. A 100 amp rated aircraft relay for power supply power switching. The relay was controlled by K2 in the high voltage control circuit.

Although the high voltage power supply battery voltage was directly monitored at the payload GSE, the design of the high voltage control circuit did not allow for a telemetry monitor for this voltage. It is recommended that this monitor be added to the system.

A major problem which occurred during power supply design was that the cell manufacturer (Yardney, Inc.) provided Visidyne with incorrect cell dimensions. Only after the cells were received did this error become evident. The cells were approximately two (2) inches higher than originally specified. The implications of this were the following:

1. Modification of the battery box.
2. Redesign and rework of the existing battery mount.

3. Redesign and rework of the high voltage power supply packaging.
4. Redesign and rework of the transmitter structure.

3.2.5 Spark Gap

The firing of the laser was initiated by a triggered spark gap which was located in the GFE energy storage capacitor housing. When a 40 kv pulse was applied to the trigger electrode of the gap, an ionized path to ground was formed between the storage capacitor inner plate and ground. This switching completed the discharge circuit through the laser xenon lamp.

The standoff voltage of the spark gap was maintained by pressurizing the gap to approximately 20 psig with ambient air. An unpressurized spark gap would spontaneously break down without being triggered when the capacitor voltage exceeded 13 to 15 kv. Standoff voltage was increased through pressurization by approximately 3 kv/psig. Since the laser output power decreased rapidly to zero when the energy storage capacitor voltage decreased to less than 18 kv, the spark gap pressurization was an essential part of the system.

The GFE spark gap was the source of many of the problems which occurred during system test. The problems are discussed in the paragraphs below.

A cracked nylon insulator ring inside the gap caused low voltage breakdown to occur. A replacement was procured and the gap reassembled and tested.

Spark gap pressure leakage was a problem throughout the program. The main cause of this was that the spark gap end plate was made of sheet metal rather than being a machined pressure flange. Sealing the plate required careful sequential tightening of the fastening screws with care so that over tightening did not strip the nylon insulation into which they were seated. The gap pressurization tubing fittings were also the cause of leakage.

During laser testing, the trigger electrode within the spark gap disintegrated. A new gap end plate was procured and the gap reassembled and tested. It should be noted that although there was a spare GFE energy storage capacitor housing, it was different dimensionally from the GFE flight unit so that they were not easily interchangeable. For example, the spark gap end plates could not be switched because they were of different designs.

During final testing, a sporadic pressure leak developed in the spark gap. Sudden depressurization occurred during occasional laser firings. The cause of this leak could not be found. Prior to shipping the payload to WSMR, the entire spark gap end plate and pressurization fittings were primed and thickly coated with RTV 11 silicone rubber. Testing at WSMR indicated the major leakage problem had been solved.

A spark gap pressure transducer was used to monitor gap pressure and the resultant data was sent to telemetry. It would have made field site testing less complicated had this data been also sent through an umbilical to the GSE for direct readout.

3.2.6 Transmitter Circuits

In addition to the High Voltage Supply, other circuits in the transmitter were the following:

Spark Gap Trigger Circuit

The GFE spark gap trigger circuit was considered unacceptable for flight primarily because of improper packaging and because of anticipated interfacing problems. Thus, a new circuit was designed, fabricated, and tested. The trigger circuit schematic is in Figure 3.11.

A TTL, asserted low, firing pulse from the timing circuit discharged C8/C9 through T2. This caused SCR1 to discharge C10 through the grid of V1. V1 went rapidly into conduction, thus discharging C6, charged to 300 volts, through the primary of T1. The secondary

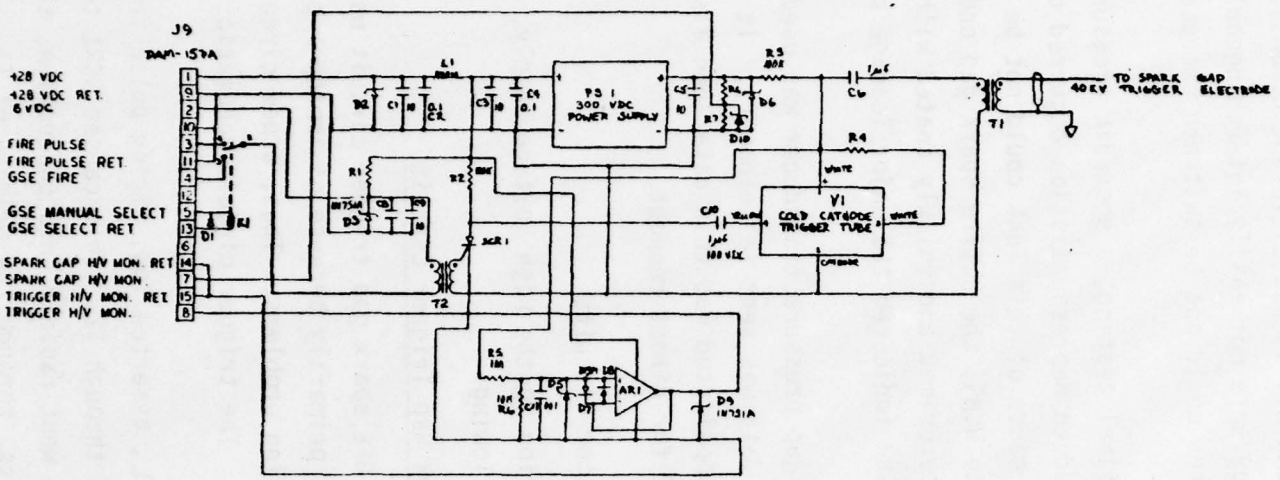

PARTS LIST			
SYM	DESCRIPTION	SYM	DESCRIPTION
T1	EG·G TR-180 B	C1, 3	CSR13G475KL
T2	PULSE ENGINEERING 6166R	C2, 4, 8	CK05BX104M
R1	TELEDYNE 412DD-26	C5	TRW X463UW .1mfd 400 WVDC
D1	IN645	C6	TRW X463UW 1mfd 400 WVDC
D2, 5, 6	TRW TRANSIENT SUPPRESSOR	C7	N/A
D3, 9, 10	IN751A	C9	CSR13 10mfd
D4	N/A	C10	CK06BX105M
D7, 8	IN914	C11	CK05BX102M
R1	15 K 1/2 W	L1	INTRONICS WEE-100
R2, 3	100 K	PS1	TECHNETICS 9503-111
R4	22 MEG	V1	EG+G KRP20
R5	1 MEG	AR1	RCA CA 3140BT
R6	10 MEG	SCR1	GE SC 146
R7	100 K		

FIGURE 3.11 TRIGGER CIRCUIT

output of T1 was a 40 kv pulse which was sent to the pressurized spark gap trigger electrode. When relay K1 was energized, the firing pulse was initiated by a manual switch closure at the GSE.

Telemetry monitors were provided for the 300 volt output of PS-1 and the charge and discharge of C6, which was the primary firing pulse capacitor. Extensive transient isolation and decoupling were included in the circuit to prevent RFI circuit effects.

Timing Circuit

The function of this circuit was to generate the timing pulses required for laser firing, sensor data gate control, and sensor calibration gate control. The circuit schematic is shown in Figure 3.12. The payload timing is discussed in Section 3.3.3.

Dye Coolant Control Circuit

The function of this circuit was to provide the laser control and monitor telemetry interface for the dye and coolant circulation system.

Temperature and Pressure Circuit

The function of this circuit was to monitor and interface transmitter section pressure and temperature data.

Power Supply

The function of this circuit was to provide $\pm$15 VDC and +5 VDC power required by the transmitter section electronics.

All of the above circuits were Visidyne designs specifically fabricated and tested for this Laser Backscatter Experiment payload. A shielded-cabling, sub-system interconnection harness was designed and fabricated. The extensive use of shielding, decoupling, and transient suppression devices in the design served to make payload RFI a minor problem.

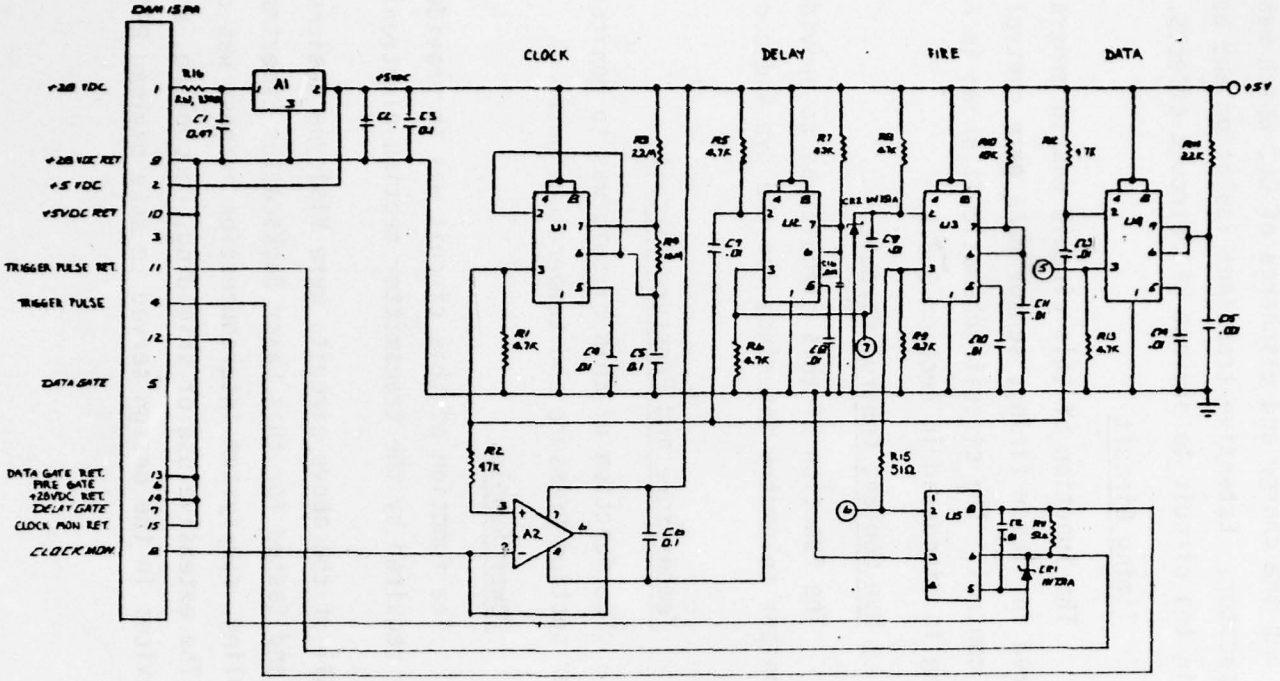

FIGURE 3.12 TRANSMITTER TIMING CIRCUIT

3.2.7 Packaging

The payload transmitter section main structure and packaging were of an entirely new design; the only parts retained from the previous payload were the energy storage capacitor housing, the laser housing, and the payload outer skin. The latter was modified by AFGL to accommodate the dye and coolant reservoirs in the payload. The transmitter section with the outer skin removed is shown in Figure 3.13.

Major features of this new design were the following:

1. Modular electronics packaging whereby all circuits were interfaced with the system using connectors, exceptions to this being the high voltage and high current interconnections.
2. Modular mechanical assembly whereby all sub-systems could be independently removed and installed as a design goal.
3. A longeron mounting system for the newly designed dye and coolant reservoirs.

Two major mechanical problems were encountered. First, the transmitter structure was mounted to the payload only by a set of screws into the optics casting. After launch and recovery several of these screws were found to be stripped from their tapped holes. It is probable that the payload exceeded its mechanical environmental specifications during chute deployment and/or ground impact. Thus, this problem was not considered significant.

Secondly, the fluid interface plate between the transmitter section and the dye coolant reservoir section was not rigidly connected to the payload structure except where it was fastened to the end plate of the lower skin section. The result of this non-rigidity was that excess flexure was imposed on the fluid lines leading from the transmitter section to the interface plate. The result of these flexures was to cause leaks in the fluid lines. By rigidly fastening this interface

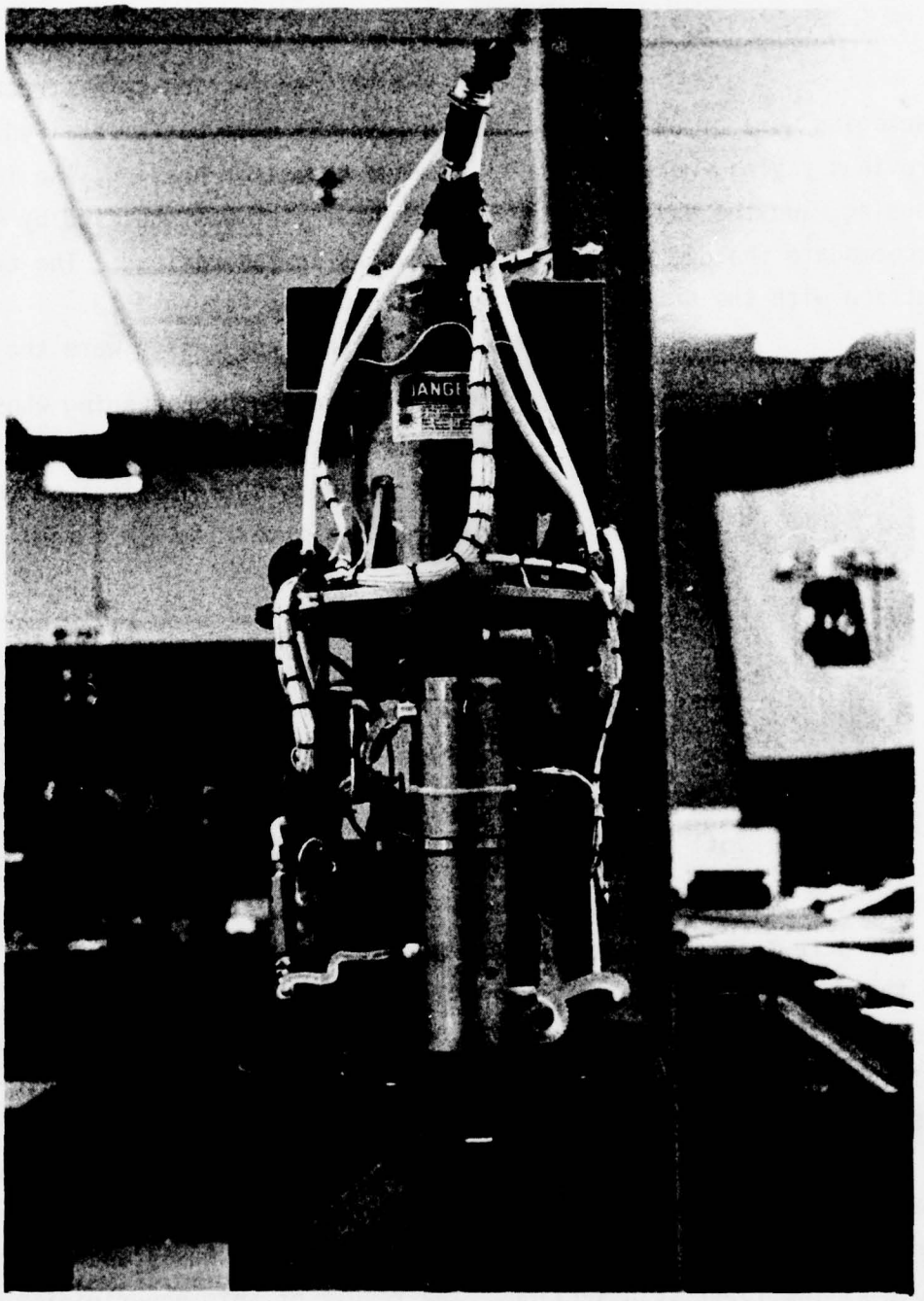

FIGURE 3.13 TRANSMITTER SECTION WITH THE OUTER SKIN REMOVED

plate to the transmitter structure, the risks of these leaks could have been minimized.

3.2.8 High Voltage and System Tests

On November 19, 1977 during the final testing of the laser payload experiment, a failure occurred in the high voltage assembly. The system had been fired approximately 100 times prior to this failure. Later investigation showed that the failure was a short-circuited high voltage rectifier. Test data has indicated that the high voltage rectifiers were subjected to excessively high frequency - high voltage inputs during initial turn-on. Inductors installed in the power supply after initial turn-on removed these high frequencies from the high voltage circuit.

Failure of the overstressed rectifiers occurred after many cycles. On the basis of these tests, no design modifications were made in the high voltage power supply.

Immediately after the above mentioned failure, the back-up high voltage assembly was installed in the payload. During the first attempt to fire the laser, a high voltage arc over occurred. The resulting transient caused extensive damage to the high voltage power supply electronics. With reluctance, Visidyne, Inc. informed AFGL on 21 November 1977 that the 6 December 1977 launch schedule could not be met.

The damaged high voltage power supply was repaired, and some transient suppression diodes were installed. It was attempted to fire the laser and again high voltage breakdown occurred, inflicting extensive damage on the high voltage power supply. Locating and testing damaged components was a major effort. The arc over also damaged the spark gap, thus requiring it to be rebuilt.

At this time, the refurbished new high voltage assembly, with new rectifiers, was installed in the payload. Arc over occurred immediately and caused the destruction of every semiconductor in the high voltage power supply. The back-up laser capacitor was then

installed in the payload and the flight unit was returned to the manufacturer for tests. No problems were found with the flight capacitor. The back-up capacitor also performed well in the payload system for approximately 15 firings when another arc over occurred. Repairs were made and additional transient suppression diodes installed. Testing was again started and final spark gap pressure capacitor high voltage and timing settings were made in preparation for the final sustained operation test. A faulty electrical connection caused the high voltage shut down circuitry to be disabled. Thus, during the next charging cycle, the capacitor was overvoltaged and breakdown again occurred. Subsequent testing showed that the breakdown voltage level had been lowered to within the operational voltage range.

Several design changes were implemented and the system was successfully tested to the approximate flight profile of 80 laser pulses in a 180 second period. The details of this effort are given below.

The extremely destructive intermittent short circuit in the high voltage section was eliminated after determining that the breakdown was occurring in the high voltage capacitor charging return wire. This wire is set at near ground potential at all times except at the instant the spark gun breaks down. When the flash lamp fires, the charging return lead voltage drops to lamp voltage (several hundred volts).

To rectify this problem, the following modifications were made to the high voltage section:

1. The high voltage capacitor charging return lead was double insulated using surgical tubing.
2. The charging resistor was replaced and relocated away from the high voltage power supply.
3. A ground plane was added between the charging return lead and the high voltage power supply.

As a result of these modifications, the breakdown was eliminated.

Next, a simulated flight test, consisting of eighty (80) laser firings, was attempted. After approximately twenty-five (25) shots the system was shut down because of excessive temperatures in the switching transistors. To locate the cause of this excessive temperature, the following power supply diagnostic measurements were made:

1. Collector-emitter voltage as a function of time.
   From this test it was found that the inverter power transistors were not fully saturated during the on period of each switching cycle. The addition of a small resistor (.025Ω) in the collector of the power switching resistor corrected this problem.
2. Collector current as a function of time.
   From this data it was found that I_c(max) was approximately 90 amps, thus permitting safe transistor operation at transistor temperatures in excess of 100^{o}C.
3. Collector current versus collector emitter voltage (load line).
   From this data it was found that the power transistors were operating within their specified safe operating area (SOA) over all operating temperatures.
4. Measurements of transistor collector current when the transistor was "off" indicated collector current of several amperes.
   This was attributed to leakage current at high junction temperatures. The leakage was eliminated by adding a capacitor to the base drive circuit so that the base was maintained

at -0.6 volts rather than 0 volts during the "off" period.

5. To further improve inverter efficiency, an inductance (40 μH) was put between the base and emitter of the power transistors. The function of the inductance was to remove charge rapidly from the transistor base region at turn-off. Since insertion of the inductance caused excessive ringing during switching, it was removed from the circuit.

6. Another attempt at continuous operation was made, but again system shut down was required when transistor temperatures exceeded 100°C. Heat sink efficiency measurements indicated that thermal equilibrium could not be maintained with the existing heat sink. Therefore, a new transistor heat sink was designed and fabricated. The new design incorporated the following improvements:

   (a) Electrical insulators were not required between transistor case and the heat sink.
   (b) Cooling liquid was circulated within .060 inches of the transistor case.
   (c) Cooling liquid was circulated around the transistor (approximately 270°).
   (d) A separate heat sink was provided for each power transistor.

   The heat sink described above was breadboarded and installed in the payload.

7. During electrical testing of the heat sink, the laser flash lamp failed. According to the manufacturer, Candela, Inc., the flash is guaranteed for 5,000 flashes and rated for 30,000 flashes at 25 kv. It is estimated that the failed flash lamp was subjected to 200 flashes at voltages averaging 22 kv. (The 5,000 flash guarantee is valid for only six months.)
8. The spare flash lamp was installed and it was found that it could not be optically aligned. The flash lamp was removed from the payload and it was found that the front window o-ring groove was too deep. The assembly was returned to the manufacturer, Candela, Inc., for repair.
9. The repaired flash lamp was returned to Visidyne and reinstalled and aligned.
10. On 10 March 1978, an engineering test was performed where constant laser operation for a period of approximately 180 seconds (80 shots) was observed.
11. On the basis of the above continuous operation test, the high voltage supply was considered to be qualified and the 24 July 1978 launch date was scheduled.

3.3 Receiver

3.3.1 Optics

The receiver optics are shown in Figure 3.4. No design changes were made in the optical components by the Visidyne modifications, but the primary and secondary mirrors of the telescope system required new optical surfaces.

The primary mirror coating as furnished was protected silver (silver 950, overcoated), but the protective coatings had obviously failed and the silver had tarnished severely. Adherence of the coating was also inferior. The decision was made to change to aluminum overcoated with SiO. Although the reflection of aluminum at 4600Å is slightly lower than silver (see Figure 5, Appendix D), its nontarnishing properties were of greater importance. Consequently, the primary mirror was sent to Applied Optics Center Corp., Burlington, Ma., where its silver coating was removed, the substrate repolished, and a new coating of aluminum applied and overcoated with SiO. The resulting physical characteristics were as follows:

Diameter: 40.00 cm
Radius of Curvature: 72.17 cm, polished to within 1/2%
Surface Finish: 80/50
Accuracy: Overall deviation $\leq 1/2\ \lambda$
Local Smoothness $\leq 1/4\ \lambda$
Astigmatism $\leq 1/4\ \lambda$

The secondary mirror was refurbished in the same manner as the primary mirror. Its radius of curvature was found to differ considerably from the value specified. Repolishing was done to its actual radius and the resulting physical characteristics were as follows:

Diameter: 18.92 cm
Radius of Curvature: 114.88 cm, polished to within 1/2%
Surface Finish: 80/50
Accuracy: Overall deviation $\leq 3/4\ \lambda$
Local Smoothness $\leq 1/2\ \lambda$
Astigmatism $\leq 1/2\ \lambda$

The spectral transmission of the receiver bandpass filter was checked at several points and at normal and 17^{o} from normal

incidence. Blocking from 2000-9000Å was also rechecked. No degradation was detected. Representative transmissions are given in Figures 6 and 7 of Appendix D.

No changes were made in the folding mirror or the relay lens. However, the relay lens was checked to see that total internal reflection was not occurring.

3.3.2 Sensor

The receiver sensor section of the experiment was located within and below the receiver optics casting. The function of the receiver sensor was to detect the backscattered photons and condition the resulting signals for payload telemetry transmission.

The backscattered photons, collected by the Cassegrainian optical system and spectrally filtered, were focussed onto the photocathode of a photomultiplier. A block diagram of the receiver electronics is shown in Figure 3.14.

The GFE receiver electronics were inspected by Visidyne, Inc. and all cables, components, and circuits were found to be unacceptable for flight. These parts were subsequently scrapped. Exceptions to the above were the photomultiplier, the photomultiplier housing, and a high voltage power supply. Thus, the receiver electronics were of a completely new design.

The detector used was an EMR 541E-01-14 photomultiplier which had a semitransparent tri-alkali photocathode which exhibited a typical quantum efficiency of 25 percent at 4270Å and a dark current of 7.5×10^{-10} amps at a gain of 10^6. This tube is a ruggedized type suitable for sounding rocket use.

The flight photomultiplier was found during flight test to be degraded such that it had excessive dark current ($>10^{-7}$ amps) and it was replaced with the uncalibrated spare.

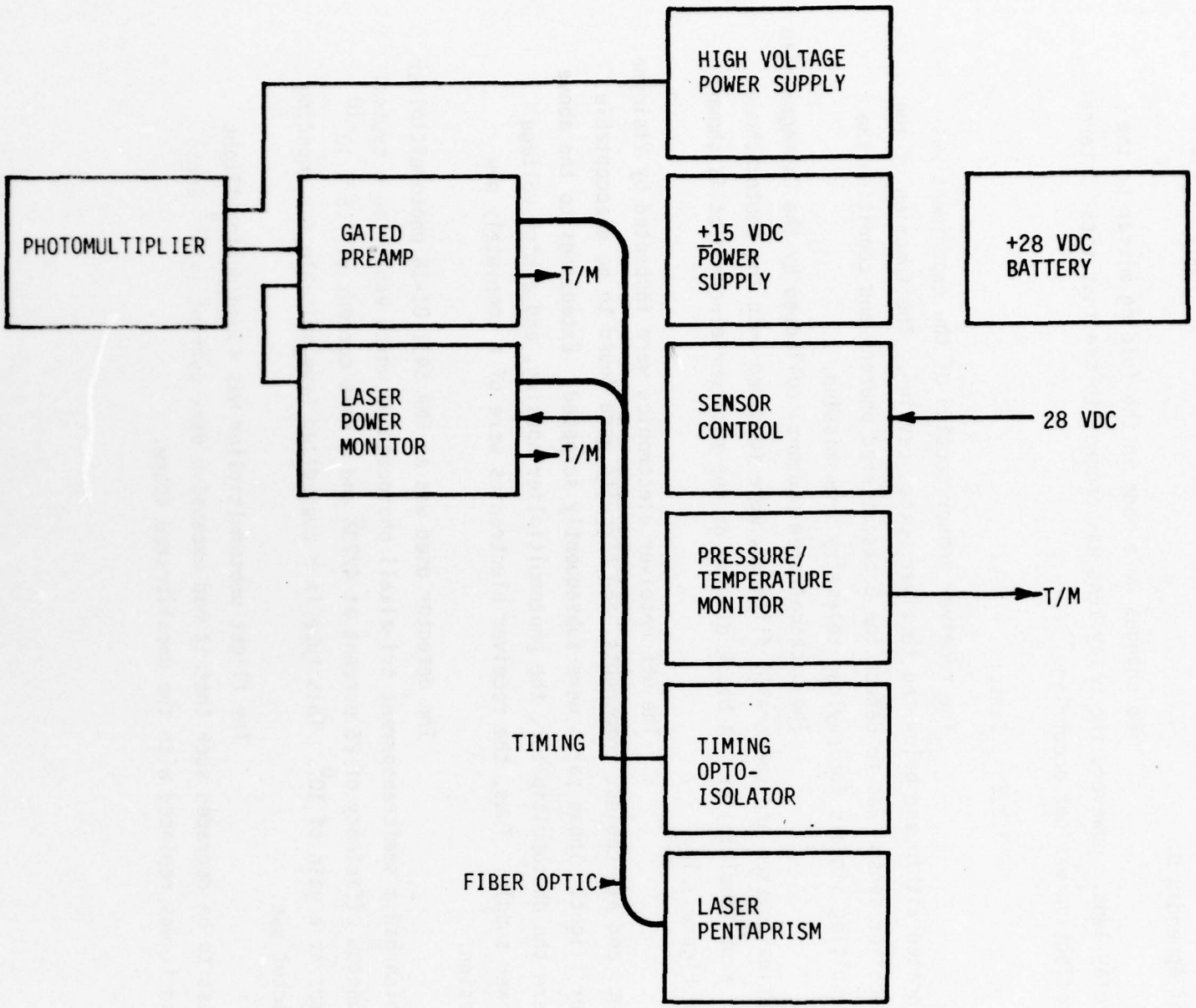

FIGURE 3.14 RECEIVER BLOCK DIAGRAM

3.3.3 Electronics

The photomultiplier data amplifier schematic is shown in Figure 3.15 and the photomultiplier signal conditioning and data distribution are shown in Figure 3.16. The preamplifier used a PMT anode capacitor to convert anode current pulses to voltage pulse heights. The 680 pf capacitor was discharged through a 10K resistor providing an effective integration time of 6.8 μsec. Thus, the voltage across the capacitor represented the time integral of counts per 6.8 μsec interval. The voltage pulse across C was then amplified and stretched to form a data pulse having a fast, sharp rise to a voltage value corresponding to backscattered photon flux but having a slow exponential decay (see Figure 3.17). In this manner, short duration data could be transmitted on relatively low frequency telemetry channels.

The IRIG FM/FM VCOs used in the payload telemetry required that the input signals be limited to the range between 0 and 5 volts. This limiting was done by zener diodes on each telemetry line. The voltages across the pulse stretching capacitor C4 were limited by the saturation voltage of the output of A1/A2, typically 12 volts, but since the peak voltage (V) of a clipped exponential can be determined from the duration of the clipping time (t_c), the dynamic range of the medium gain channel was extended by a factor of 2.4.

The clipped exponential waveforms prevalent in the flight data was a normal data format.

If the voltage (V_c) across C1 exceeded 2 volts, the output of A1/A2 would saturate. This was the maximum useful medium gain data. A resistor divider network across C2 attenuated this high level signal and applied it to a pulse stretching circuit from which it was inverted and sent to telemetry. Thus, the dynamic range of this data amplifier chain was determined at the low level by the telemetry system noise. It is assumed that a 10 mv signal could be observed on the high gain channel. The maximum observable signal on the low gain data channel was probably limited by the absolute maximum input voltage to A1/A2, 15 volts; hence, the dynamic range R of the system can be defined as:

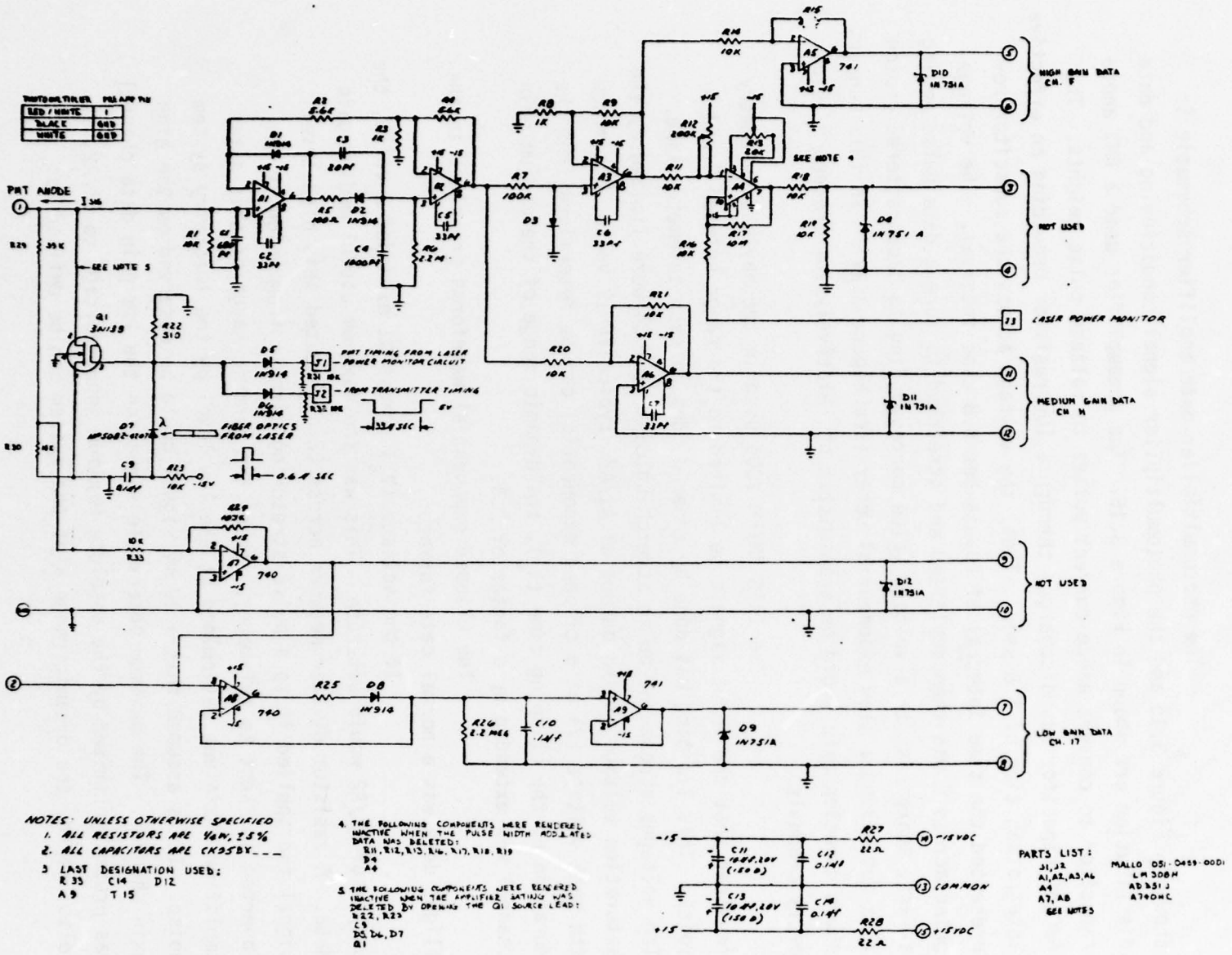

NOTES: UNLESS OTHERWISE SPECIFIED

1. ALL RESISTORS ARE ¼W, 5%
2. ALL CAPACITORS ARE CK05BX___
3. LAST DESIGNATION USED:
   R 35 C14 D12
   A 9 T 15
4. THE FOLLOWING COMPONENTS WERE RENDERED INACTIVE WHEN THE PULSE WIDTH ADJUSTABLE DATA WAS DELETED:
   R11, R12, R13, R16, R17, R18, R19
   D4
   A4
5. THE FOLLOWING COMPONENTS WERE RENDERED INACTIVE WHEN THE AMPLIFIER GATING WAS DELETED BY OPENING THE Q1 SOURCE LEAD:
   R22, R23
   C9
   D5, D6, D7
   Q1

PARTS LIST:

J1, J2	MALLO 051-0459-0001
A1, A2, A3, A6	LM 308H
A4	AD 351 J
A7, A8	A740HC
SEE NOTES	

FIGURE 3.15 DATA AMPLIFIER

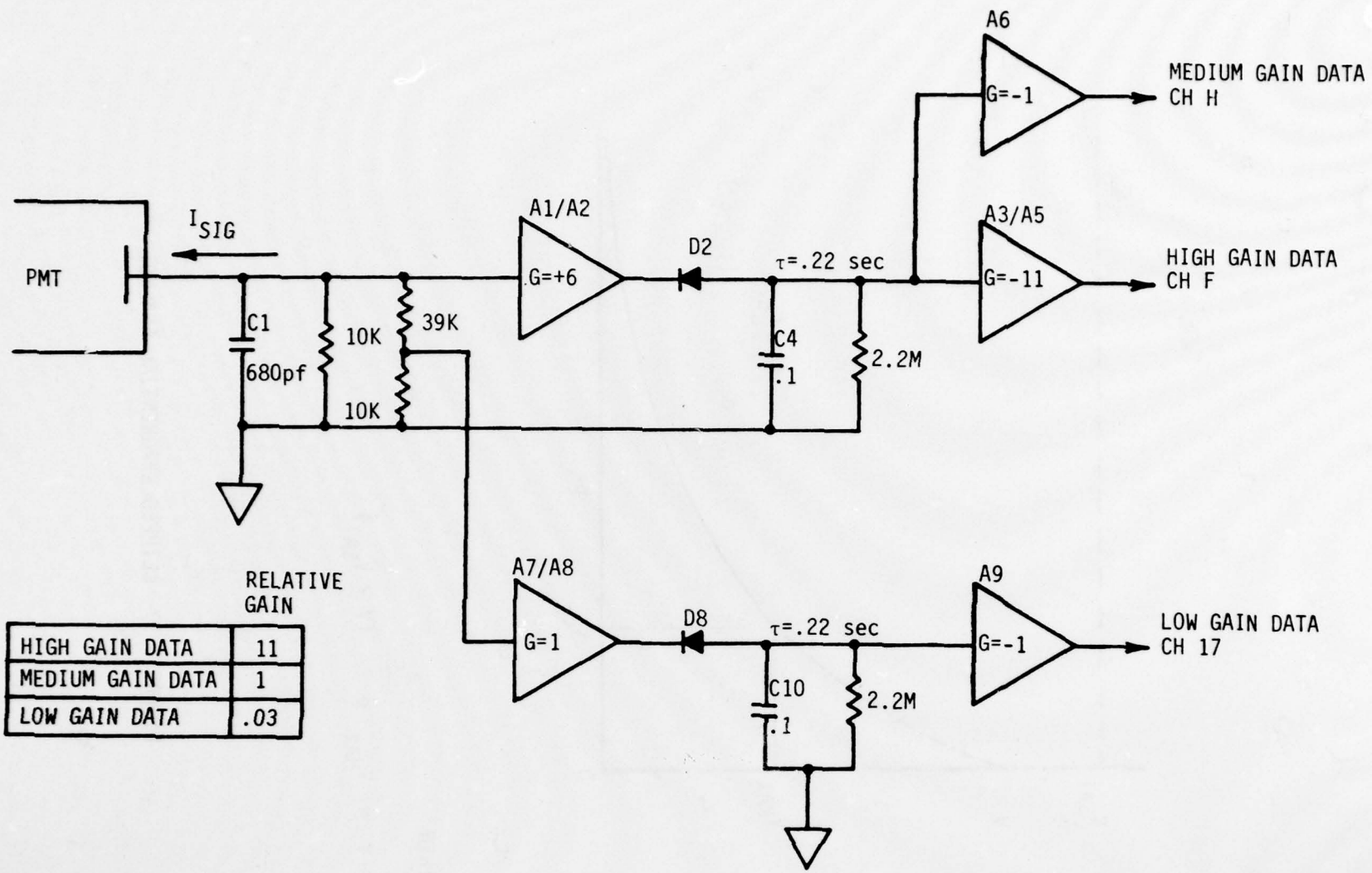

RELATIVE GAIN	
HIGH GAIN DATA	11
MEDIUM GAIN DATA	1
LOW GAIN DATA	.03

FIGURE 3.16 RECEIVER DATA AMPLIFIER CHAIN

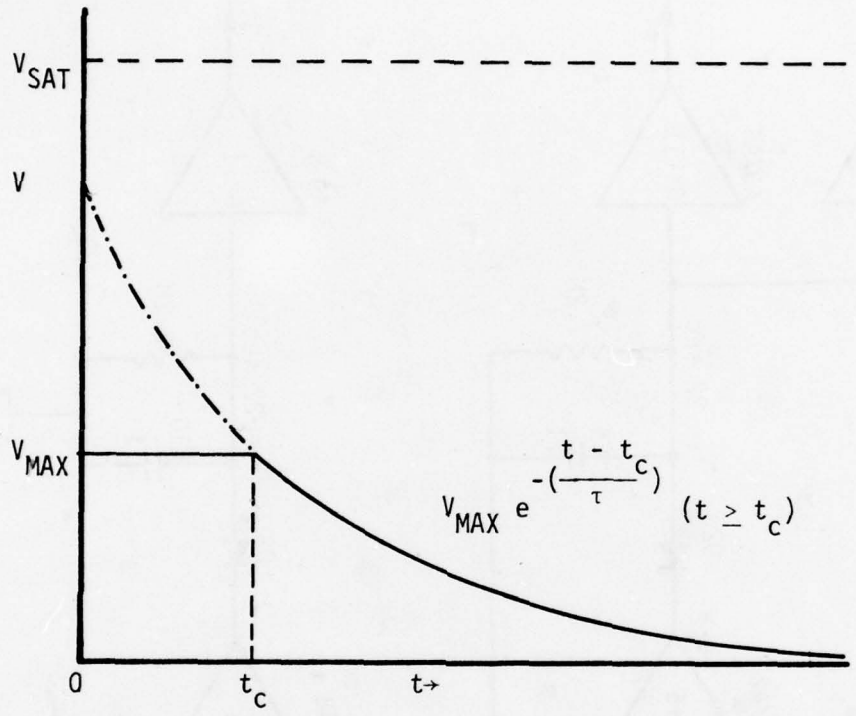

THEN

$$V = V_{MAX}\, e^{\frac{t_c}{\tau}} \quad (V \leq V_{SAT})$$

FIGURE 3.17 CLIPPED EXPONENTIAL ANALYSIS

$$R = \frac{\text{maximum unsaturated signal}}{\text{minimum detectable signal}} = 10^5 \text{ (100 db)}.$$

It should be noted that this data amplifier circuit is a peak detector. Any time a bright point source is observed, the amplifier output rapidly rises to a voltage corresponding to the source brightness, and then as the point source leaves the field-of-view, the voltage will decay exponentially with a characteristic .22 second time constant. Any radiating sources subsequently viewed which generate voltages less than the instantaneous value of that decaying previous source will not be detected. That is, the voltage on the pulse stretching capacitor (C4, C10) will not be changed because the charging diodes D2, D8 will be back-biased.

It was originally planned to use the pulse width modulation format discussed in Reference 2, where the primary data output is a pulse whose width is proportional to the ratio of backscatter return to laser output power. Although this format is attractive from a data analysis viewpoint, it was not used because (1) its reliable operation (and thus all primary data) depended upon the proper operation of two independent sensor systems (PMT and laser power monitor), and (2) it had a limited dynamic range ($\sim 10^3$).

Acknowledgement is herewith given to Reference 2 for the design of the input amplifier A1/A2 circuit.

The receiver used a gated amplifier circuit which was designed, fabricated, and tested. During final testing, this circuit was intentionally rendered inoperable. The function of the gating was to improve the data signal-to-noise ratio by the reduction of the contribution of PMT dark current and night sky background to the backscatter data. The gating was accomplished by shorting C1 except when backscatter data was expected.

The voltage across the capacitor was held at zero volts by a silicon, insulated gate, N-channel, depletion type, field effect transistor (FET) utilizing metal oxide semiconductor (MOS) construction

(RCA 3N138). This device will provide a very high input resistance (10^{14} ohms typical) during the time the PMT current is to be gated on. During all other times, the switch is turned on, thereby shorting out the anode capacitor through 240 ohms (on resistance) with an inherently zero offset voltage.

A block diagram of the payload timing system is shown in Figure 3.18 and an experiment timing diagram is shown in Figure 3.19. The master timing circuit is located in the transmitter. The circuit schematic is shown in Section 3.2.6, Figure 3.13.

The clock pulse determines the laser firing repetition rate, set for 0.45 pulse per second. A negative transition of the clock pulse initiates a 33 μsec wide Primary Data Gate, which is sent to the preamplifier through an optical isolator. The function of this isolator is to provide electrical isolation between the transmitter and receiver sections of the payload in order to minimize RFI and ground loops.

A 5 μsec Delay Gate is generated simultaneously with the data gate. At the end, or negative transition, of the Delay Gate, the laser FIRE pulse is sent to the spark gap trigger circuit through another optical isolator. Hence, the gated amplifier is always enabled 5 μsec prior to laser firing in this primary mode of operation.

A secondary mode of operation was designed into the system which provided a properly timed data gate to the preamplifier whenever the laser fired. Thus, if the laser self-fired (fired out of synchronization with timing circuit clock), backscatter data would still be obtained.

An optical pick-up was mounted behind the laser pentaprism (reference Section 3.2.2). The pentaprism was coated on a reflective surface so that approximately 2 percent of the incident 4600Å radiation was transmitted through the surface. This radiation was then focused onto the face of a fiber optic bundle. This noncoherent fiber optic bundle was split into two bundles so that half of the sample laser output was transmitted to the data amplifier PIN photodiode (D7) which controls the PMT anode switch (Q1). The other half of the fiber optic provided the optical input to the laser power monitor circuit.

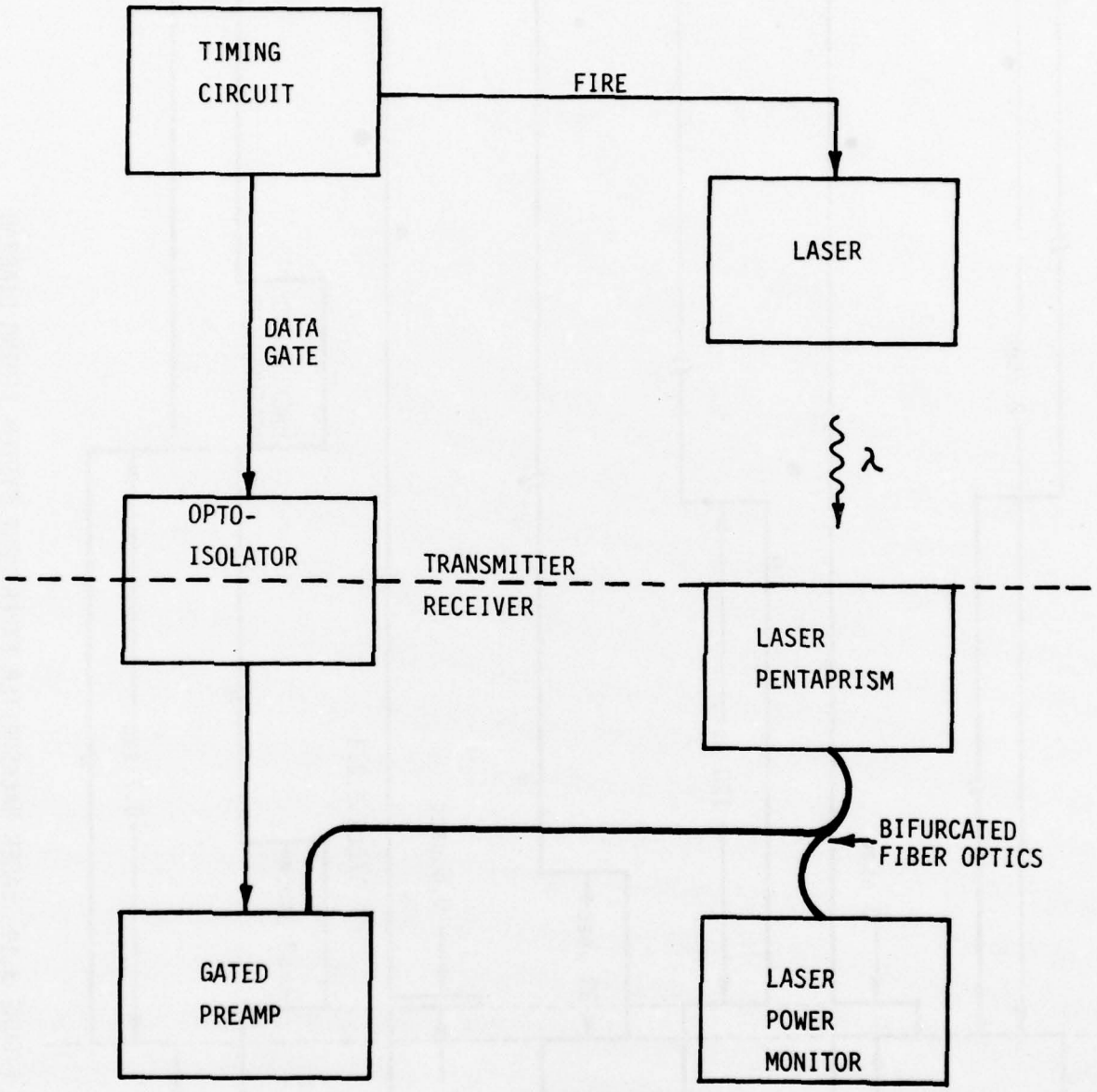

FIGURE 3.18 TIMING SYSTEM DIAGRAM

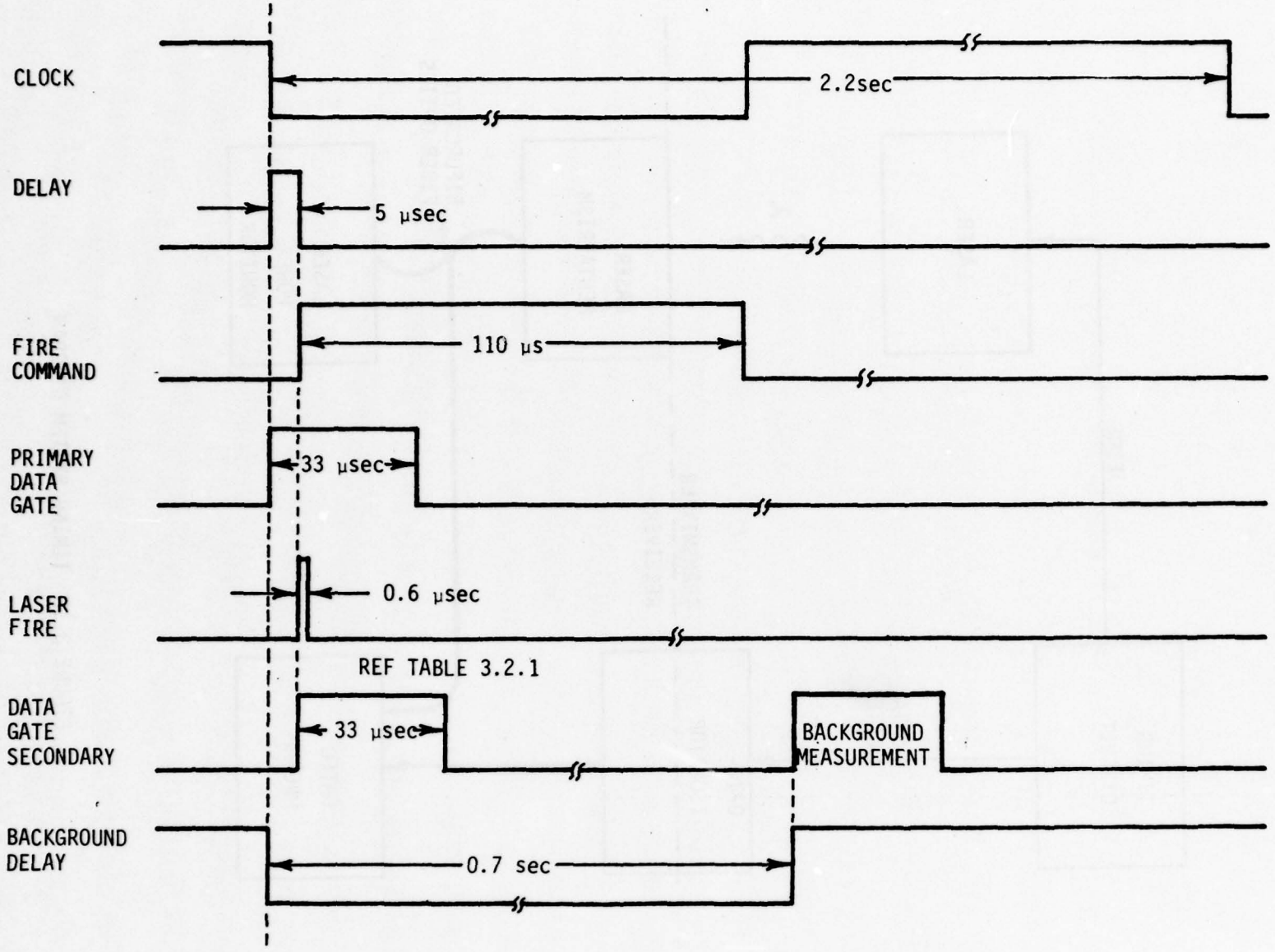

FIGURE 3.19 LASER BACKSCATTER EXPERIMENT SYSTEM TIMING DIAGRAM

A design study (Table 3-1) indicated that the time of flight of the laser emitted photons to the PMT anode was greater than the time required for the laser emitted photons to open the PMT anode switch (Q1). Since the laser pulse duration was only 0.6 μsec, a sustaining gate was required to maintain the PMT anode switch open for an additional 20 μsec. This sustaining gate was generated in the laser power monitor circuit by using the laser emitted photons from the second half of the bifurcated fiber optic bundle to trigger a one-shot multivibrator. This gate pulse was then applied to the PMT anode switch.

Optical coupling of the laser radiation into the fiber optic bundle was difficult. It was found that it was necessary to integrate the entire laser beam pattern spatially in order to have a signal which represented the total laser output power. Spatial inhomogeneities in the laser beam as a function of time history (first few firings) were observed. These inhomogeneities were probably caused by the fact that the dye within the laser cavity was not completely replaced between laser firings. Thus, for the first four or five shots, beam pattern variations were noted, but then a steady state condition was attained for the remaining shots of a series.

In addition to spatial integration, it was required that the intensity of the sampled radiation be maximized because of the large fiber optic end-coupling losses and the relative insensitivity of the PIN photodiode detectors. Because of the ultra-fast switching speed requirements of this system, the use of amplifiers was precluded.

During final system test, a failure of the secondary or back-up data gating system occurred. Whenever the laser self-triggered, no receiver data were obtained. To prevent this problem from causing a catastrophic experiment failure, the PMT anode gate switch was rendered inoperable by opening the Q1 source circuit on the amplifier printed circuit board. The conditions which led to this decision were:

TABLE 3.1

COMPARISON OF TRANSIT TIMES

LASER BEAM	Length (m)	Time (nsec)	PMT ANODE SWITCH CONTROL	Length (m)	Time (nsec)
To minimum sensitive range	2	6.7	Fiber optic (n=1.5) from laser to PIN diode	1	5
Return to receiver optics	2	6.7	PIN diode response time (1)	-	1
Receiver optics path length	.5	1.7	FET switch turn-off time (2)		2.7
Photomultiplier electron propagation time	-	25			
TOTAL		40.1 nsec			8.7 nsec

(1) HP 5082-4207

(2) RCA 3N138

1. The previous backscatter experiment attempt (Reference 2) had failed because of a timing problem.
2. The spark gap pressure leakage problem had as yet to be solved so that there was a high probability of laser self-triggered firings which would yield no data with the improperly functioning back-up timing system.
3. Greater emphasis was now being placed on obtaining backscatter data from the lower (<100 km) altitudes. At these altitudes, the magnitude of the backscattered signal was much greater than at the higher (>100 km) altitudes, and thus the advantages in signal-to-noise obtained by amplifier gating were not required.
4. The program launch schedule and resources would not permit enough time for the effort required to solve the problem.

The laser power monitor circuit, shown schematically in Figure 3.20, provided an analog signal whose amplitude was proportional to the laser output radiation power. The detection circuit was based upon the one described in Reference 2. Extensive modifications were required to the circuit in order to make it operable. The PIN photodiode signal was amplified and sent to telemetry as the Laser Power Monitor.

Included on this circuit board was the monostable multivibrator which generated the PMT anode switch sustaining gate and the background gate. The function of the latter was to open the PMT anode switch approximately one (1) second after each laser firing to permit a sky background measurement to be made.

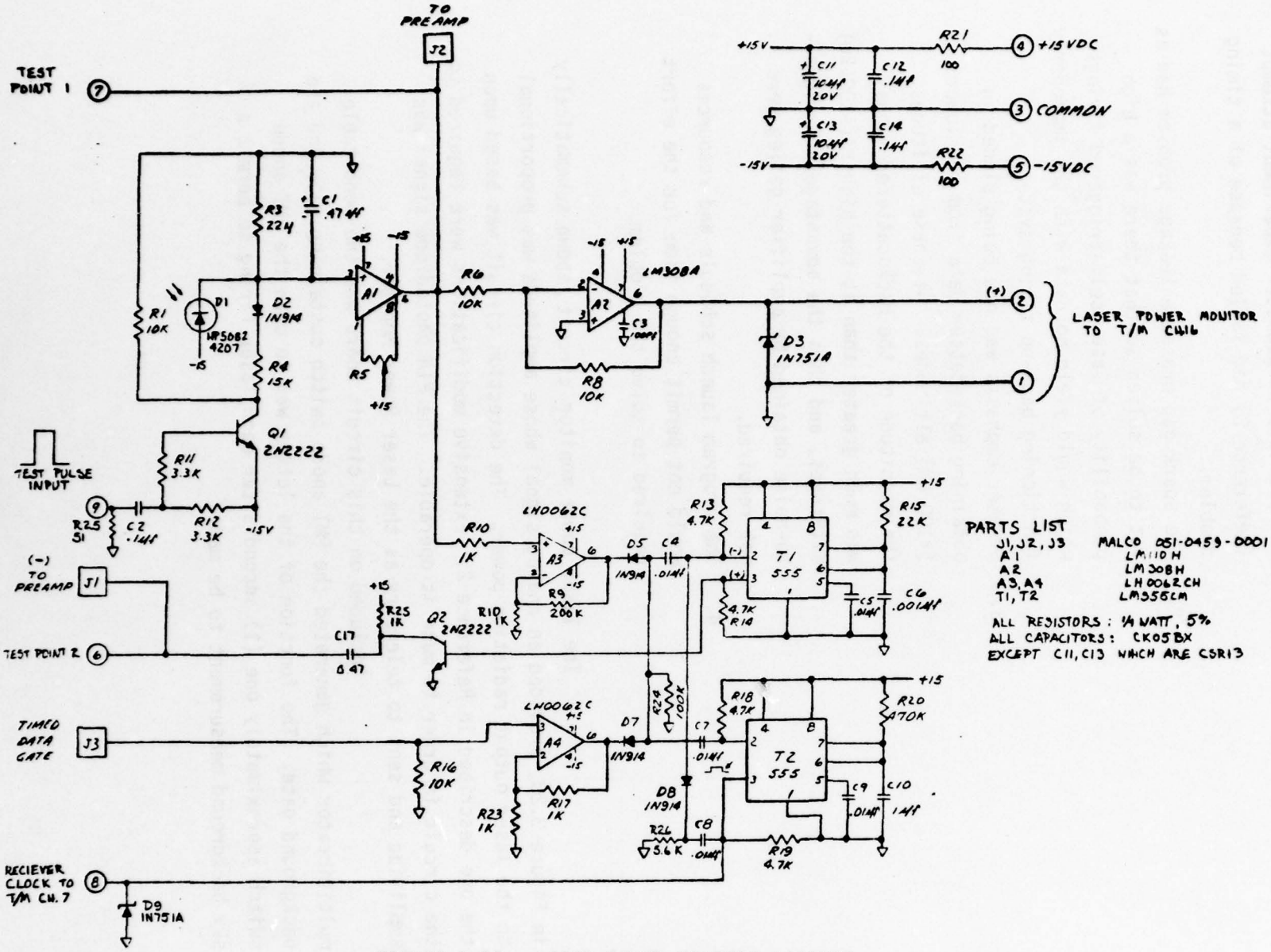

PARTS LIST

J1, J2, J3	MALCO 051-0459-0001
A1	LM110H
A2	LM308H
A3, A4	LH0062CH
T1, T2	LM355CM

ALL RESISTORS : ¼ WATT, 5%
ALL CAPACITORS : CK05BX
EXCEPT C11, C13 WHICH ARE CSR13

FIGURE 3.20 LASER POWER MONITOR CIRCUIT

Other components of the receiver electronics and their functions were the following:

1. Pressure and temperature monitor.
   To provide a telemetry monitor of receiver compartment temperature and absolute pressure.
2. Sensor Control.
   To provide power internal/external switching, battery charging circuitry, and voltage monitors.
3. ±15 VDC Power Supply.
   To provide a highly regulated dc voltage to all other receiver circuits.
4. High Voltage Power Supply.
   To provide the PMT high voltage (~2000 volts) bias.
5. +28 VDC Battery.
   A NiCd battery which provided all receiver power.

A major problem encountered in the receiver was in the packaging of the PMT sensor. Both the preamplifiers and the laser power monitor circuit boards were packaged in the PMT housing. Great difficulty was encountered in testing each of these circuits because of the high density packaging.

3.4 Ground Support Equipment

The GFE Ground Support Equipment was inspected and found to be not compatible with the modified payload.

A new Ground Support Equipment (GSE) (Figure 3.21) was designed and fabricated for use with the Laser Backscatter Experiment payload. The functions of this equipment were:

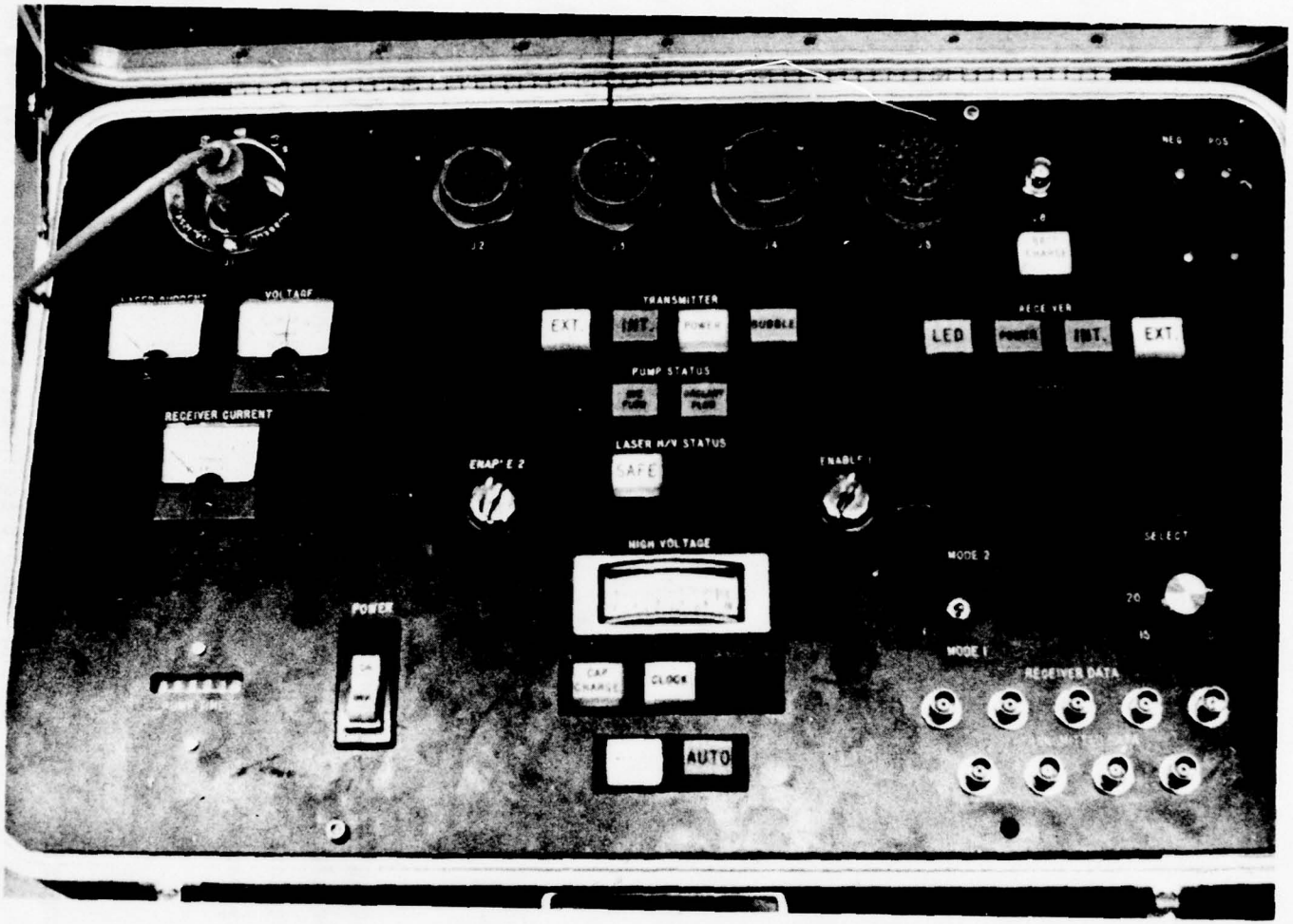

FIGURE 3.21 GROUND SUPPORT EQUIPMENT (GSE)

a. Laser Transmitter Test.
b. Receiver Test.
c. Payload System Test.
d. Experiment External Power and Timing Function Control through the Umbilical Laser and Receiver.
e. Laser and Receiver Battery Charge.
f. All Direct and Commutator Point Data Read-Out on a panel digital voltmeter (DVM).
g. Laser High Voltage ARM/SAFE Control.
h. Laser Firing Control.

The Ground Support Equipment fabricated for the Laser Backscatter Experiment was designed for maximum flexibility and utilization. Three modes of operation were possible with this GSE system as follows:

a. Laser Transmitter Module Interface.
In this mode, the GSE interfaced directly with the transmitter module. DC power was provided to the module while the GSE controlled the high voltage functions in the module. The power batteries were able to be charged in this mode. All diagnostic monitor data voltages could be read out on a panel digital voltmeter.

b. Receiver Module Interface.
In this mode, the GSE interfaced with the receiver and DC power from the GSE was supplied to the laser rocket payload. All of the direct telemetry channel data points could be monitored by the panel DVM as could each point of the commutator data. Payload timing pulses could be simulated by the GSE panel switch closure. These functions permitted the entire payload instrumentation to be checked out independent of the payload power and telemetry system.

c. Umbilical Interface.

In this mode, the GSE provided monitor and control functions of the payload through the umbilical cable. All these functions could be performed adjacent to the payload or between the blockhouse and the launch tower. These functions were:

1. Provide external 28 VDC to both receiver and laser transmitter.
2. Provide timing function simulation, set, and reset.
3. Provide ARM-SAFE control for the laser high voltage power supply. A meter readout provided a monitor of the high voltage status.

The GSE was provided with a two-key safety system to prevent accidental damage to the laser system. In this system, it was necessary for two keys to be inserted into the GSE panel key switches simultaneously for the laser high voltage power supply to be enabled and the laser fired. To eliminate inadvertent laser turn on, each of the project personnel had only a single key.

Safety procedures established for laboratory and field testing of the laser instrumentation are documented in Appendix F.

4.0 CALIBRATION

The laboratory calibration of the Laser Backscatter Experiment was designed to be a complete throughput test of the transmitter and receiver. This calibration required three separate tests, as follows:

a. Measure the laser radiant power output, using a calorimeter, as a function of the laser power monitor voltage.
b. Map the receiver sensor relative response as a function of distance along laser line of sight.
c. Measure receiver sensitivity (i.e., signal voltage) as a function of backscattered photon intensities at the receiver entrance pupil.

4.1 Laser Calibration

The absolute measurement of the laser radiant energy output was made using a calorimeter (Scientech, Inc., Model 36-0401). The calorimeter was positioned so that the laser beam was incident on the sensitive area. The observable drift on the calorimeter meter was manually zeroed and the laser was fired. Because of the time required for the calorimeter sensitive area to reach thermal equilibrium, the calorimeter meter reading was taken 10 seconds after the laser firing. The laser power monitor signal was displayed on an oscilloscope and photographed.

During laser calibration beam homogeneity was monitored using blue line Diazo paper (Charrette 2920, Speed 1). The paper was held over the laser output aperture, the laser fired, and the blue line paper developed. This provided a permanent record of beam homogeneity. From these measurements it became evident that the beam uniformity was subject to large variations during the first five shots of a rapid (1 shot/2.2 seconds) firing sequence. After this, spatial uniformity became established.

Lord Rayleigh's formula for the intensity, I, of scattered, unpolarized light in a direction making an angle, β, with the incident ray varies with β as:

$$I \propto (1 + \cos^2 \beta) \qquad (4\text{-}1)$$

Thus, the intensity is twice as great in the direction of the incident ray as in a direction perpendicular to it (Reference 7).

A test was performed to confirm that the radiating wavelength of the laser was within the passband of the receiver interference filter. The laser was fired into the calorimeter with the filter in the beam path. The calorimeter reading was then compared to the reading taken when the laser was fired without the filter in the path. Since the difference in the readings of the two shots was consistent with the filter peak transmission value, it was concluded that the laser was radiating at the proper wavelength.

4.2 Receiver Response vs. Distance

The response of the laser rocket receiver system as a function of distance along the laser beam axis, R (ℓ), was determined with the results shown on a linear plot in Figure 4.1 and a semi-log plot in Figure 4.2.

For this experiment, a replacement EMR PMT, operated as a photodiode, was mounted in the payload in place of the flight PMT and the payload was placed on its side. Using a Metrologic He-Ne laser and a beamsplitter cube, the laser signal was reflected off the rear mirror of the dye laser. By adjusting the payload, the axis of the laser beam was made parallel to the laboratory floor to within 2.6 minutes of arc, or less than one milliradian. With plumb lines, the position of the laser was marked on the laboratory floor. A high intensity light source, chopped and diffused with opal glass, was moved along the laser beam path out to a distance of 12 meters. The PMT signals were monitored on an oscilloscope.

4.3 Experiment Throughput

Visidyne, Inc. designed and implemented a new calibration procedure for use with the Laser Backscatter Experiment payload which provided a complete transmitter, receiver test, and, in addition, the receiver absolute sensitivity calibration factor was obtained.

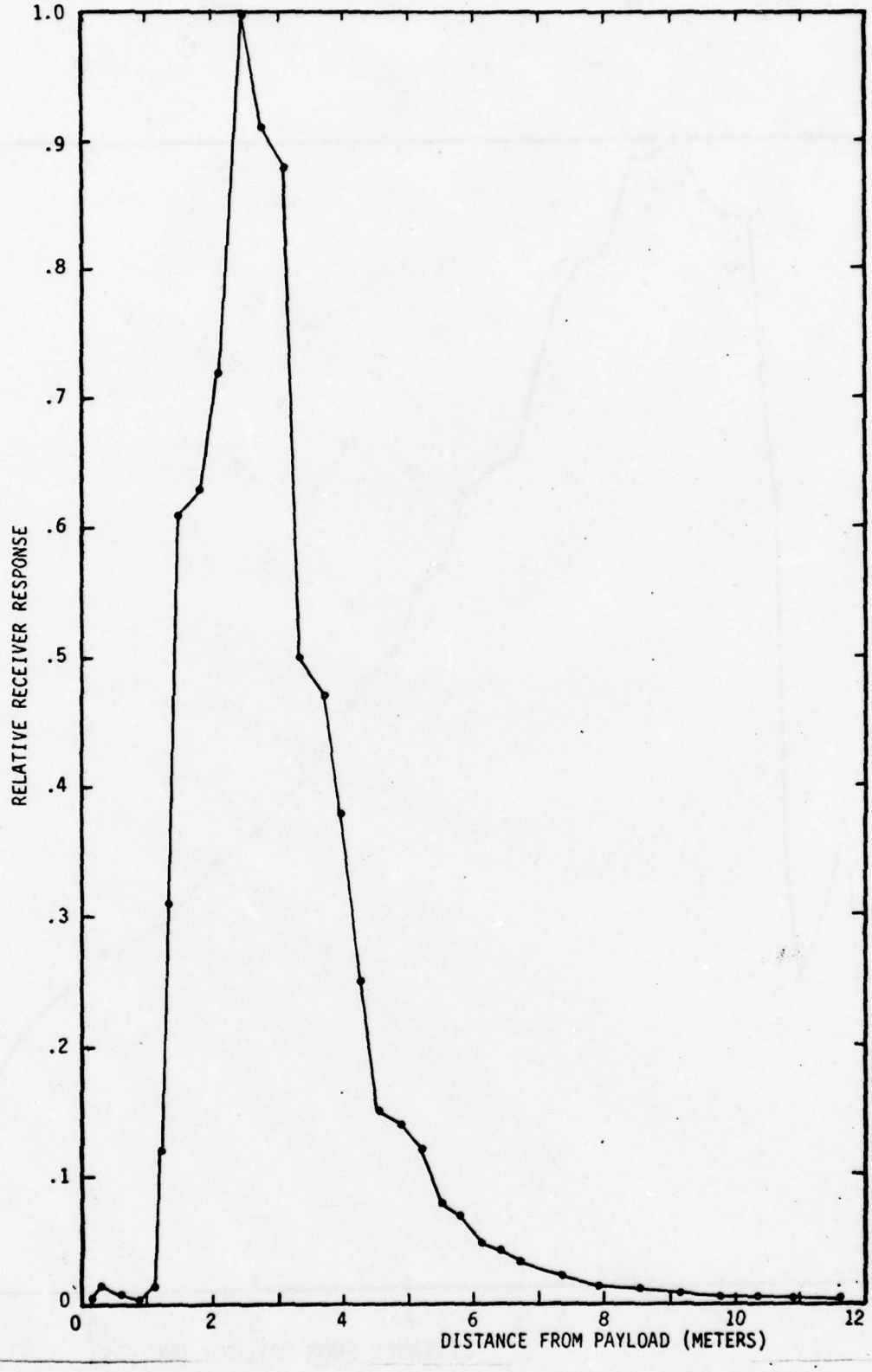

FIGURE 4.1: LASER ROCKET RECEIVER RESPONSE VS. DISTANCE ALONG LASER AXIS, LINEAR PLOT

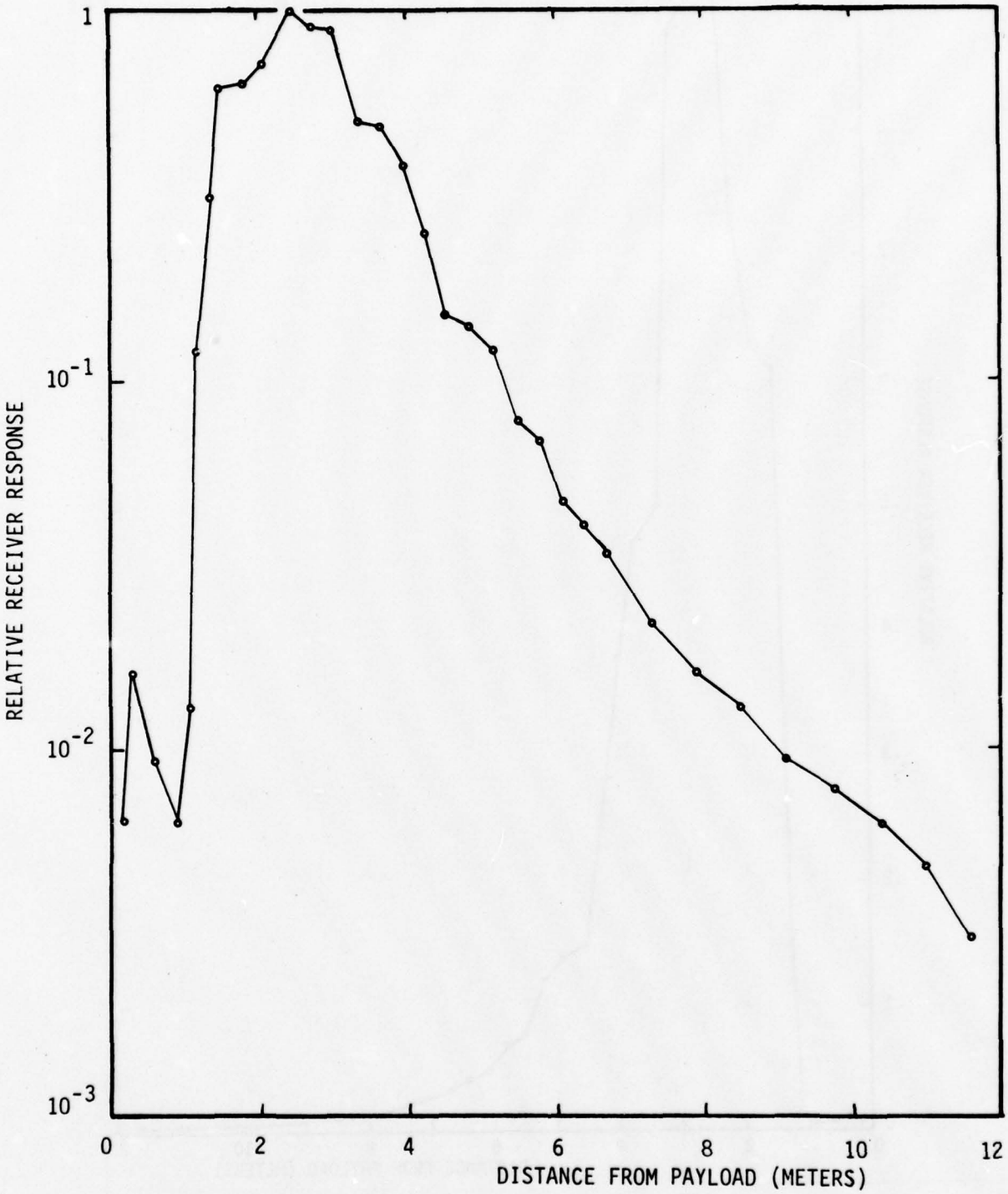

FIGURE 4.2 LASER ROCKET RECEIVER RESPONSE VS. DISTANCE ALONG LASER AXIS, LOGARITHMIC PLOT

A near ideal diffusing surface, made of Eastman White Reflectance Paint (Reference 6), was positioned in and normal to the laser beam path at a distance of 2.2 meters away from the payload. This distance corresponds to the point of maximum receiver response (reference Figure 4.1). When the laser was fired, the photon flux was incident on a screen which acted as a lambertian surface.

Because this backscattered flux was many orders of magnitude greater than that predicted to be observed during the flight, it was necessary to attenuate the received photon flux. A stack of Kodak Wratten N.D. 2.0 filters was mounted in front of the receiver relay lens (reference Figure 3.4) for this calibration. An attenuating factor of 10^{-8} was used for most of the calibration tests.

When the laser was fired, both the laser power monitor signal and one of the three analog data signals were displayed on an oscilloscope and photographed.

In summary, the receiver sensitivity constant:

$$K\ \{\text{photons/volt}\} = \frac{P}{\pi}\ \frac{A_c}{\ell_{cal}^2}\ \alpha\ \frac{1}{V_{cal}} \qquad (4\text{-}2)$$

where: P = number of photons radiated by the laser during a single pulse- determined from the laser power monitor data.

A_c = Receiver telescope collecting area = 700 cm^2.

ℓ_{cal} = Distance from defocusing screen to payload = 2.2 m.

α = Neutral density filter attenuation factor = 10^{-8}.

V_{cal} = Measured analog data voltage as referenced to the medium gain data voltage.

The receiver sensitivity constant, K, is then used to convert analog data voltages to corresponding density values through Equation 4-2.

An advantage of this calibration technique was that it was easily repeated at WSMR during the payload horizontal test. Thus, complete

experiment operational capability was fully demonstrated at the latest possible time prior to launch.

In addition and in conjunction with throughput testing, the payload was subjected to RFI and light leak testing. For these latter tests, the neutral density filters were completely blocked and the laser fired. The high gain data signals were monitored on an oscilloscope and no detectable signals were observed.

Another advantage of this calibration technique is that it includes and compensates for any timing, spectral, or optical geometry effects in the system.

The measured value of receiver sensitivity was found to be:

$$K = 2.5 \times 10^{6} \text{ photons/volt (medium gain).}$$

5.0 PAYLOAD INTEGRATION

The fully assembled experiment payload was delivered to AFGL during August 1977 for payload integration. The following integration tests were performed:

a. Mechanical Interface.
   The experiment section was mated to the telemetry can.

b. Electrical Interface.
   All interface and umbilical connectors were checked out and mated.

c. GSE Interface.
   The experiment GSE and telemetry GSE were used to operate the payload on both external and internal power.

d. Telemetry Transmission of Payload Data.
   The laser payload was operationally tested, including laser firing, while transmitting telemetry data. Data quality and channel assignments were checked.

e. RFI Test.
   No interference with payload or telemetry support systems were observed during laser firing.

f. Payload Timer Test.
   Payload timers were run and proper functional operation confirmed and actuation time measured.

g. Vibration Test.
   The payload was subjected to a longitudinal vibration test as specified for Aerobee 150 payloads (reference Appendix G). No vibrational problems were observed.

h. Payload Door Ejection Test.
   Proper payload door ejection was confirmed.

i. Payload Pressurization Test.
   The transmitter section, optics casting, and telemetry can were all pressurized to approximately 14 psig and the leakage rate monitored. In no case did the leakage rate

exceed 10 psi/10 minutes. The purpose of this test was to insure that excessive depressurization of either the receiver or transmitter did not compromise the high voltage reliability of either system.

Upon completion of this integration, the high voltage transformer failed. This failure caused the launch date to be rescheduled. A new transformer was designed, fabricated, and tested. It was subjected to a subassembly vibration test as specified in Appendix G.

In June 1978, the payload was delivered to AFGL where it again underwent the same series of integration tests. The tests were successfully completed.

This series of tests, with the exception of the vibration tests, was repeated during the horizontal payload testing at WSMR.

An inspection and cleaning of the receiver optics cavity was performed in a Class 100 clean area at AFGL prior to shipment of the payload to WSMR. The telescope optics were removed and their reflecting surfaces carefully rinsed with Freon TF. The cavity was inspected for dust particles by using a high intensity ultraviolet lamp which caused them to fluoresce. They were then removed with a combination of microdusters and vacuuming. The optics were then reinstalled and the payload sealed. The inspection procedure was repeated in the field prior to launch. The entire external surface of the payload was also washed off with Freon TF before being sealed in Velostat and transported to the launch tower from the vehicle assembly building.

6.0 LAUNCH SUPPORT

The field trip to launch the laser rocket was during the period from July 17 to July 26, 1978. Three of the appendices of this report are concerned with this phase of the contract. Appendix H gives the field schedule, Appendix J is a copy of the completed preflight conference form, and Appendix K is the launch countdown. Figure 6.1 shows the assembled payload in the Vehicle Assembly Building (VAB), Launch Complex 36 at White Sands Missile Range and Figure 6.2 is a photograph of Launch Tower A, Launch Complex 35. The azimuthal positioning of the rocket is shown in Figure 6.3.

The schedule in Appendix H was adhered to closely with a few minor exceptions as follows:

1. The laboratory set-up did not begin until Tuesday because the area was closed for a rocket launch.
2. A change in the timing sequence required an extra disassembly of the telemetry section.
3. The payload was taken to the launch tower on Saturday. The final bubble check revealed one bubble in the laser cavity. The ogive skin was raised so the laser could be dismounted and tilted to remove this bubble. At this point, a rare shower suddenly struck and the rain started to leak through the launch tower enclosure on to the transmitter section of the open payload. At this time, the payload skin was replaced and all openings in the payload were covered with velostat. The following morning, the payload skin was removed and the transmitter section was inspected. No evidence of moisture was found anywhere within the transmitter section. The payload was reassembled and dry nitrogen gas flushed through the forward section of the payload for approximately the next 40 hours.

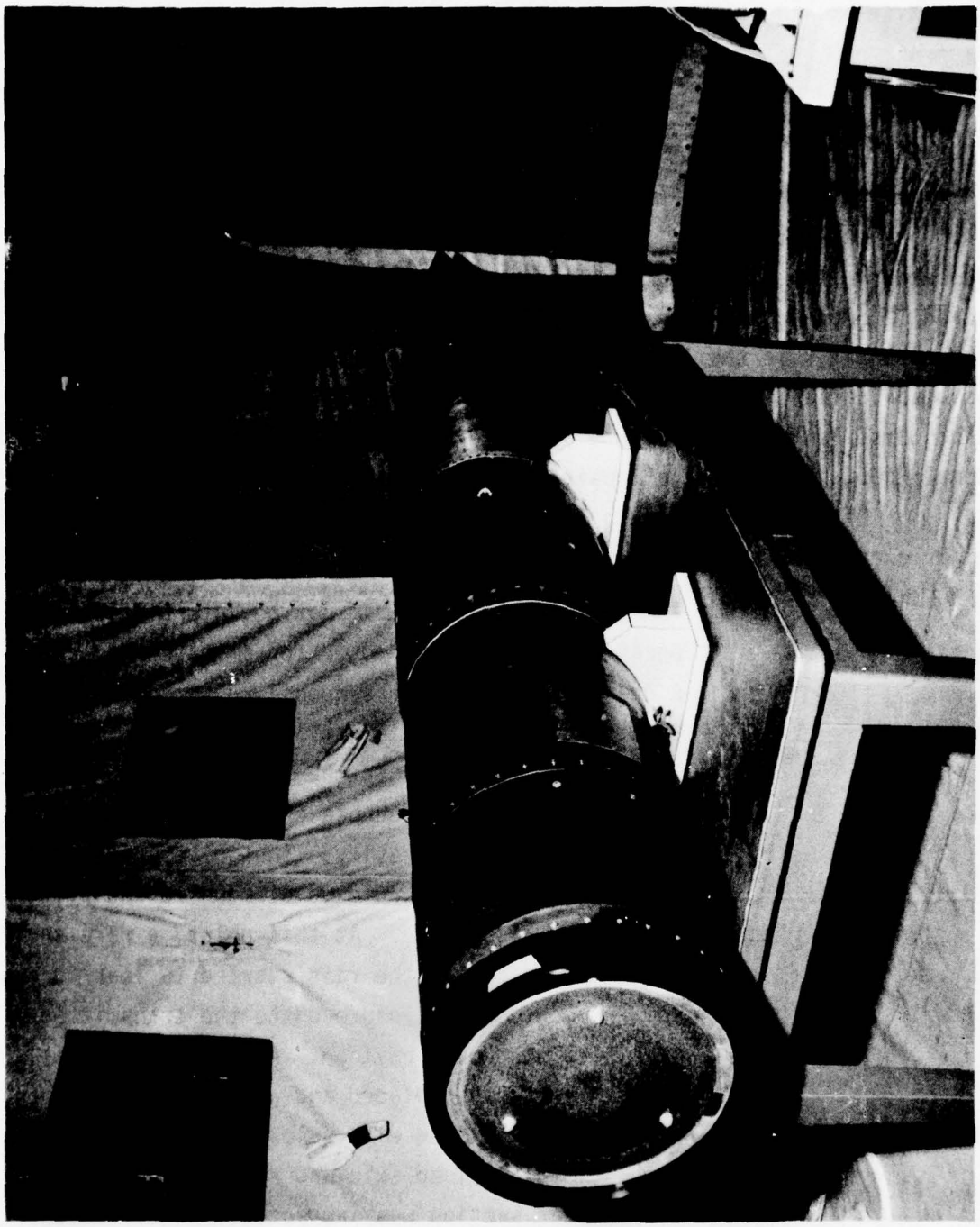

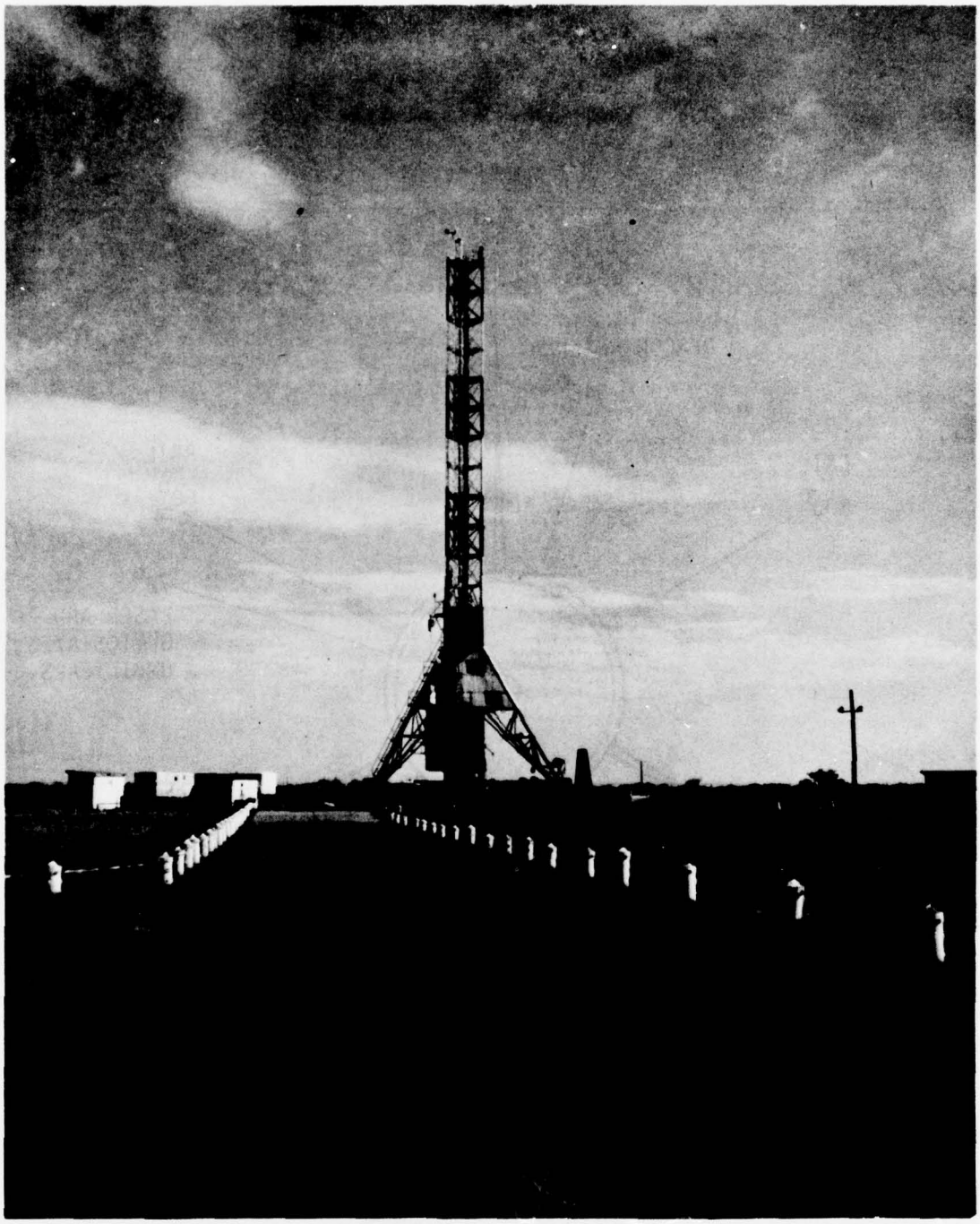

FIGURE 6.2 LAUNCH TOWER A, LAUNCH COMPLEX 35, WSMR

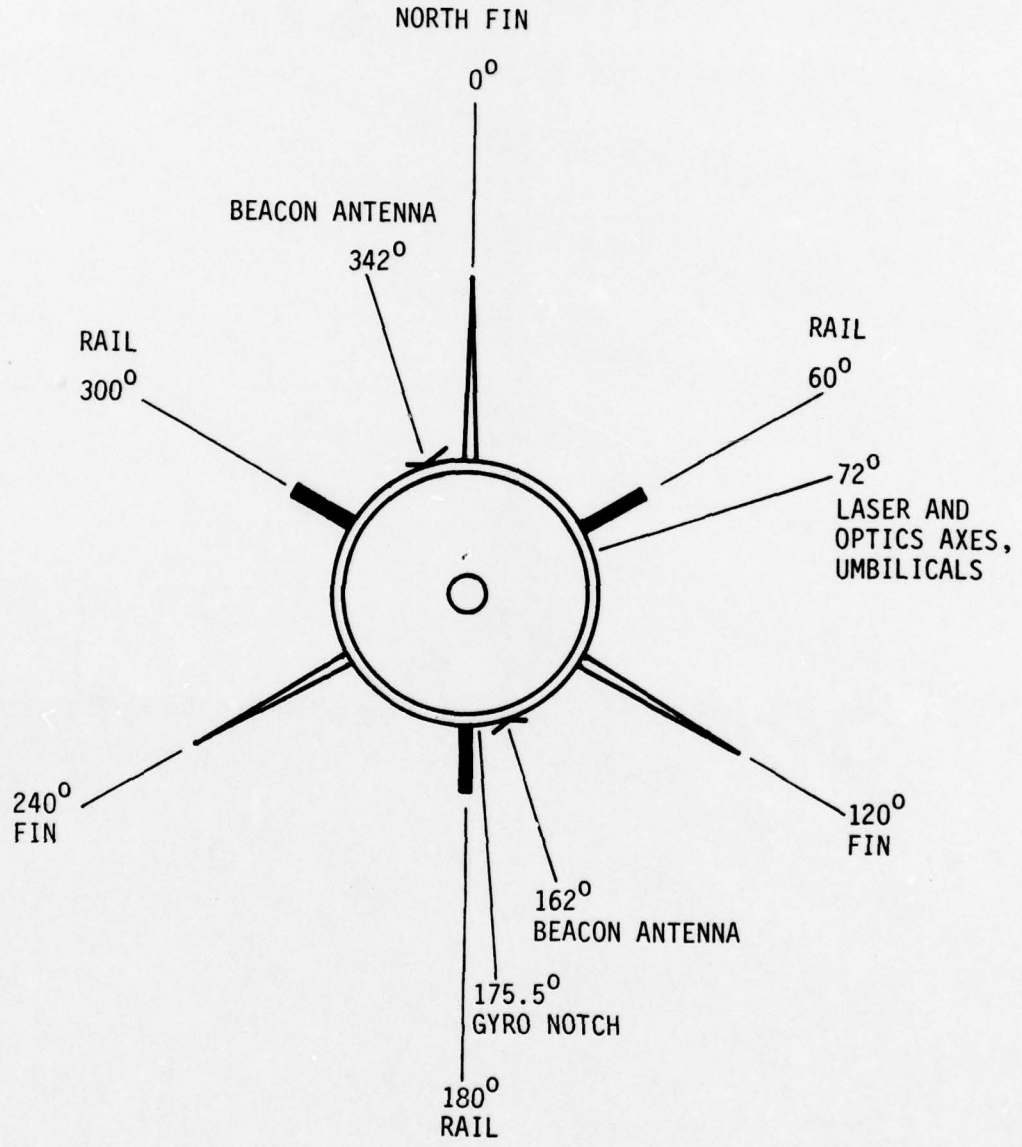

FIGURE 6.3 ROCKET A03.604, AZIMUTHAL LOCATIONS

Launch took place as scheduled at 2205 hours on July 24, 1978. The launch tower settings were 84.1^{o} elevation and 332.5^{o} azimuth. The rocket trajectory is shown in Figure 6.4 and its track on a map of the region is shown in Figure 6.5. All phases of the launch programming went essentially as planned. The apogee (143.8 km) was slightly lower than expected and the winds that were expected to have blown the parachute-borne payload to the east failed to materialize with the result that the payload touched down in the San Andres Mountains near Skillet Knob. Fortunately, the payload came to rest at a place that was fairly accessible to the recovery helicopter team the next morning.

Examination of the payload showed no leakage of either laser dye or coolant and damage to be minimal, as follows:

1. The nose tip was broken off and lost.
2. The six screws holding the laser to the receiver casting (magnesium alloy) had all pulled out. (No Helicoil inserts were used in these particular screw holes.)
3. The ogive skin was dented out by the motion of the internal structure.
4. The monitor fiber optics inside the open receiver optics cavity had been buffeted to the point of disintegration.

Further discussion can be found in Section 7.1.

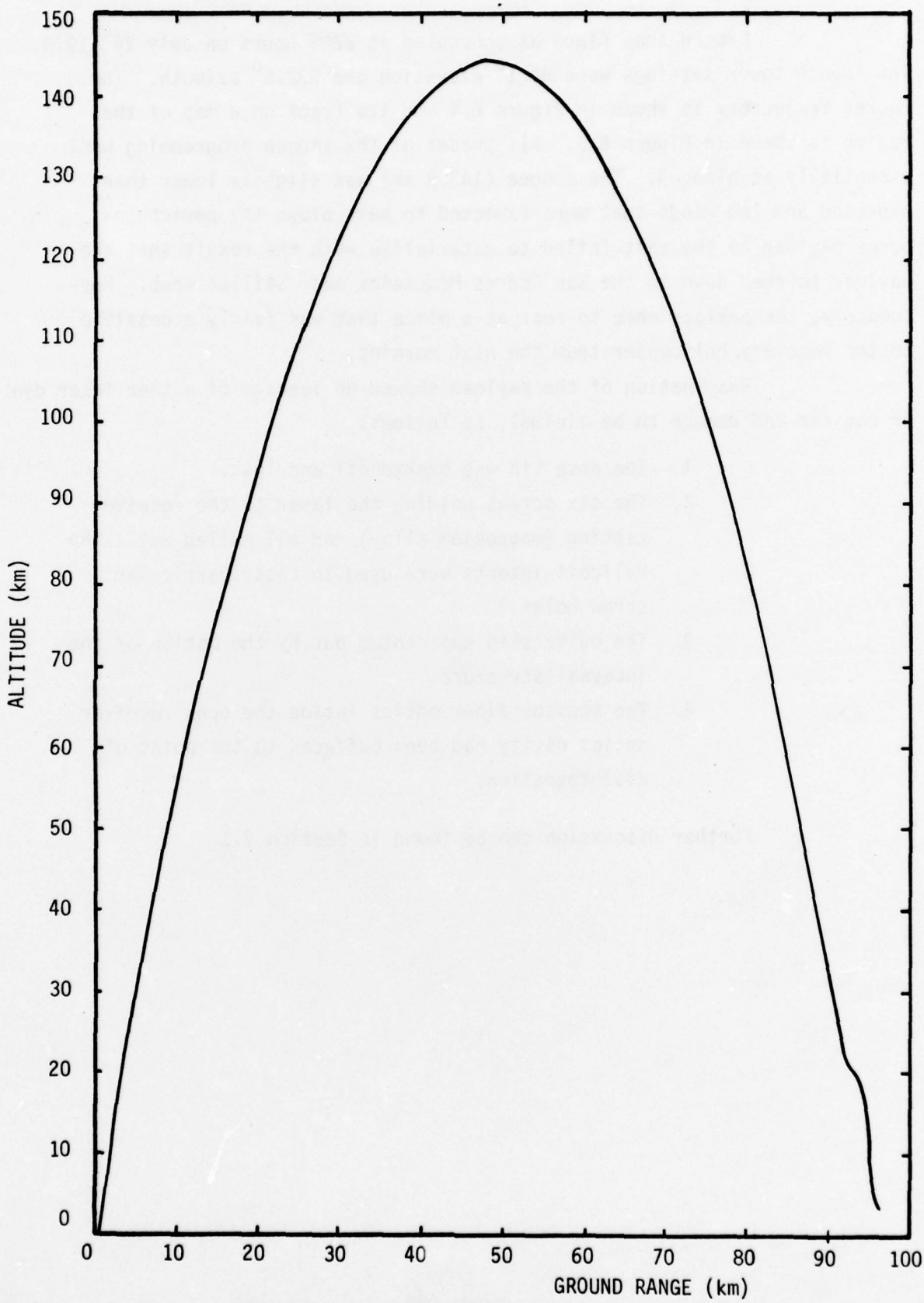

FIGURE 6.4 ROCKET A03.604 TRAJECTORY

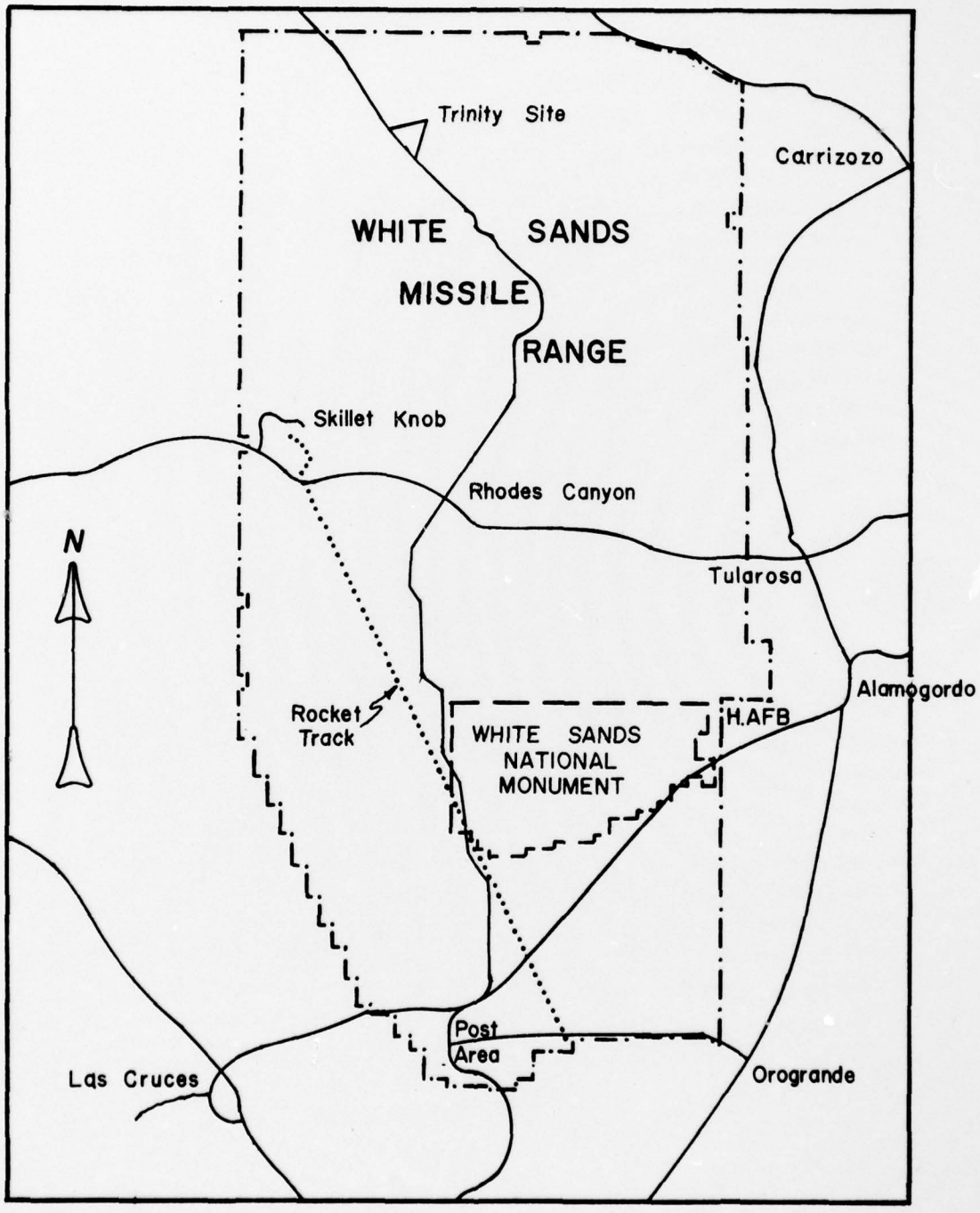

FIGURE 6.5 MAP OF WHITE SANDS MISSILE RANGE SHOWING TRACK OF ROCKET A03.604

7.0 POST FLIGHT ENGINEERING EVALUATION

7.1 Instrumentation

The recovered payload was packed and shipped from WSMR to AFGL without internally inspecting the payload. Later on in August 1978, the payload was unpacked and inspected. The results of this inspection were as follows:

1. The transmitter skin had been dented from the inside. This was caused by the laser transmitter structure partially stripping its hold down screws out of the tapped holes in magnesium optical casting. The six screws which mounted the laser housing to the casting were also completely stripped from their tapped holes. These screws were found loose in the payload when it was first opened. The loosening of these screws permitted the laser mounting structure to impact with the skin and form various dents. One of the laser end mirror clamps was bent and the spark gap pressurization tubing was deformed.

   It should be noted that all of these tapped holes which failed in the casting were installed prior to the current effort. The additional tapped holes which were installed during this phase of the program all had Helicoil inserts.

   The probable cause of this stripping was that g forces in excess of those specified for the Aerobee 150 payload were encountered during recovery parachute opening or ground impact.
2. The 28 VDC High Current Battery which provided power for the laser high voltage power supply was found to be completely discharged. This was

unexpected because since the laser had not operated during the flight, the battery had essentially not been loaded. In addition, the laser high voltage was shut-off by the payload timers at T+375 seconds. This shut-off was confirmed by a telemetry monitor. After considerable testing and investigation, the only reasonable explanation is that the same high "g" shock caused a magnetic latching relay to change status and thus turn the laser high voltage power on. Even though it was inoperable, the laser power supply would had drawn sufficient current to run down the battery over a period of several days.

Electrical testing at AFGL, using the GSE, confirmed proper operation of all experiment functions except for the laser high voltage power supply. It was observed that upon actuation, the high voltage supply would turn on, and when the capacitor voltage exceeded 1 kv (approximately), the driver circuit for the supply was shut off. The circuit remained off until the capacitor high voltage dropped below 500 volts (approximately) when this cycle would be repeated.

Diagnostic testing showed that this operation was being caused by a shorted OVP (over voltage protection) diode in the high voltage shut-off circuit. The purpose of this circuit is to prevent the high voltage capacitor voltage from exceeding the rated voltage of the capacitor. A schematic of the OVP circuit is in Figure 7.1. The shorted diode was removed from the circuit and replaced. Proper operation of the high voltage power supply and trigger circuits were confirmed.

The faulty diode was sent to Assurance Technology, Inc., Carlisle, Massachusetts for a comprehensive failure analysis. The complete failure analysis report is in Appendix L. The conclusion of this report is that the diode was damaged by excessive current.

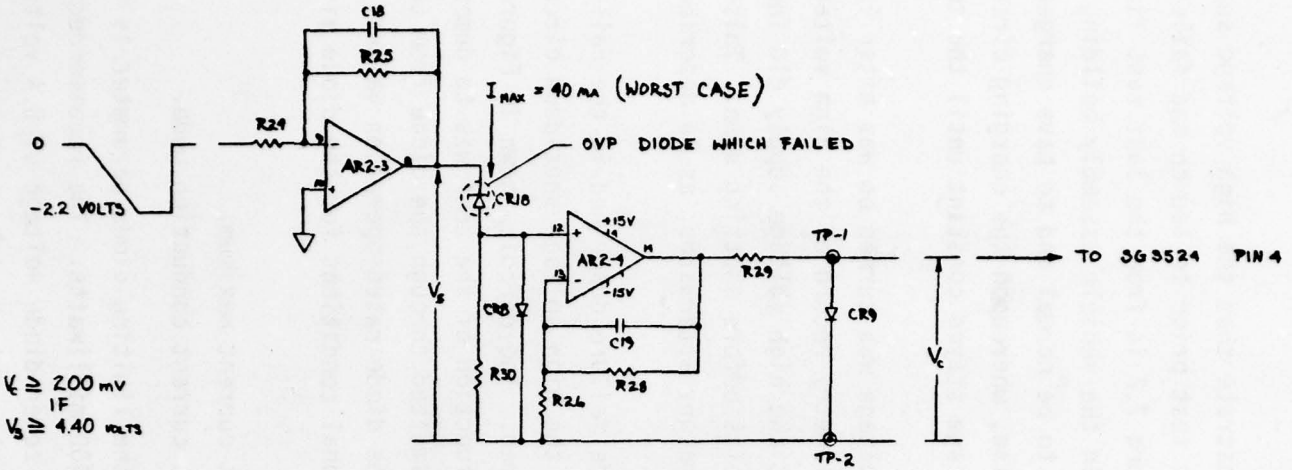

REF. DWG. 645-807

PARTS LIST		
ITEM	SYM	TYPE
1	R24	5.1 K ¼ WATT 5%
2	R25	11 K
3	R26	60K
4	R28	1K
5	R29	1K
6	R30	10K ¼ WATT 5%
8	CR8	1N914
9	CR9	1N645
10	CR18	1N751A
11	C18	0.1 CK05BX105
12	C19	0.1 CK05BX105
13	AR2-3	1/4 HA4741-5
14	AR2-4	1/4 HA4741-5

FIGURE 7.1 OVER VOLTAGE PROTECTION CIRCUIT

Figures 7.2 and 7.3 demonstrate that the high voltage supply was operating properly through the last test prior to launch and failed to operate properly after launch. Figure 7.2 is from the last test firing series of the laser, which took place in the vehicle assembly building at WSMR. The high voltage supply appears to be normal and to have charged up to 11.5 kv following the last laser pulse, whereupon the charging circuit was manually turned off. The high voltage stayed constant until the test was ended.

The next time the high voltage was turned on was after launch at T+90 seconds. Figure 7.3 is the telemetry record of the high voltage monitor at that instant. It shows that the high voltage supply did indeed turn on but reached only about 1,000 volts before shutting down. This malfunction was duplicated in the laboratory afterwards, as is described elsewhere in this report.

To determine how the diode failure described in the Failure Analysis Report could have occurred in the high voltage shut-down circuit, a "worst case" circuit test was performed. The circuit shown in Figure 7.4 was assembled and power applied. The function of the test was to demonstrate that the absolute maximum current transmitted through the diode from the amplifier was signifiently less than the diode rated operation values.

The "worst case" operational conditions for the diode within the circuit were as follows:

1. Amplifier output current maximum.
2. Diode in reverse current conduction mode.

Under these conditions, the limiting diode parameter is the power dissipation P_d (T+25C) which is 400 milliwatts. The recommended maximum reverse current of 40 ma and a zener diode voltage of 5.4 volts yield a maximum 220 milliwatt power level. This "worst case" test was run for 36 hours and no degradation was observed.

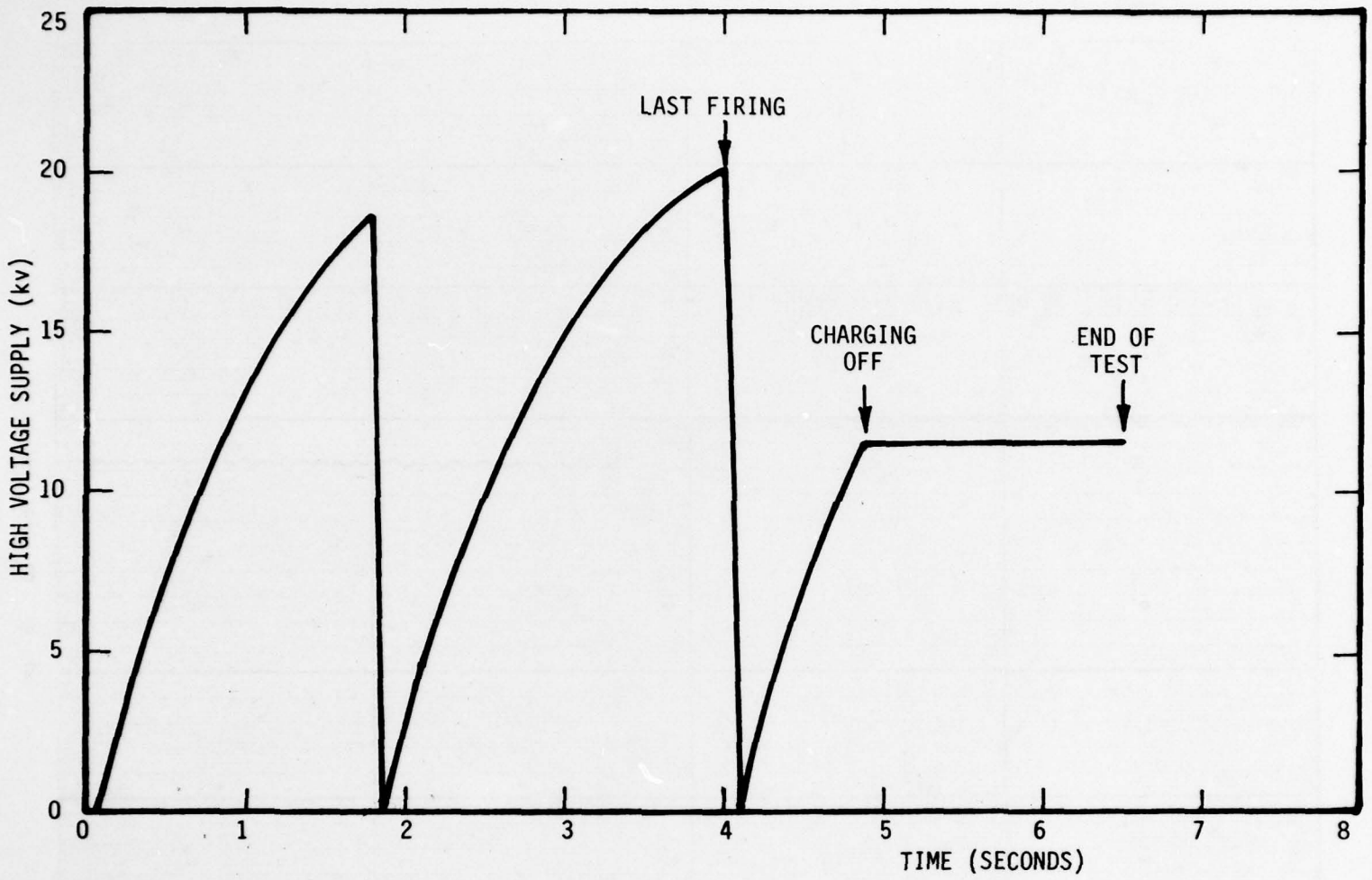

FIGURE 7.2 HIGH VOLTAGE SUPPLY MONITOR FROM TELEMETRY RECORDS OF LAST FIRING TEST PRIOR TO LAUNCH

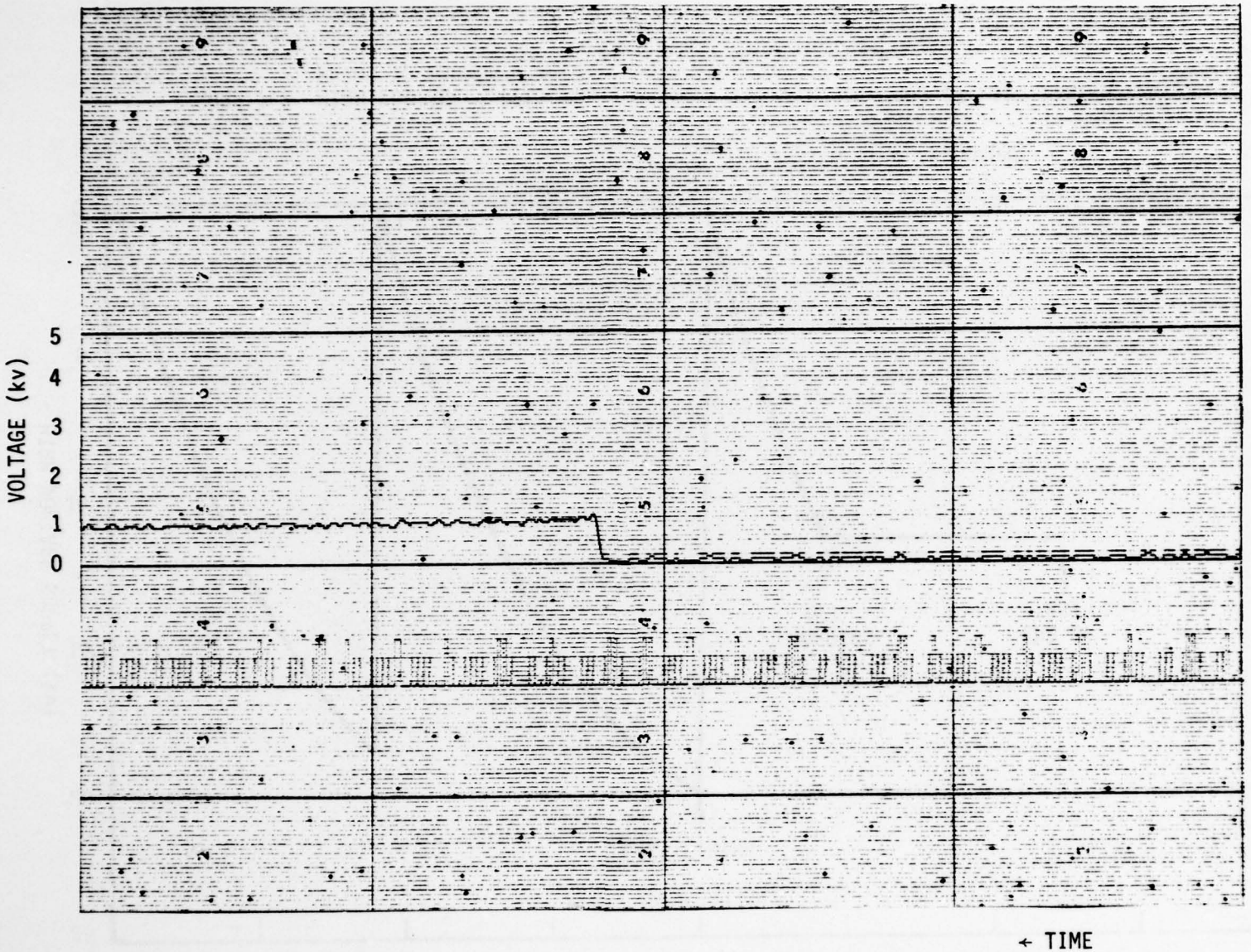

FIGURE 7.3 TELEMETRY RECORD OF HIGH VOLTAGE MONITOR, FIRST TURN-ON AFTER LAUNCH AT T+90 SECONDS

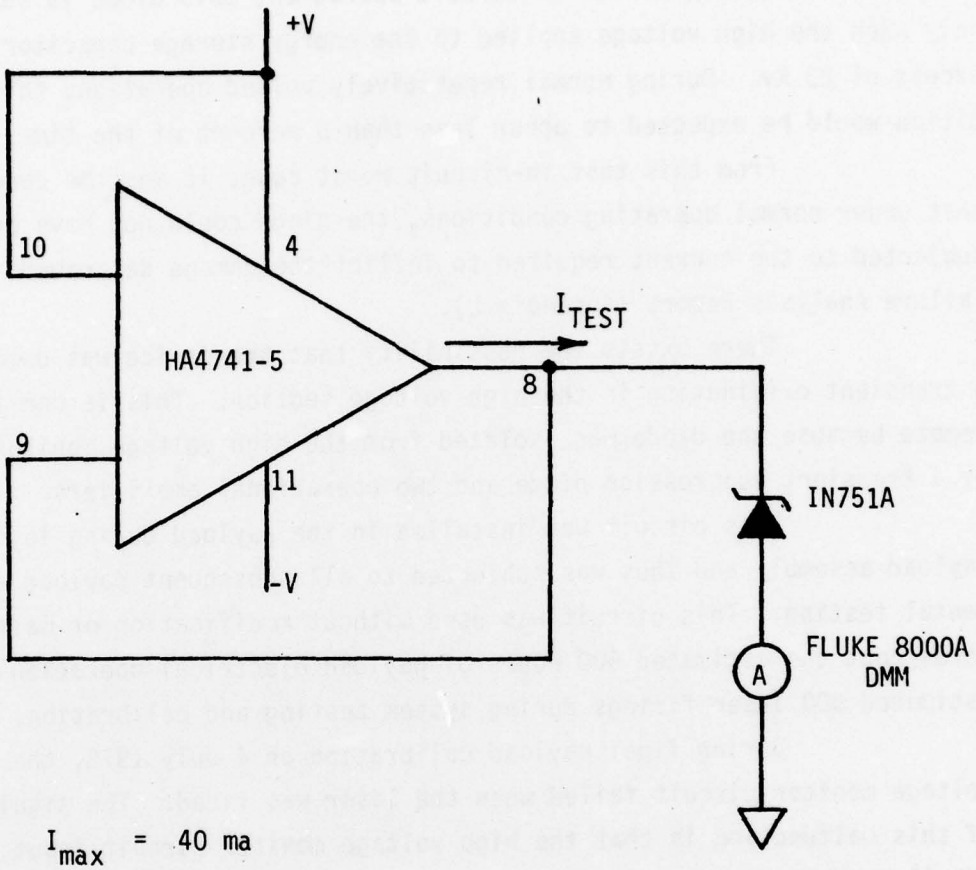

I_{max} = 40 ma

TEST DURATION = 36 HOURS

FIGURE 7.4 HIGH VOLTAGE POWER SUPPLY OVERVOLTAGE PROTECTION CIRCUIT, WORST CASE TEST CONFIGURATION

During normal in-circuit operation, this diode is conducting only when the high voltage applied to the energy storage capacitor is in excess of 23 kv. During normal repetitively pulsed operation, this condition would be expected to occur less than 5 percent of the time.

From this test in-circuit worst case, it must be concluded that under normal operating conditions, the diode could not have been subjected to the current required to inflict the damage described in the Failure Analysis Report (Appendix L).

There exists the possibility that the device was damaged by a transient originating in the high voltage section. This is considered remote because the diode was isolated from the high voltage monitor input by a transient suppression diode and two operational amplifiers.

This circuit was installed in the payload during initial payload assembly and thus was subjected to all subsequent payload environmental testing. This circuit was used without modification or malfunction throughout the estimated 500 hours of payload electrical operation and an estimated 500 laser firings during system testing and calibration.

During final payload calibration on 4 July 1978, the high voltage monitor circuit failed when the laser was fired. The significance of this malfunction is that the high voltage monitor circuit input, the OVP (Over-Voltage Protection) circuit, and the OVP operational amplifier are on the same chip as the high voltage monitor operational amplifier (a quad operational amplifier was used to conserve circuitry area). Since the maximum current through the OVP zener diode is limited by an amplifier on this chip, it is possible that when this chip failed, excessive current was conducted by the OVP diode so that partial destruction of the junction occurred at this time.

The quad operational amplifier was replaced and proper system operation was confirmed through a subsequent 28 laser firings. On 5 July, 1978, the payload was packed and shipped to WSMR in preparation for launch. An additional 16 laser firings were performed at WSMR.

The component printed circuit board upon which the OVP circuit was located was subjected to considerable rework. The reason for these modifications was that to make the original launch schedule, it was required that this printed circuit be designed using a preliminary schematic. Subsequent testing indicated that certain design changes were required. An inherent constraint to all of these changes was that they conform as closely as possible to the preliminary printed circuitry. It was such a constraint that defined the OVP circuit configuration discussed herein. The circuit might be described as unelegant while functionally adequate. It is not evident that this reworked circuitry contributed to the OVP diode failure.

At the time of the engineering evaluation testing of the payload, it was not possible to follow up the determination of an OVP zener diode failure with a complete set of payload electrical documentations. Because of limited program resources, the mechanical and electrical documentation updating throughout the program were maintained solely by the project engineer as a single set of unreproductable marked-up drawings and a laboratory notebook. It is an objective of this report to formalize the relevant sections of this engineering documentation package.

The conclusions of this failure analysis are the following:

1. The OVP diode did not fail because of a faulty circuit design.
2. The OVP diode did not fail because of inadequate system testing.
3. Had the OVP diode been partially damaged during final system testing, such damage would not have been detected nor corrected with the control procedures in force at the time.

4. The OVP circuit was shown to be operational during the last scheduled high voltage test performed at WSMR during the payload horizontal tests. Thus, the diode failure occurred at some time between the horizontal tests and cessation of the in-flight high voltage operation which occurred approximately 0.5 seconds after high voltage turn-on.
5. The cause of the OVP diode failure has not been determined, and it is unlikely that additional investigation or measurements would provide greater understanding of the failure in question.

7.2 Measurements

The telemetry worked well and sent back good data on all channels. Unfortunately, the laser itself never did turn on for the reasons discussed earlier in this section so that no atmospheric density information was provided by the laser rocket experiment. However, the telemetry did return some surprising background data, an example of which is shown in Figure 7.5. These data are characterized by the following:

1. The brightness is orders of magnitude greater than the values predicted for the night sky.
2. The background signal is clearly periodic with the rocket spin.
3. The leading edge of the background signal, as can be seen in Figure 7.5, is not an abrupt rise, which is typical throughout the data taking period.

The conclusions to be drawn from the above are discussed in the following section.

7.3 Evaluation of Background Data

We have conducted a rather detailed and lengthy attempt to determine an explanation of the unexpected background signals. Of great

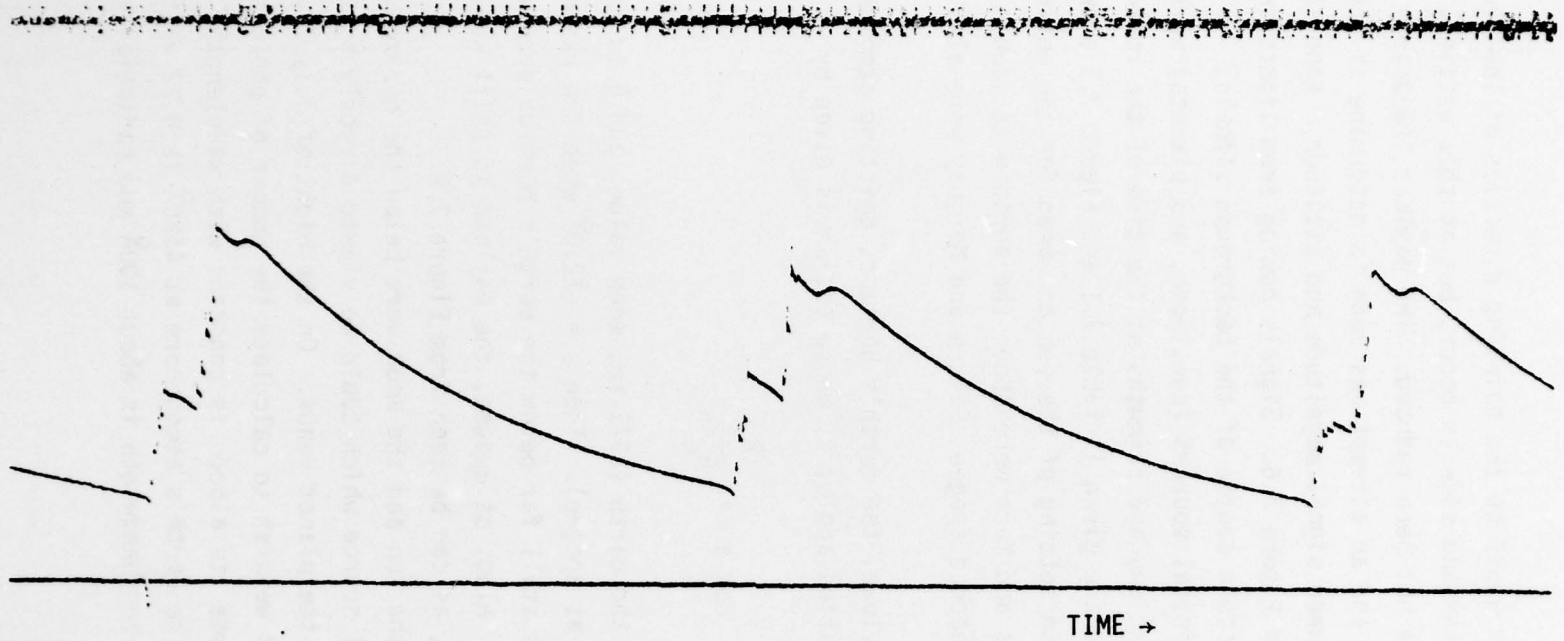

FIGURE 7.5 LASER ROCKET RECEIVER BACKGROUND SIGNALS AT T+265 SECONDS

importance to this attempt would be the pointing direction of the receiver axis at the times the background signals occur, but at this writing, the payload attitude data have not been reduced. The payload trajectory has been determined, however, and an attempt was made to determine if there were any relationship between signal magnitude and altitude. None is apparent from the plots in Figure 7.6. Signals coming from lights on the ground are also a possible source of the background signals.

Natural celestial sources (sun, moon, and planets) were investigated. Their elevations and azimuths at the time of the rocket launch were determined and are given in Table 7.1 and Figure 7.7 shows the times of the rising and setting of the sun and moon for the entire launch window. Only Venus and Mars were above the horizon at launch, but by the time the payload reached apogee, Saturn and Mercury were also above the horizon.

From the payload, the earth's horizon, omitting atmospheric refraction, is at an elevation angle, θ, whose cosine is given by

$$\cos \theta = \frac{R_e}{R_e+h}$$

where R_e is the radius of the earth (6371 km, mean value) and h is the rocket altitude (143.8 km at apogee). Then $\theta = -12.0^o$ when the payload is at apogee. The moon is still far below the earth's horizon even when the payload is at apogee. Also, at apogee, the payload is still well within the earth's shadow, as can be seen from Figure 7.8.

Since both the sun and the moon were below the horizon, the brightest astronomical source which could be viewed directly by the laser rocket receiver was the planet Venus. On the night of July 24, 1978, its magnitude was -3.7 and we wish to calculate the number of photons per second collected. We assume its albedo is constant with wavelength. The solar irradiance outside the earth's atmosphere at 4580Å is 0.22 watts/m^2-Å[8]. The receiver filter bandwidth is about 100Å and radiation at

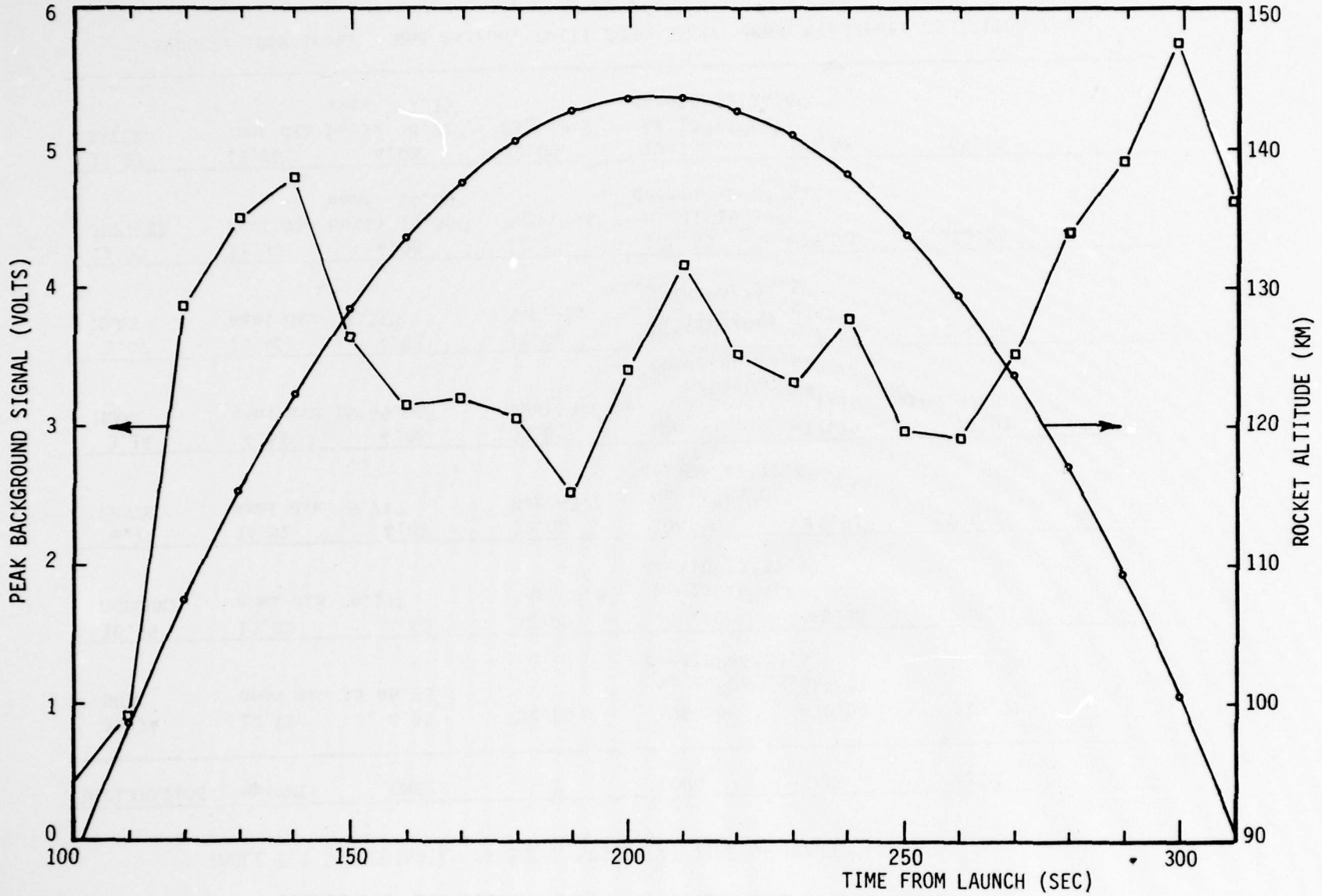

FIGURE 7.6 BACKGROUND SIGNAL AND ROCKET ALTITUDE VS. TIME

TABLE 7.1 COORDINATES OF SOLAR SYSTEM AT TIME OF ROCKET LAUNCH

DECLINATION	mp(GMT)	GMT	LAT	LONG	ELEV	AZIM
19.74	12.11	4.08	32.80	106.50	-20.92	312.57
SUN	semi dia 15 46.33"			mp $12^h06^m26.44^s$		
				dec+19°44'33.8"		
10.55	13.83	4.08	32.80	106.50	-8.38	288.37
MERCURY	semi dia 4.11"		Mag +0.8	mp $13^h49^m36^s$		
				dec+10°32'57.9"		
6.79	14.92	4.08	32.80	106.50	2.91	276.19
VENUS	semi dia 8.74"		Mag -3.7	mp $14^h55^m06^s$		
				dec+06°47'12.6"		
3.14	4.55	4.08	32.80	106.50	-17.79	74.01
MOON	semi dia 15'49.00"		age:19.8days	Fraction Illuminated:0.68		
				mp $04^h32^m47.4^s$		
				dec+03°08'12.82"		
3.07	15.45	4.08	32.80	106.50	7.58	268.76
MARS	semi dia 2.31"		Mag +1.7	mp $15^h26^m52.3^s$		
				dec+03°04'24.5"		
21.95	11.33	4.08	32.80	106.50	-25.73	323.54
JUPITER	semi dia horiz 15.86"		Mag -1.4	mp $11^h19^m59"$		
	vert 14.80"			dec+21°56'47.63"		
12.37	13.96	4.08	32.80	106.50	-5.48	289.15
SATURN	semi dia horiz 8.21"		Mag +0.9	mp $13^h57^m44^s$		
	vert 7.35"			dec+12°52'24.4"		

SUNSET: 1859 local End Astron, Twil: 2030 local MOON Rise/Set: 2257/1104 local

AD-A073 853 VISIDYNE INC BURLINGTON MASS F/G 20/6
ROCKETBORNE LASER BACKSCATTER EXPERIMENT.(U)
MAR 79 O SHEPHERD, A G HURD, W H SHEEHAN F19628-76-C-0253
UNCLASSIFIED VI-475 AFGL-TR-79-0081 NL

2 OF 2
AD
A073853

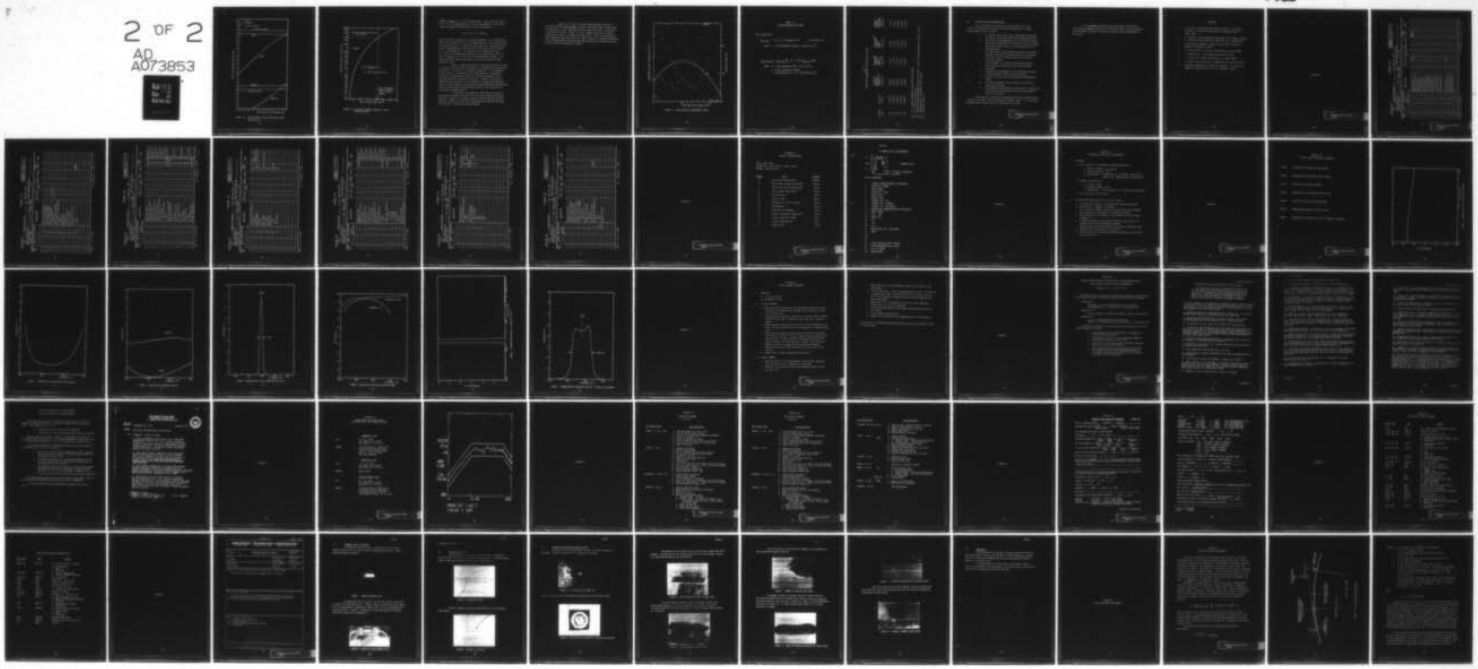

END
DATE
FILMED
10-79
DDC

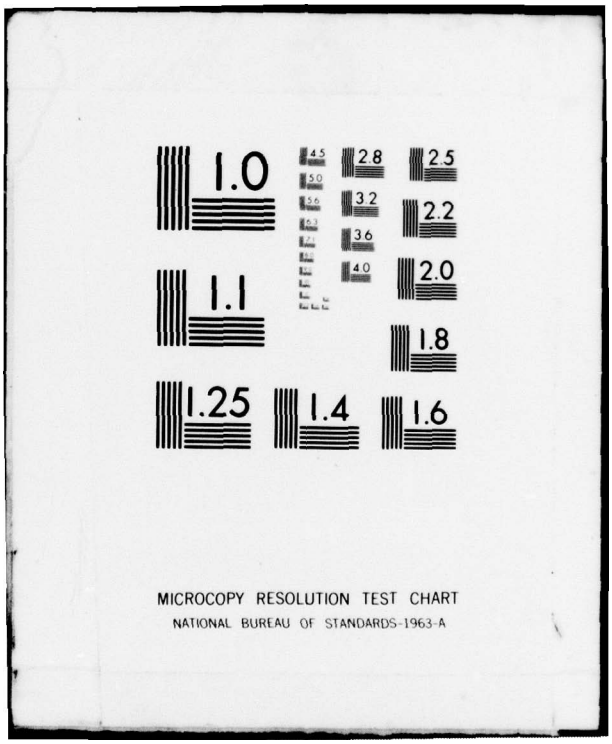
1.0
1.1
1.25
1.4
1.6
1.8
2.0
2.2
2.5
2.8
3.2
3.6
4.0
4.5
5.0
5.6
6.3
MICROCOPY RESOLUTION TEST CHART
NATIONAL BUREAU OF STANDARDS-1963-A

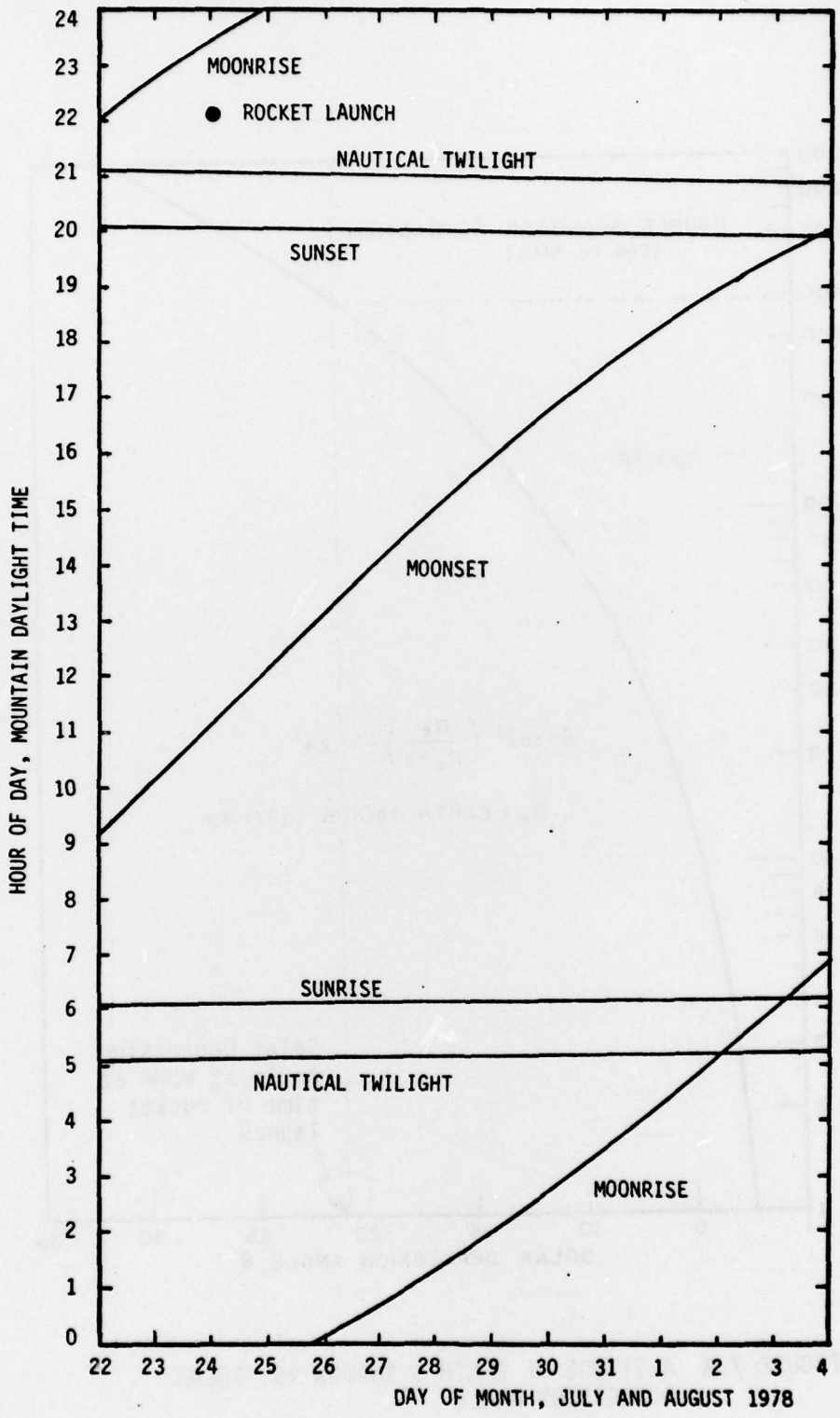

FIGURE 7.7: SUN AND MOON RISINGS AND SETTINGS DURING LAUNCH PERIOD.

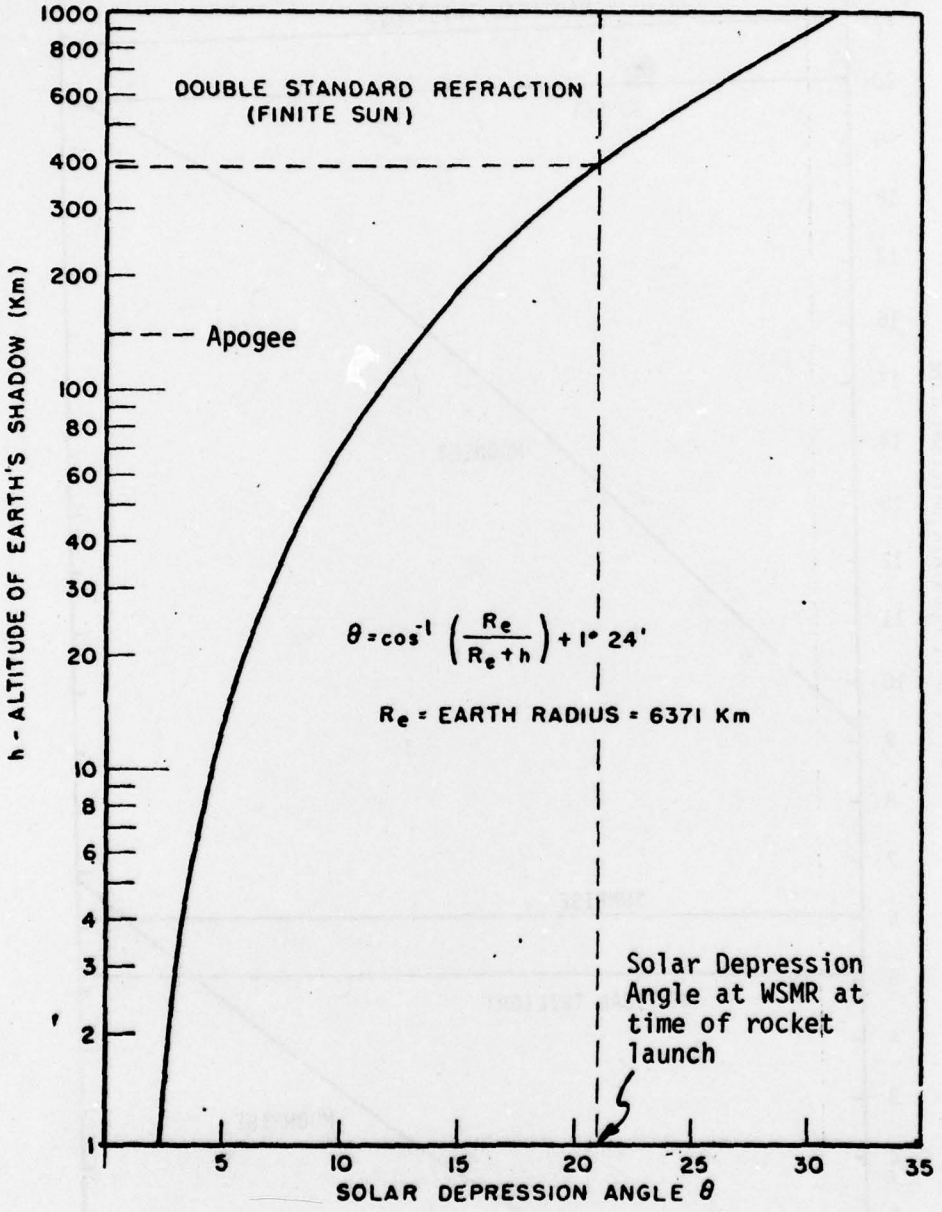

FIGURE 7.8 ALTITUDE OF EARTH'S SHADOW VS. SOLAR DEPRESSION ANGLE

4580Å corresponds to 2.2×10^{18} photons/joule. Thus, the solar photon flux is 5×10^{15} photons/cm^2-sec. The solar magnitude is -26.8, and by using the equation defining magnitude, M, from intensity, I,

$$\log \{I_1/I_2\} = -0.4 \ (M_1-M_2)$$

then, the ratio of intensities of the Sun to Venus is 1.7×10^9 and the photon flux from Venus is 2.9×10^6 photons/cm^2-sec. The collecting area of the receiver optics is essentially the area of the primary minus the area of the secondary, or about 700 cm^2, so that the signal from Venus is 2.1×10^9 photons/sec. The data amplifier integration time of 6.8×10^{-6} seconds would have resulted in an average photon signal of 1.4×10^4 photons or 6×10^{-3} volts on the medium gain channel. This signal would have been of the order of the receiver sensor minimum detectable level.

There is another source that is worth considering, and that is scattering from the earth's atmosphere as illuminated by the below-the-horizon sun. This source is discussed in Appendix M. The brightness of this source is very difficult to estimate because of atmospheric absorption, distant weather conditions, and local geography, and is certainly beyond the scope of this contract. However, this source is considered to be the most likely candidate for the measured background signal principally because of the previously mentioned data characteristic that the leading edge of the background signal is not an abrupt rise, indicating an extended source.

In conclusion, the problem of identifying the source of the background cannot be resolved until the rocket aspect data becomes available. However, the intense background signals measured indicate potential problems for this type of measurement and they must be taken into account in planning future measurements.

Figure 7.9 is a plot of the measured background signals as obtained from the flight telemetry records. The voltage level of the medium gain detectors, at the times when the laser would have fired, is plotted as a function of altitude. Tables 7.2 and 7.3 compare these data to the predicted signal levels. The comparison shows that in spite of the abnormally high backgrounds measured during the flight, there was a reasonable probability that valid backscatter data would have been obtained for altitudes less than 90 km had the laser operated as planned.

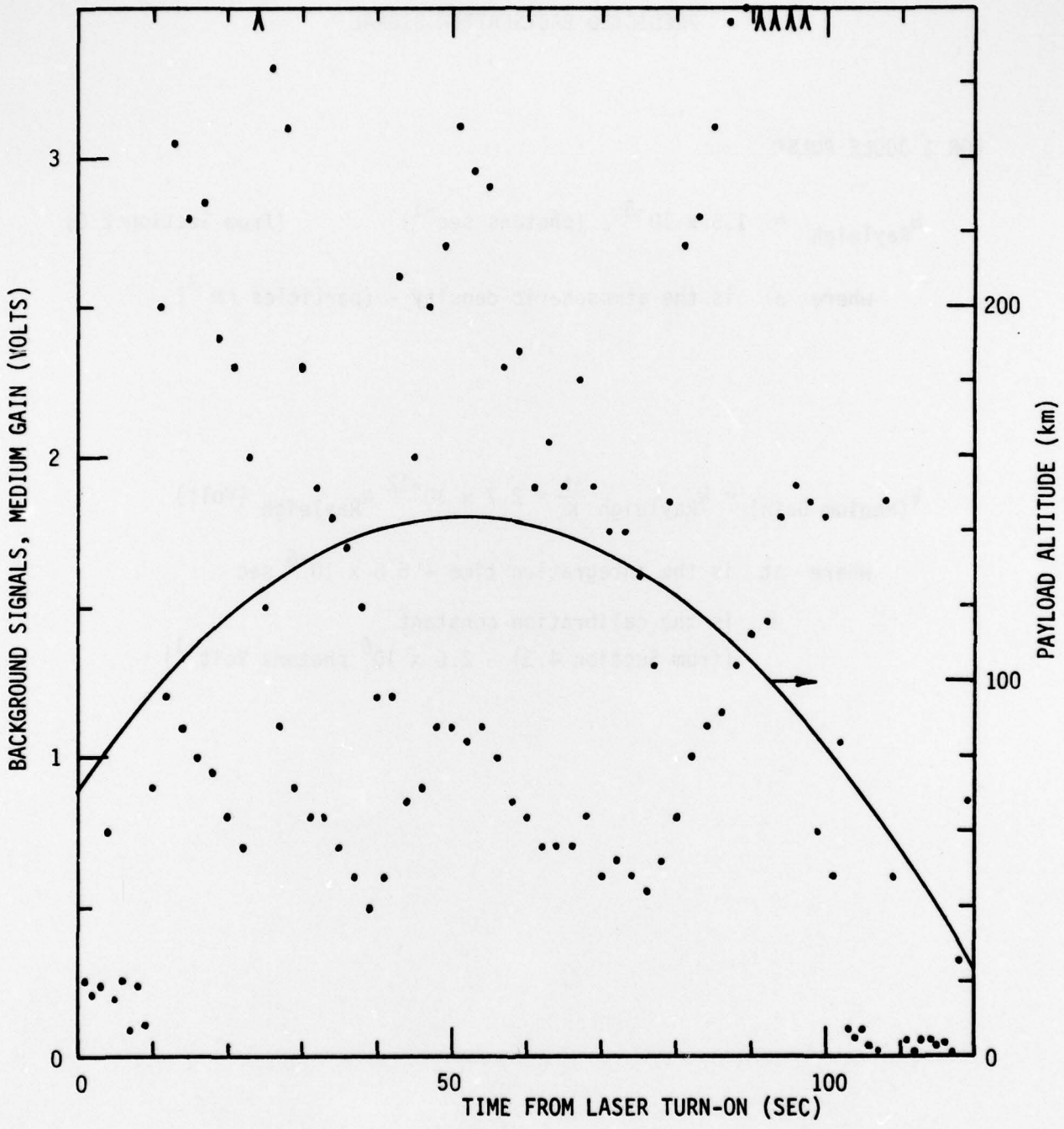

FIGURE 7.9 LASER CORRELATED BACKGROUND SIGNALS

TABLE 7.2

PREDICTED BACKSCATTER SIGNAL

FOR 1 JOULE PULSE

$N_{Rayleigh} = 1.5 \times 10^{-3} \rho$ (photons sec^{-1}) (from Section 2.0)

where ρ is the atmospheric density - (particles cm^{-3})

$V_{(Medium\ Gain)} = N_{Rayleigh} \frac{\Delta t}{K} = 2.7 \times 10^{-12} N_{Rayleigh}$ (Volt)

where Δt is the integration time - 6.8×10^{-6} sec

K is the calibration constant
(from Section 4.3) - 2.5×10^{6} photons $Volt^{-1}$)

TABLE 7.3

SIGNALS AND BACKGROUNDS FOR VARIOUS ALTITUDES

ALTITUDE (km)	DENSITY[1] (cm^{-3})	CALCULATED RAYLEIGH BACKSCATTERED SIGNAL[2] (Volts)[3]	CALCULATED BACKGROUND SIGNAL, NIGHT SKY (Volts)[3]	CALCULATED[4] BACKGROUND SIGNAL, VENUS (Volts)[3]	MEASURED AVERAGE BACKGROUND SIGNAL[5] (Volts)[3]
60	6.4×10^{15}	2.6×10^{1}	1.1×10^{-4}	5.7×10^{-3}	7.5×10^{-1}
80	3.8×10^{14}	1.6×10^{0}	1.1×10^{-4}	5.7×10^{-3}	1.0×10^{0}
100	1.2×10^{13}	4.9×10^{-2}	1.1×10^{-4}	5.7×10^{-3}	4.0×10^{0}
120	5.1×10^{11}	2.1×10^{-3}	1.1×10^{-4}	5.7×10^{-3}	2.0×10^{0}
140	9.3×10^{10}	3.8×10^{-4}	1.1×10^{-4}	5.7×10^{-3}	2.5×10^{0}

(1) U.S. Standard Atmosphere, 1976 (NOAA-S/T76-1562)

(2) For a one joule laser pulse

(3) Medium Gain Channel/Maximum saturation voltage: 1.2×10^{2}; minimum detectable voltage: 1×10^{-3})

(4) Assuming Venus in instrument field of view

(5) Reference Figure 7.9

8.0 CONCLUSIONS AND RECOMMENDATIONS

The Laser Backscatter Experiment program proved to be long, difficult, and expensive, and the end results disappointing. Program accomplishments were as follows:

a. The design, fabrication, test, integration, calibration, and launch of the Laser Backscatter Experiment payload.

b. The design and implementation of laser and high voltage operational procedures which resulted in not one incident where the personal safety of any individual was in any way jeopardized.

c. The development of experimental techniques for assembly alignment, operating, and dye mixing for a rocketborne dye laser system providing reliable and consistent radiational output.

d. The development of a state-of-the-art high voltage power supply and associated high voltage assembly procedures.

e. The design and development of a new payload calibration procedure which provided a single test point.

f. A state-of-the-art data timing system was designed and tested.

g. A unique rocketborne liquid storage and circulation system was developed.

h. The payload system exhibited a minimum of RFI considering the radiation source (pulsed laser) and the sensitive receiver electronics.

The payload was successfully recovered and with minor modifications, alignment, and repair could be prepared for another flight. It is currently operational and ready for use as a laboratory test system.

It is recommended that the rocket aspect data, when available, be analyzed to determine the source of the unanticipated, intense background radiation which could have a significant impact on future measurements of this source.

REFERENCES

1. A. Tomlinson, "Laser Backscatter Density System", Final Report, Contract No. F19628-72-C-0363, AFCRL-TR-74-0460, GCA Corp., (Sept. 1974).

2. A. Tomlinson, "Laser Backscatter Experiment", Final Report, Contract No. F19628-75-C-0006, AFCRL-TR-75-0444, GCA Corp., (August 1975).

3. "Electro-Optics Handbook", Technical Series EOH-11, RCA Corp., Commercial Engineering, (1974).

4. H.W. Furumoto and H.L. Ceccon, Applied Optics, 8, 1613 (1969).

5. L.H. Weeks, AFGL, private communication, January 1976.

6. F. Grum and G.W. Luckey, Applied Optics, 7, 2289, (1968).

7. R.W. Wood, "Physical Optics", The MacMillan Co., New York, (1929).

8. "Handbook of Geophysics and Space Environments", S.O. Valley, ed., Chapter 16, McGraw Hill Bo. Co., Inc., New York, (1965).

APPENDIX A

VISIDYNE, INC.

CHECKED	
APPROVED	

WIRE RUN LIST

TITLE: TRANSMITTER UMBILICAL WL- 645-1-701 REV. -

CABLE FABRICATED BY: _____ REF. CABLE FABRICATION DWG. _____

ESTIMATED LENGTH _____ FT ACTUAL LENGTH _____ FT.

WIRE No.	SOURCE P____	DESTINATION J- 100 DM5605-37S	DESCRIPTION	V VOLTS	I MA	f kHz/ BPS	Z OHMS	CLASS	WIRE TYPE	NOTE
		1	Pump Ext 28 vdc		2000				AWG 22 Type E	
		2	Pump Ext 28 vdc Return		--					
		3	Pump On Command							
		4	Pump Off Command							
		5	Command Return							
		6	Pump On Indication							
		7	Pump Off Indication							
		8	Indication Return							
		9	Coolant Flow Switch							
		10	Dye Flow Switch							
		11	Flow Switch Return							
		12	Pump Battery Charge							
		13	Pump Battery Monitor							
		/								
		14	Laser Ext 28 vdc		1000					
		15	Laser Ext 28 vdc Return							
		16	Laser Battery Charge							
		17	Laser Battery Monitor							
		/								

PAGE 1 OF 2 PAGES

WL- 645-1-701 REV. _____

VISIDYNE, INC.

CHECKED	
APPROVED	6.79

WIRE RUN LIST

TITLE: TRANSMITTER UMBILICAL WL- 645-1-701 REV. ____

CABLE FABRICATED BY: _____ REF. CABLE FABRICATION DWG. _____

ESTIMATED LENGTH _____ FT ACTUAL LENGTH _____ FT.

WIRE No.	SOURCE P____	DESTINATION J____	DESCRIPTION	V VOLTS	I MA	f kHz/ BPS	Z OHMS	CLASS	WIRE TYPE	NOTE
		18	Laser Int 28 vdc Command							
		19	Laser Ext 28 vdc Command							
		20	Laser H/V Enable Command							
		21	Laser H/V Safe Command	——	——	—(+)		X		
		22	Command Return	——	——	—(-)		Y		
		23	Laser Inspection Lamp Power							
		24	Laser Inspection Lamp Power Ret							
		25	Shield							
		26	Payload Ground							
		27	Timing Monitor							
		28	Timing Monitor Return							
		29	Laser H/V Monitor							
		30	Laser H/V Monitor Return							
		31	Shield						Copper Braid	
		32-37	Spares							

WL- 645-1-701 REV. _____

VISIDYNE, INC.

CHECKED	
APPROVED	

WIRE RUN LIST

TITLE: TRANSMITTER INTERFACE WL- 645-1-702 REV. -

CABLE FABRICATED BY: _____ REF. CABLE FABRICATION DWG. _____

ESTIMATED LENGTH _____ FT ACTUAL LENGTH _____ FT.

WIRE No.	SOURCE P____	DESTINATION J-101 HPSE07-18-325	DESCRIPTION	V VOLTS	I MA	f kHz/ BPS	Z OHMS	CLASS	WIRE TYPE	NOTE
		A	Spark Gap Trigger	5					2 CondSh	FM/FM CH10
		B	Spark Gap Trigger Return	-					↓	Ground at T/M
		C	Spark Gap H/V Mon.	5					↓	FM/FM CH8
		D	Spark Gap H/V Mon. Return	-					↓	Ground at T/M
		E	Laser H/V Supply Mon.	5					↓	FM/FM CH9
		F	Laser H/V Supply Mon. Return						↓	Ground at T/M
		G	Clock Monitor						↓	FM/FM CH14
		H	Clock Monitor Return						↓	Ground at T/M
		J	Shield						DaisyChan	Ground at T/M
		K	Laser 28 vdc Battery Mon						3 CondSh	PAM
		L	Laser 28 vdc Power Mon						↓	PAM
		M	Return						↓	Ground at T/M
		N	Spark Gap 300 vdc Mon						↓	PAM
		P	Spark Gap Pressure Mon						↓	PAM
		R	Return						↓	Ground at T/M
		S	Dye Flow Mon						↓	PAM
		T	Coolant Flow Mon						↓	PAM
		U	Return						↓	Ground at T/M
		V	Dye Temperature Mon						4 CondSh	PAM
		W	Coolant Temperature Mon						↓	PAM

WL- 645-1-702 REV. _____

VISIDYNE, INC.

CHECKED	
APPROVED	

WIRE RUN LIST

TITLE: TRANSMITTER INTERFACE WL- 645-1-702 REV. -

CABLE FABRICATED BY: _____ REF. CABLE FABRICATION DWG. _____

ESTIMATED LENGTH _____ FT ACTUAL LENGTH _____ FT.

WIRE No.	SOURCE P____	DESTINATION J____	DESCRIPTION	V VOLTS	I MA	f kHz/ BPS	Z OHMS	CLASS	WIRE TYPE	NOTE
		X	Laser Compartment Pressure						↓	PAM
		Y	Return						↓	Ground at T/M
		Z	Laser H/V Enable						3 CondSh	From Payload Tim
		a	Laser H/V Off						↓	
		b	Return						↓	
		c	Signal Ground						4 CondSh	Ground at T/M
		d	Power Ground						↓	" "
		e	Case Ground						↓	" "
		f	Shield Ground						↓	" "
		g	Shield						DaisyChain	" "
		h	Spare						↓	" "
		j	Outer Shield						↓	" "

PAGE 2 OF 2 PAGES WL- 645-1-702 REV. _____

VISIDYNE, INC.

CHECKED	
APPROVED	

WIRE RUN LIST

TITLE: RECEIVER INTERFACE WL- 645-1-703 REV. ____

CABLE FABRICATED BY: _____ REF. CABLE FABRICATION DWG. _____

ESTIMATED LENGTH _____ FT ACTUAL LENGTH _____ FT.

WIRE No.	SOURCE P____	DESTINATION J- 201 HPSE07-20-41S	DESCRIPTION	V VOLTS	I MA	f kHz/ BPS	Z OHMS	CLASS	WIRE TYPE	NOTE
		A	Medium Gain Data						2 CondSh	FM/FM CH H
		B	Medium Gain Data Return							Ground at T/M
		C	High Gain Data							FM/FM CH F
		D	High Gain Data Return							Ground at T/M
		E	Low Gain Data							FM/FM CH 17
		F	Low Gain Data Return							Ground at T/M
		G	Laser Power Monitor							FM/FM CH 16
		H	Laser Power Monitor Return							Ground at T/M
		J	Receiver Clock							FM/FM CH 7
		K	Receiver Clock Return							Ground at T/M
		L	Shield						Daisy Chain	Ground at T/M
		M	Spare							Ground at T/M
		N	Receiver 28 vdc Battery Mon						5 CondSh	PAM
		P	+15 vdc Mon							PAM
		R	-15 vdc Mon							PAM
		S	+ 5 vdc Mon							PAM
		T	PMT H/V Mon							PAM
		U	Return							Ground at T/M
		V	Calibration LED Mon						2 CondSh	PAM
		W	Calibration LED Mon Return							Ground at T/M

VISIDYNE, INC.

CHECKED	
APPROVED	8/4/70

WIRE RUN LIST

TITLE: RECEIVER INTERFACE WL- 645-1-703 REV. ____

CABLE FABRICATED BY: _____ REF. CABLE FABRICATION DWG. _____

ESTIMATED LENGTH _____ FT ACTUAL LENGTH _____ FT.

WIRE No.	SOURCE P____	DESTINATION J____	DESCRIPTION	V VOLTS	I MA	f kHz/ BPS	Z OHMS	CLASS	WIRE TYPE	NOTE
		X	PMT Temperature Mon						3 CondSh	PAM
		Y	Receiver Compartment Pressure						↓	PAM
		Z	Return						↓	Ground at T/M
		a	Shield						DaisyChain	
		b	Calibration Command 1						3 CondSh	Timer
		c	Calibration Command 2						↓	Timer
		d	Command Return						↓	
		e	Spare							
		f	Spare							
		g	Spare							
		h	Spare							

WL- 645-1-703 REV. _____

VISIDYNE, INC.

CHECKED	
APPROVED	

WIRE RUN LIST

TITLE: RECEIVER UMBILICAL WL- 645-1-704 REV. -

CABLE FABRICATED BY: _____ REF. CABLE FABRICATION DWG. _____

ESTIMATED LENGTH _____ FT ACTUAL LENGTH _____ FT.

WIRE No.	SOURCE P____	DESTINATION J - 200 DM5605-37S	DESCRIPTION	V VOLTS	I MA	f kHz/ BPS	Z OHMS	CLASS	WIRE TYPE	NOTE
		1	Receiver Ext 28 vdc							
		2	Receiver Ext 28 vdc Return							
		3	Receiver Battery Charge							
		4	Receiver Battery Monitor							
		5	Receiver Int 28 vdc Command							
		6	Receiver Ext 28 vdc Command							
		7	Command Return							
		8	Receiver Ext 28 vdc Ind							
		9	Receiver Int 28 vdc Ind							
		10	Ind Return							
		11	Calibration LED Command						2 CondSh	
		12	Calibration LED Command Return						↓	
		13	Shield							
		14-20	Spares							
		20-32	Reserved to T/M Use							

PAGE 1 OF 1 PAGES

WL- 645-1-704 REV. _____

APPENDIX B

APPENDIX B

A03.604 TM ALLOCATIONS

FM/FM - 2279.5 mHz

TRANSMITTER: Vector T102-S, 2 watts nominal

ANTENNA: BBRC Stripline

CHANNEL	DATA	LOW PASS
"H"	(Recvr) PMT Med Gain Data	4,950 Hz
"F"	(Recvr) PMT High Gain Analog Data	2,790 Hz
17	(Recvr) PMT Low Gain Analog Data	790 Hz
16	(Recvr) Laser Power Monitor	600 Hz
15	Gyro Multiplex	790 Hz
14	(Trans.) Clock	600 Hz
13	*Commutator (2.5 RPS x 30 Seg.)*	220 Hz
12	Accelerometer	160 Hz
11	Capacitor Discharge Mon.	110 Hz
10	(Trans.) Spark Gap trigger Pulse	81 Hz
9	(Trans.) Laser H.V. Supply	59 Hz
8	(Trans.) Spark Gap H.V.	45 Hz
7	(Recvr) Clock	35 Hz

A03.604

COMMUTATOR ASSIGNMENT

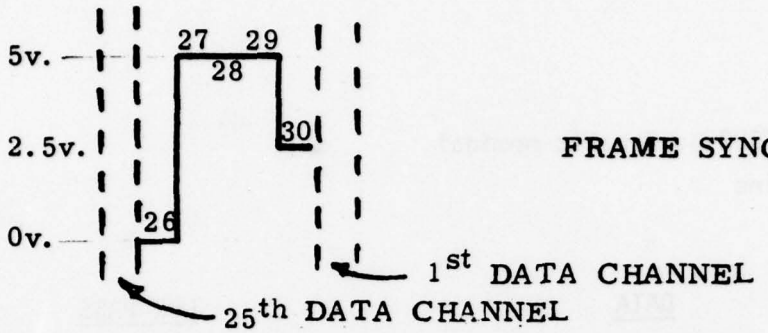

DATA CHANNEL	
1	LASER COMPARTMENT PRESSURE
2	COOLANT TEMP.
3	DYE TEMP.
4	COOLANT FLOW
5	DYE FLOW
6	SPARK GAP
7	SPARK GAP 300v.
8	LASER +28v. POWER
9	LASER +28v. BATTERY
10	RECEIVER COMPARTMENT PRESSURE
11	PMT TEMP.
12	CAL. LED
13	PMT H.V.
14	+5v.
15	-15v.
16	+15v.
17	RECEIVER +28v. BATTERY
18	GND.
19	
20	
21	
22	GYRO ANALOG ROLL RATE
23	ACCELEROMETER B+ MON.
24	28v. B+ MON.
25	DOOR MON.

APPENDIX C

APPENDIX (C)
INSTRUCTIONS FOR LASER DYE PREPARATION

I. MATERIALS

a. Dye: Coumarin 2 (4,6-Dimethyl-7-ethylamino coumarin)

1. Empirical Formula: $C_{13} H_{15} NO_2$
2. Molecular Weight: 217.27
3. Manufacturers: Eastman Kodak Co., Rochester, New York and Candela Corp., Needham Heights, Massachusetts

b. Methanol, Certified ACS

1. Formula: CH_3OH
2. Molecular Weight: 32.04
3. Manufacturer: Fisher Scientific Co., Pittsburgh, Pennsylvania

c. Distilled Water, Certified Pure

II. MIXING INSTRUCTIONS (Volume to Fill Laser System)

a. Use only glass, teflon, or stainless steel containers and tools.
b. Pour 3333 ml of methanol in container.
c. Fill container to 6666 ml mark with distilled water (this methanol-water mixture is an azeotrope at atmospheric pressure).
d. Mix continuously for 30 minutes with a magnetic stirrer to remove trapped air.
e. In another container, add 210 mg of Coumarin 2 dye to 500 ml of methanol and stir until completely dissolved.
f. Add dye mixture to solvent mixture and stir until completely mixed. Resulting dye laser solution is 1.5×10^{-4} M.
g. Store in clean, air-tight glass containers and keep in a dark place until ready to use.

APPENDIX D

APPENDIX (D)
SPECTRAL CURVES FOR OPTICAL COMPONENTS

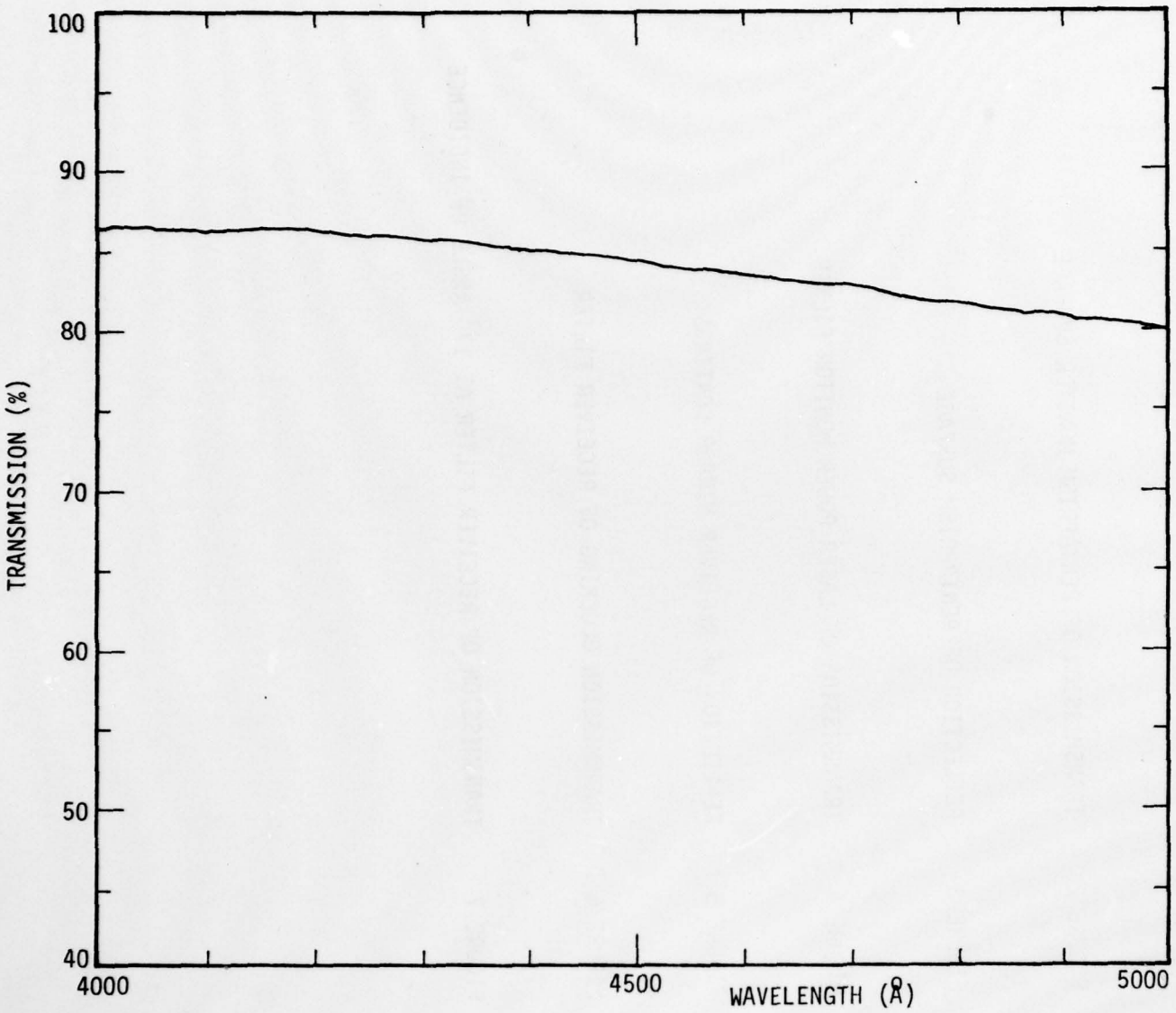

FIGURE 1 TRANSMISSION OF FRONT END LASER MIRROR

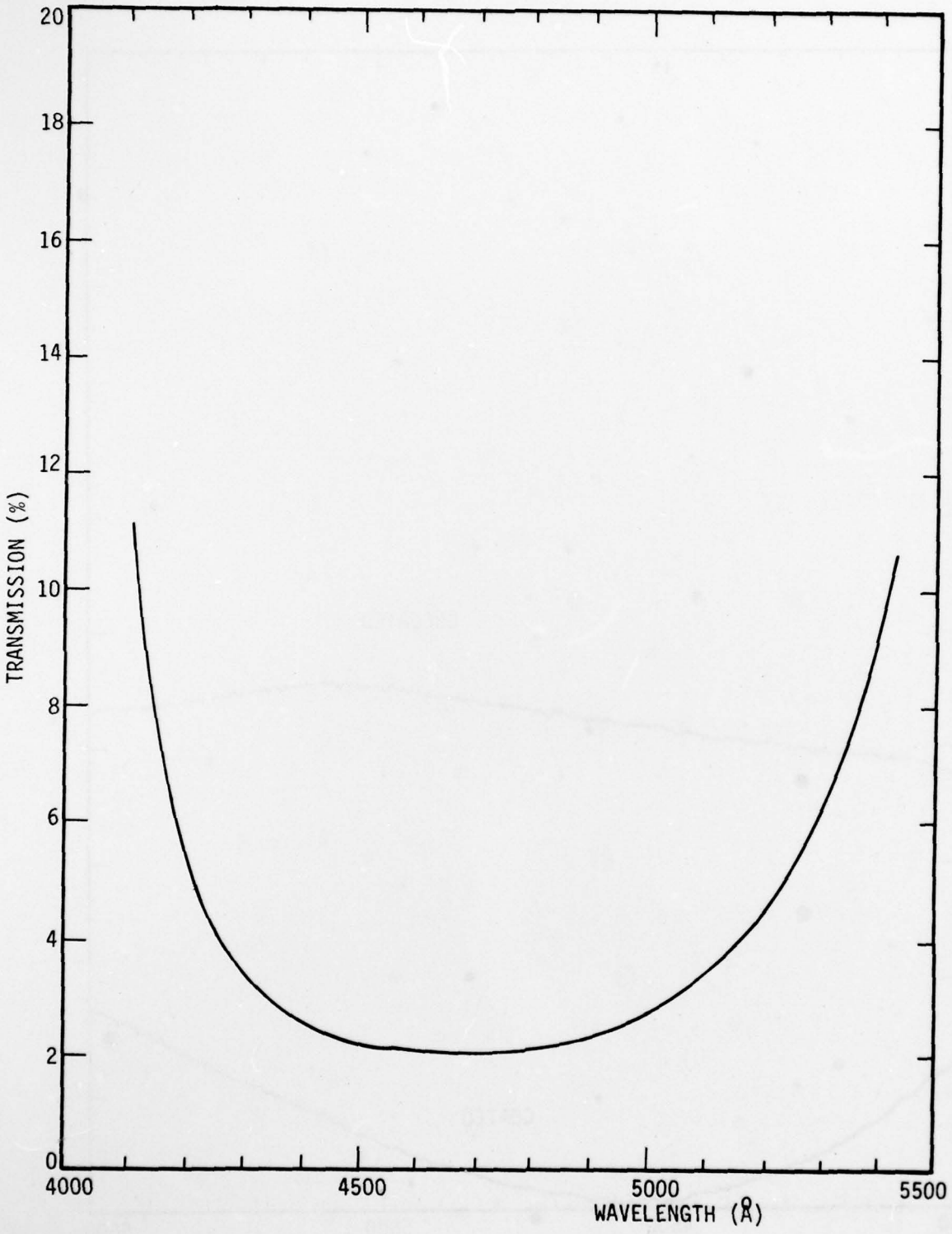

FIGURE 2 TRANSMISSION OF PENTAPRISM MONITOR SURFACE

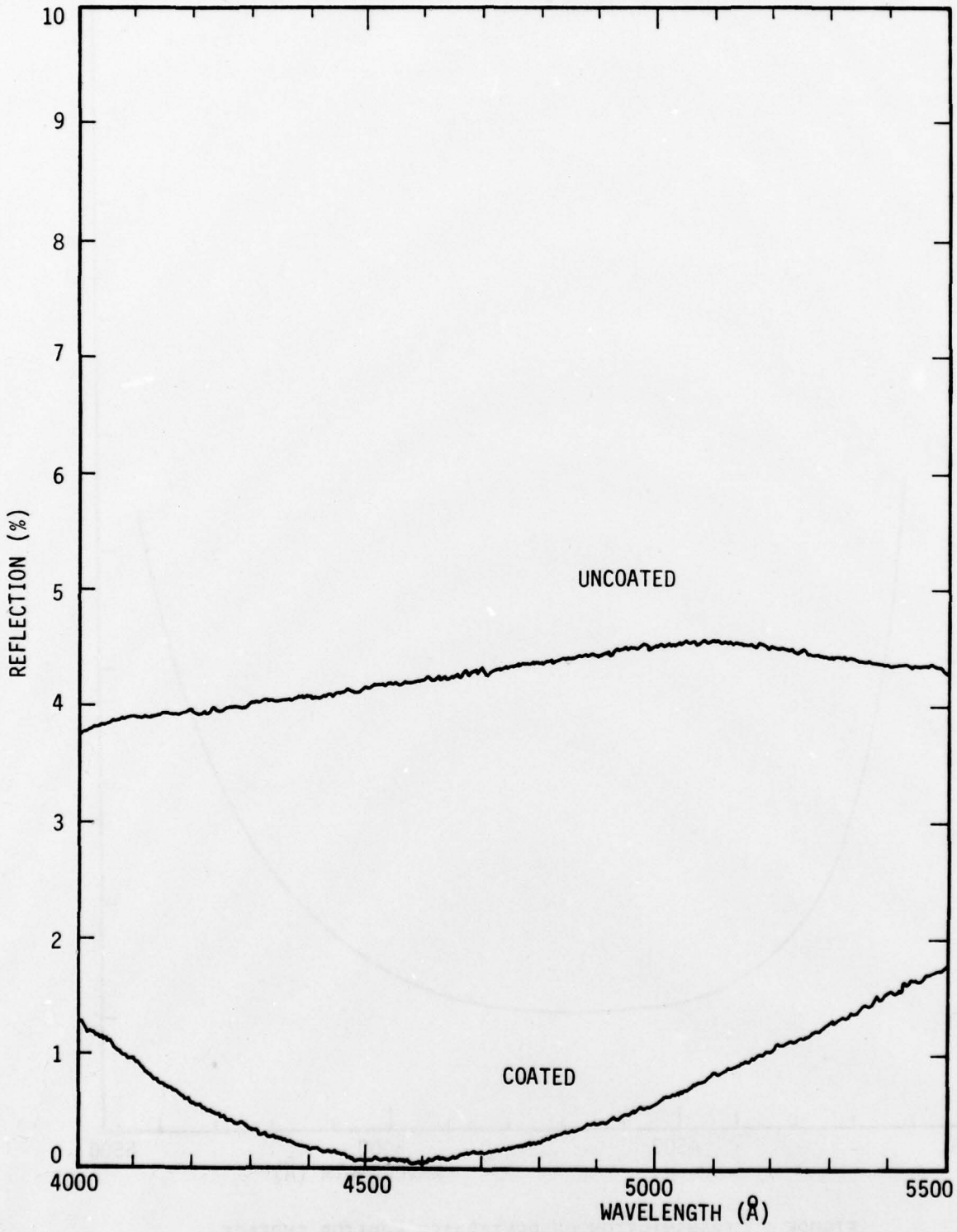

FIGURE 3 REFLECTION OF PENTAPRISM SURFACE

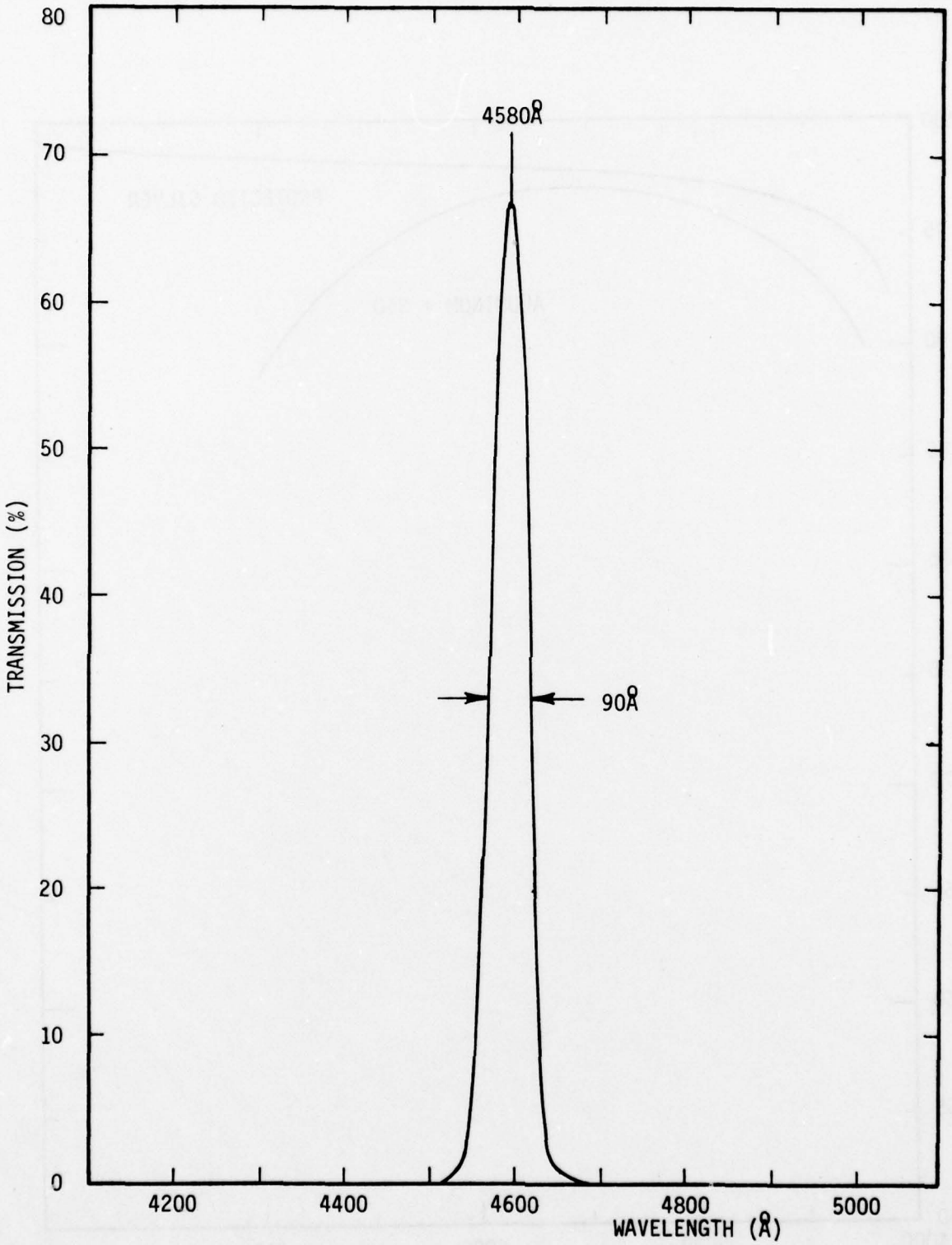

FIGURE 4 TRANSMISSION OF LASER POWER MONITOR FILTER

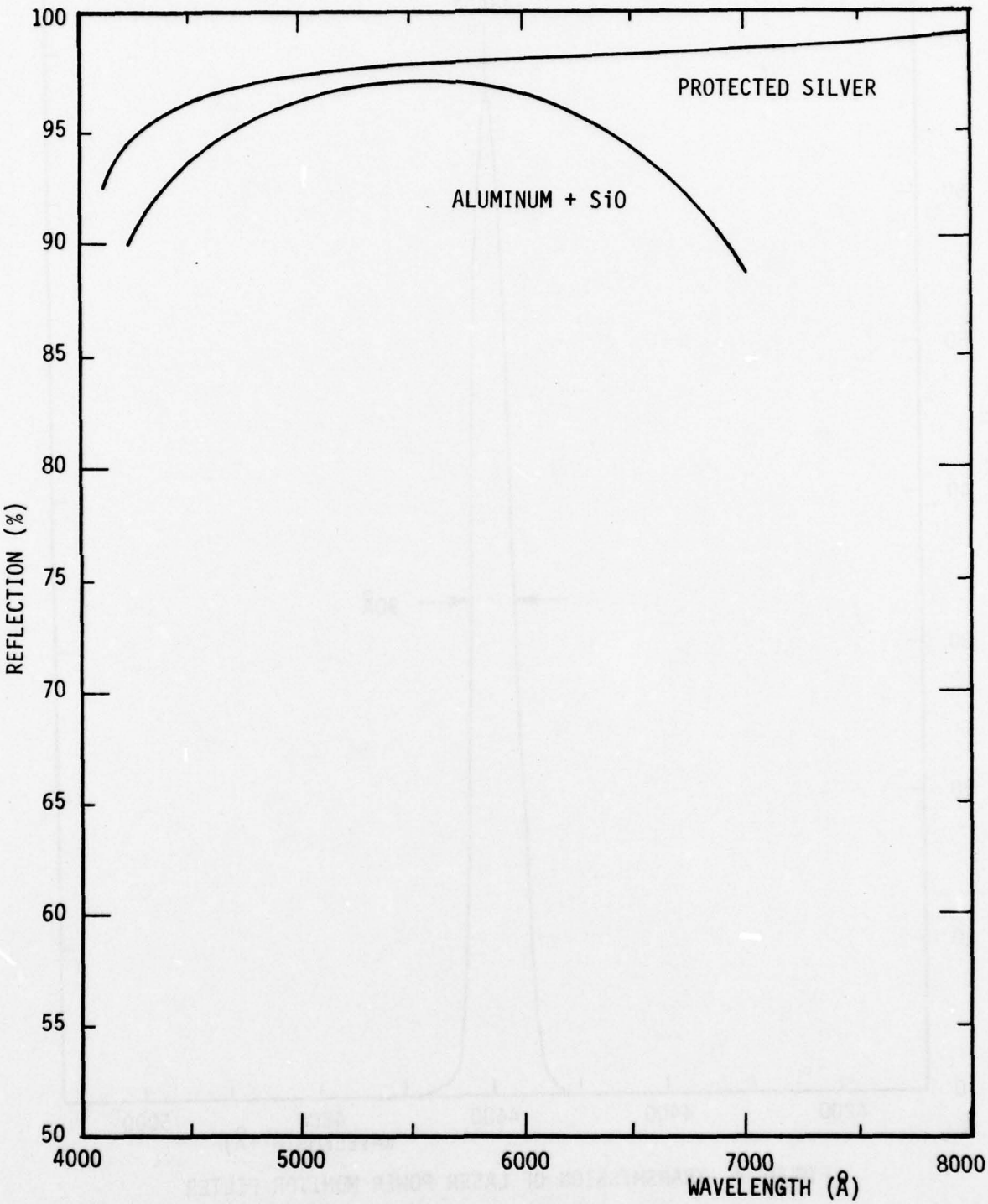

FIGURE 5 REFLECTION OF RECEIVER MIRROR COATINGS

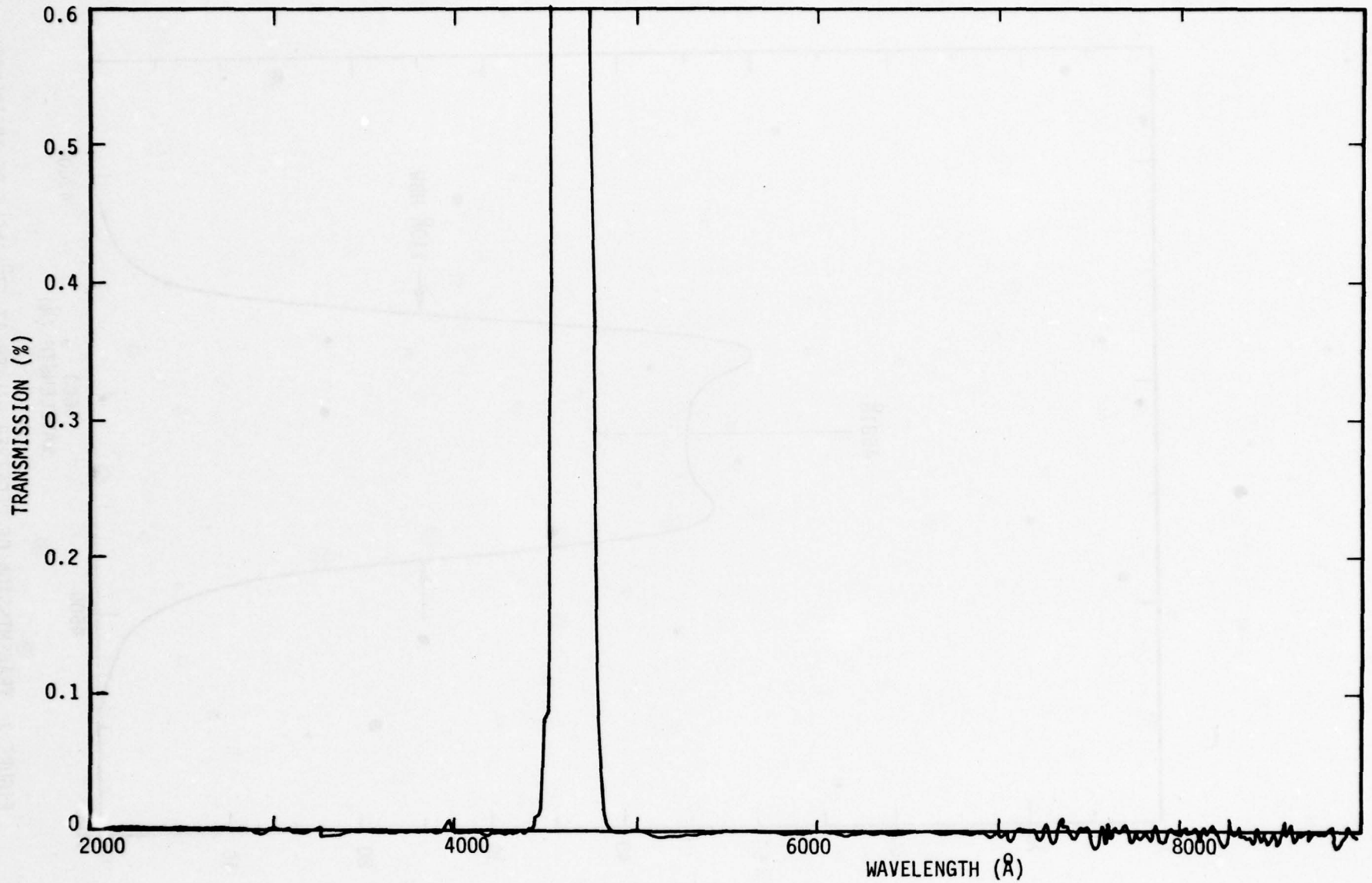

FIGURE 6 TRANSMISSION BLOCKING OF RECEIVER FILTER

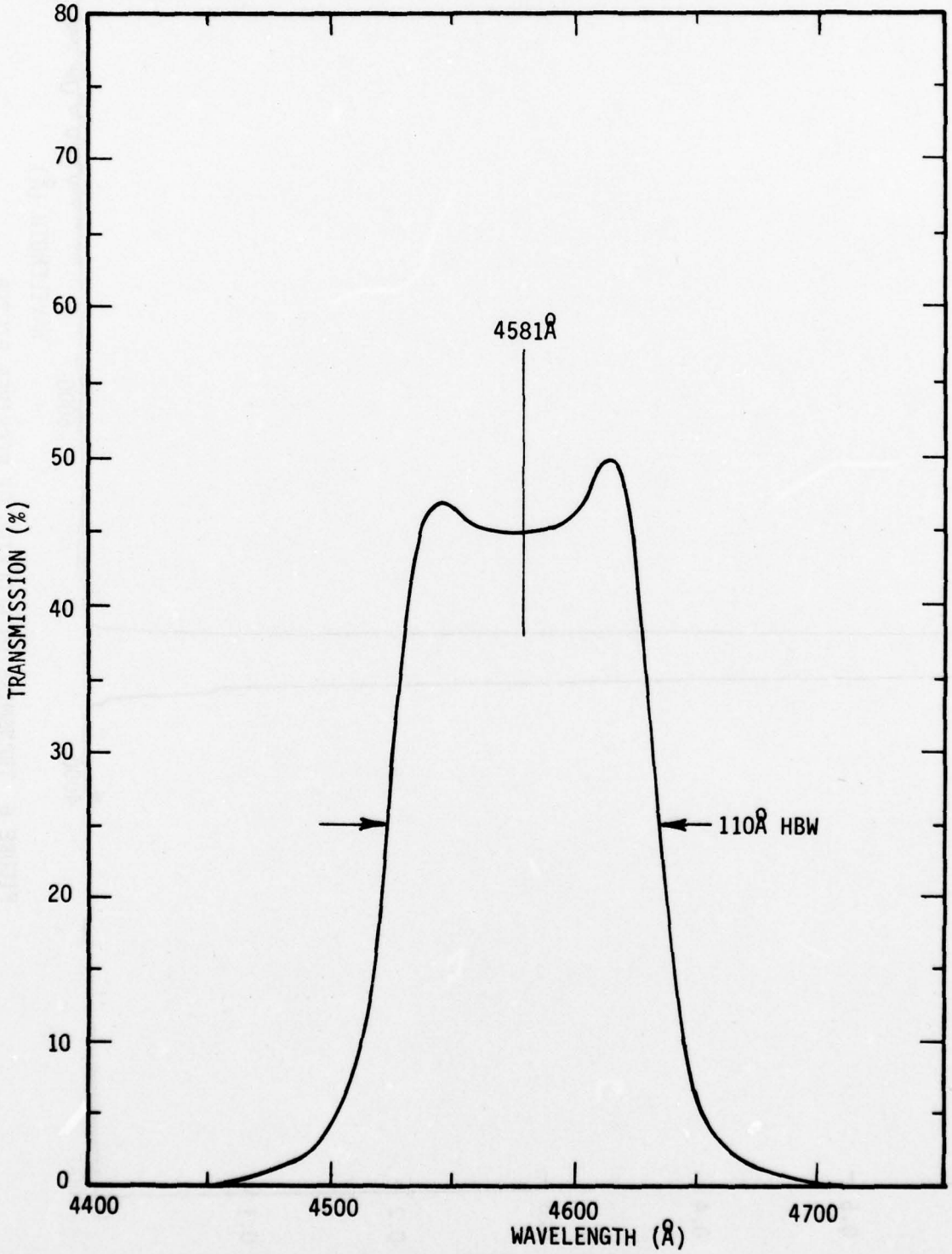

FIGURE 7 TRANSMISSION OF RECEIVER FILTER AT 17° ANGLE OF INCIDENCE

APPENDIX E

APPENDIX (E)
LASER ALIGNMENT PROCEDURES

I. MATERIALS

a. 0.5 mW He-Ne Laser
b. Alignment Fixtures

II. INITIAL ALIGNMENT

a. Mount dye laser horizontally on an adjustable stand and set He-Ne laser about five meters away with axes of both lasers coincident.
b. Turn on He-Ne laser.
c. Using apertures in place of end mirrors on the dye laser, determine that He-Ne laser beam is centered on dye laser axis. Adjust as needed.
d. Remove apertures and mount front end mirror (20% reflectance) with mirror side out (pointed end of mark on substrate is toward mirrored side).
e. Using the three mounting screws, adjust reflection of He-Ne beam from the front end mirror so that it shines directly back into the He-Ne aperture. A white card with a hole centered on the He-Ne output is helpful for this operation. Caution: End mirrors are sometimes 30 arc min. wedges and give multiple reflections.
f. Mount rear end mirror (99.9% reflectance) on laser tube, mirror side out.
g. Repeat step "e" except adjusting rear end mirror.

III. FINAL ALIGNMENT

a. After dye laser is filled and mounted in the payload, reposition laser so that its axis is external to the payload.
b. Position a first surface mirror (on an adjustable mount) on the dye laser axis.

c. Mount He-Ne laser on an adjustable tripod about five meters from the payload.

d. Turn on He-Ne laser. Adjust its beam position so that it is centered in the dye laser tube. (The rear end mirror of the dye laser has sufficient transmission through pinholes so that the beam position can be determined.)

e. Repeat step "II e" as required to reflect the He-Ne laser beam directly back into the laser aperture.

f. Turn on dye laser pumps and check that reflected beam position has not shifted.

g. Turn off pumps and He-Ne laser.

h. Remove first surface mirror and remount dye laser in the payload.

The accuracy of the above procedure consistently resulted in successful lasing of the dye laser.

APPENDIX F

APPENDIX (F)

SAFETY PROCEDURES TO BE USED IN CONNECTION WITH THE LASER BACKSCATTER EXPERIMENT

Visidyne, Inc. - July 28, 1977

Safety procedures to be observed during the laboratory and field testing of the laser backscatter experiment payload must include the following:

Attachment 1

"Guidelines for the Safe Operation of Laser Systems"
ESD Supplement 1 to AFR 161-24, 17 November 1970

Attachment 2

"Laser Backscatter Experiment Payload Recovery Procedures"

Attachment 3

"Dye Laser (Preinstallation Certification)"
Memo to L. Weeks from Lt Col C.W. Winney, 5 December 1973

In addition to the above, the following procedures must be observed during laboratory operation:

1. The payload electrical ground shall be strapped to a suitable laboratory ground.
2. At least one Class A-B-C fire extinguisher shall be immediately available in case of fire.
3. Firing of the laser shall require double key switching to prevent unauthorized operation.
4. All personnel directly involved with operation of the laser shall have had retinal photographs taken and be familiar with first aid procedures to be followed for victims of electrical shock.

GUIDELINES FOR THE SAFE OPERATION OF LASER SYSTEMS

These guidelines of general principles and practices for the safe operation of most laser systems will be followed by all laser users unless other safety operating procedures are substituted. Additional specific procedures for safe operation of lasers may be required if scattering or unusual applications constitute a hazard to personnel or equipment.

1. Laser equipment will be operated by personnel who have received adequate training in the use and operation of the specific system, and who are thoroughly familiar with the associated hazards, safety precautions, and protective measures for the particular system.

2. When practicable, the "buddy-system" will be used; i.e., two qualified persons will be present during high-voltage laser operations.

3. Areas using laser systems will be restricted areas. Only persons directly associated with the operations will be permitted access.

4. The entrances to laser areas will be posted with warning signs.

5. In work with laser systems when scattered light from rough surfaces to any point in the room is above the safe tolerance level, entrances to the area will be marked with a visual warning system and/or an interlock system. An audible signal may detract from safety since it could draw attention to the laser light during firing.

6. Visitors to operating laser areas will be accompanied by an escort and will comply with established safety precautions.

7. Avoid aiming the laser by eye; looking along the beam axis increases the hazard from reflections.

8. Avoid looking into the primary beam at any time.

9. Avoid looking at specular reflections of the beam, including those from lens surfaces.

10. Avoid having the laser beam impinge on exposed skin surfaces.

11. When exposure is at close range, all personnel within the room will be warned to turn their heads away during the firing of a pulse type laser unless the laser and all portions of its beam and target are inclosed by thick opaque shields or a light-tight housing.

12. Exposure to laser radiations will be held to a minimum.

13. A verbal count-down will be used prior to firing a laser.

14. Use appropriate goggles or filter eye shields when working lasers.

15. The safety or filtered eye shields will be marked to indicate type and amount of protection afforded; i.e., wave lengths filtered, percent transmission, etc. Safety glasses will never be relied upon to provide full protection since no one set of glasses provides protection for all wave lengths.

16. When possible, a high general illumination will be maintained in laser areas to keep the pupil diameter as small as possible; darkened areas cause the pupils of the eyes to dilate, thereby increasing the amount of laser energy which might enter the eye.

17. When any degradation in acuity or field of vision is noted, or if persistent after-image is experienced following exposure to an operating laser system, report as soon as possible to the Dispensary.

18. Medical evaluations will be required prior to and at termination of work with laser systems. Annual examinations will also be required.

19. Flash tubes will be shielded since misfires or accidental firing can occur. With unshielded units, energy density decreases approximately with the inverse square of the distance. Avoid looking directly at the unshielded flash tube.

20. Flash tube explosions, although rare, are potential hazards, and adequate precautions will be taken, e.g., use of shields, laminated glass, etc.

21. Walls, ceiling, and floors will be coated or painted with non-reflecting material when practicable. All windows and glass surfaces will be covered with similar material on the interior sides, when practicable.

22. Minimum use will be made of instruments and materials which have specularly reflecting surfaces for the wave lengths being used. If possible, such surfaces will be covered with a diffusely reflecting material.

23. Under field conditions, consideration will be given to the scattering caused by terrain, particulate matter, fog, snow, rain, and smoke. Some of these scattering media might apply equally as well under certain laboratory conditions.

24. The laser beam will be discharged into a background that is fire-resistant and non-reflective.

25. Personnel will be aware of the generation of beryllium compounds due to beryllium impurities in firebrick.

26. When viewing a laser beam pattern on a diffuse screen, view from the same side as the laser source to avoid direct illumination through pin hole leaks.

27. Never leave a laser unattended in a potentially operative condition if it constitutes a hazard to personnel, unless you can secure the area from access to other persons.

28. Prior to any maintenance or inspection of the laser equipment, remove all power cables from the power receptacle.

29. Avoid exceeding the manufacturer's recommended operating limits.

30. Adequate ventilation will exist to prevent the displacement of oxygen with noxious gases such as nitrogen, carbon dioxide, ozone, etc. Other toxic compounds can be generated by the action of lasers upon particular materials.

31. When ultraviolet radiation is generated, ozone will be generated; hence, caution must be exercised to insure that ozone concentrations do not exceed recommended safe levels.

32. Adequate precautions will be taken with high voltage equipment insuring equipment is properly grounded, wires adequately insulated, and interlocks properly used.

33. Proper precautions will be taken to insure capacitor banks are adequately grounded and discharged automatically after use.

34. Extra caution must be exercised around laser systems operating at wave lengths invisible to the human eye.

35. Personnel will become familiar with first aid procedures especially with artificial respiration techniques and the handling of electric shock victims. Medical aid will be summoned as soon as possible.

36. The light gathering characteristics of optical instruments, such as binoculars and microscopes, must be taken into consideration, and will be avoided when possible. To approximate the factor by which the laser energy is increased by such optical instruments, the square of the magnification power can be used; i.e., a magnification power of 7 will increase the energy 49 or 50 times. As an example, if the safe exposure level for the cornea of the eye is 10^{-7} joule/cm^2, then the optical instrument should not be used in a laser field exceeding 2×10^{-9} joul /cm^2.

LASER BACKSCATTER EXPERIMENT
PAYLOAD RECOVERY PROCEDURES

The experiment payload is potentially dangerous and no recovery should be attempted until after inspection and approval for recovery by AFGL. The payload hazards are:

1. Potential eye injury due to laser radiation.
2. Potential shock from lethal high voltage within the payload.

Both the laser and the high voltage will be automatically shut-off by an onboard payload timing prior to parachute deployment. Only in the case of a failure in the payload timer system will these hazards be present.

It is recommended that the following safety precautions be adhered to during the payload recovery operations:

1. All recovery time personnel should wear AFGL approved laser safety glasses when approaching within two km of the payload recovery site.
2. Personnel under direction of AFGL will inspect the payload for potential laser or high voltage hazards prior to attempting to move the payload.
3. The payload optical cavity will be covered using an AFGL furnished door and the laser aperture covered. (Laser aperture cover to be provided AFGL by Visidyne, Inc.)
4. AFGL will approve the commencement of recovery operations.

The payload personnel assigned to the recovery team will be required to have had retinal photographs as required by AFGL regulations.

It is requested that a range photographer accompany the recovery team.

DEPARTMENT OF THE AIR FORCE
USAF CLINIC LG HANSCOM (AFSC)
L. G. HANSCOM FIELD, BEDFORD, MASS. 01730

REPLY TO:
ATTN OF: SGPM/MSgt Klett, 2574 5 December 1973

SUBJECT: Dye Laser (Preinstallation Certification)

TO: AFCRL/LKB ATTN: Mr. Weeks

1. The 4500-4600Å dye laser on order has a Permissible Exposure Level (PEL) of 2.0×10^{-7} Joules for the eyes, $0.01 J/cm^2$ for the skin and the Safe Eye Exposure Distance (SEED) is 6,500 feet. The optical density (OD) required for eye protection is 6.7 and for the skin a protection with an OD of 2.4 is required.

2. Each time the laser is operated, safety precautions should include adequate procedures so that the direct beam does not impinge on the skin, the area is posted as a laser hazard area and protective eye wear will be required for all individuals in the area when ever the laser is firing.

3. Laser glasses recommended by the Laser Labs at Brooks AFB are Model LGS-A, which are soft glasses, O.D. 10, visible transmission of 45% and cost $25.00 per pair. Protective glasses are available from Glendale Optical Company, Inc., 130 Crossways Park Dr., Woodbury L.I. N.Y. 11797.

4. Laser physicals will be required for all personnel who routinely operate the laser. Support personnel may require a physical but it is tentatively planned to treat them as visitors to the area. The responsibility of contractors operating the laser and their subsequent physicals is under consideration and must be resolved. Command assistance has been requested.

CHARLES W. WINNEY, Lt Col, USAF, MSC
Director of Base Medical Services

Cy to: AFCRL/SU

APPENDIX G

APPENDIX (G)

LONGITUDINAL VIBRATION TESTING
ACCEPTANCE LEVELS FOR AEROBEE PAYLOADS

COMPONENTS TESTS

SINE	15 g's 0 - PEAK 20 - 2000 Hz @ 2 OCT/MIN (DISP LMT'D TO .5 IN. D.A.)
RANDOM	.15 g^2/Hz PSD 100 - 1000 Hz WITH 6 DB/OCTAVE ROLL OFF EACH END TO 20 Hz LOWER & 2000 Hz UPPER (RMS g's ~ 15.3 g's RMS) FOR 3 MIN DURATION

SUBASSEMBLY TESTS

SINE	7.5 g's 0 - PEAK 20 - 2000 Hz @ 2 OCT/MIN (DISP LMT'D TO .5 IN D.A.)
RANDOM	SAME AS ABOVE

PAYLOAD ASSEMBLY TESTS

SINE	2 g's 0 - PEAK 20 - 2000 Hz @ 2 OCT/MIN (DISP LMT'D TO .5 IN D.A.)
RANDOM	.05 g^2/Hz PSD 100 - 1000 Hz WITH 6 DB/OCTAVE ROLL OFF EACH END TO 20 Hz LOWER & 200 Hz UPPER FOR 1 MIN DURATION (TOTAL ~ 8.7 g's RMS)

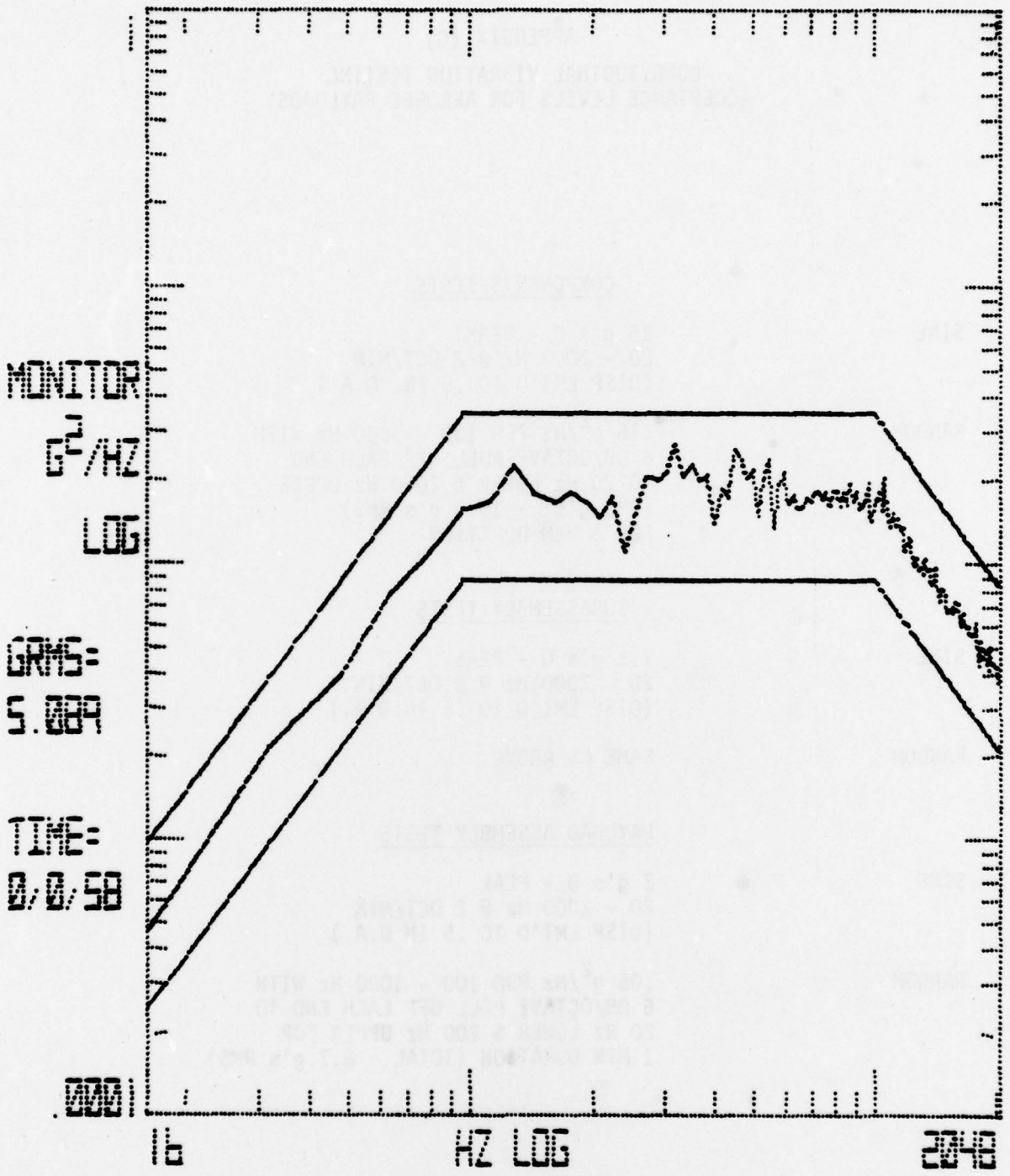

RANDOM TEST 17 AUG 77

A 03.604 G. GEARY

APPENDIX H

APPENDIX (H)

LASER ROCKET PROGRAM

FIELD TRIP

DATE AND/OR TIME	TASK DESCRIPTION
MONDAY - 17 JUL - 0700	1. Crew Deployment to El Paso, Texas 2. Pick up station wagon at Avis 3. Pick up 3 crates at Emery WB50987 and WB50993 4. Drive to Las Cruces 5. Check in at Century 21 Motel 6. Drive to WSMR and check security clearances 7. Take crates to Building 36 in launch area 8. Begin lab set-up
TUESDAY - 18 JUL	1. Complete lab set-up 2. Refocus scope camera 3. Fill flight batteries and set at Angle #1 4. Mix dye and fill dye and coolant tanks 5. Inspect P/L and GSE 6. Mount P/L in test configuration 7. Perform GSE-P/L Test 8. Align laser 9. Test fire laser with calorimeter, one shot and photo 10. Test fire laser with cal. surface, one shot and photo 11. Set batteries at Angle #2 12. Check spark gap leakage rate 13. Check shipment of spare laser
WEDNESDAY - 19 JUL - a.m.	1. Attend Prefire Conference 2. Clean receiver optics 3. Install batteries in payload 4. Test fire laser with calorimeter, one shot and photo 5. Test fire laser with cal. surface, one shot and photo 6. Perform mechanical check of P/L
THURSDAY - 20 JUL	1. Ring out umbilical cables 2. Mount rocket skin and lay P/L horizontal 3. Mate P/L to T/M 4. Mount P/L vertically 5. Perform pre-horizontal tests a. External Power - T/M check b. Internal Power - Six shots on automatic fire, calibration surface at 2.2m. Save printout of T/M and tape c. Remove rocket skin d. Mount door and squibs e. Timer and door tests

APPENDIX (H)

LASER ROCKET PROGRAM

FIELD TRIP

DATE AND/OR TIME	TASK DESCRIPTION
MONDAY - 17 JUL - 0700	1. Crew Deployment to El Paso, Texas 2. Pick up station wagon at Avis 3. Pick up 3 crates at Emery WB50987 and WB50993 4. Drive to Las Cruces 5. Check in at Century 21 Motel 6. Drive to WSMR and check security clearances 7. Take crates to Building 36 in launch area 8. Begin lab set-up
TUESDAY - 18 JUL	1. Complete lab set-up 2. Refocus scope camera 3. Fill flight batteries and set at Angle #1 4. Mix dye and fill dye and coolant tanks 5. Inspect P/L and GSE 6. Mount P/L in test configuration 7. Perform GSE-P/L Test 8. Align laser 9. Test fire laser with calorimeter, one shot and photo 10. Test fire laser with cal. surface, one shot and photo 11. Set batteries at Angle #2 12. Check spark gap leakage rate 13. Check shipment of spare laser
WEDNESDAY - 19 JUL - a.m.	1. Attend Prefire Conference 2. Clean receiver optics 3. Install batteries in payload 4. Test fire laser with calorimeter, one shot and photo 5. Test fire laser with cal. surface, one shot and photo 6. Perform mechanical check of P/L
THURSDAY - 20 JUL	1. Ring out umbilical cables 2. Mount rocket skin and lay P/L horizontal 3. Mate P/L to T/M 4. Mount P/L vertically 5. Perform pre-horizontal tests a. External Power - T/M check b. Internal Power - Six shots on automatic fire, calibration surface at 2.2m. Save printout of T/M and tape c. Remove rocket skin d. Mount door and squibs e. Timer and door tests

DATE AND/OR TIME		TASK DESCRIPTION
THURSDAY - 20 JUL (cont'd)		6. Perform final cleaning of receiver section 7. Remove neutral density filters 8. Install HV power supply fuse plug 9. Mount rocket skins 10. Charge batteries overnight
FRIDAY - 21 JUL	0900	1. Check batteries 2. Perform horizontal tests a. External Power - spark gap pressure check b. Internal Power - T/M check (30 sec) 3. Perform external mechanical check 4. Make laser bubble check 5. Perform final receiver optics dust check 6. Install door with squibs 7. Perform final pressure test 8. Clean P/L exterior and seal in plastic
SATURDAY - 22 JUL		1. Take P/L to rail 2. Perform GSE-P/L check 3. Clean up clean room
SUNDAY - 23 JUL		Reserved for schedule slippage
MONDAY - 24 JUL	a.m.	1. Perform vertical tests a. Laser bubble check b. External Power - spark gap pressure check c. Internal Power - T/M check (30 seconds) 2. Top off batteries
	2205-2220	3. Launch window
TUESDAY - 25 JUL	0500	1. Recovery P/L from range 2. Pack crates for reshipment
WEDNESDAY - 26 JUL		Crew Redeployment

APPENDIX J

APPENDIX (J)

SOUNDING ROCKET PREFLIGHT CONFERENCE **NOMTF 8040**

Held on July 19, 1978 **Flight No.** A03.604

Scheduled for launch 7/24/78 (time & date) **Window** 2205-2220 (time to time of day)

For scheduling information, phone 678-5502

Evacuation? ____ Yes __X__ No **Area(s)** ____

Horizontal scheduled for 1000 (time) **to** 1100 (time) **on** 21 (day) **of** July (month)

Vertical scheduled for 0900 (time) **to** 1000 (time) **on** 24 (day) **of** July (month)

4 **hour check scheduled for** 1800 (time) **to** 1900 (time) **on** 24 (day) **of** July (month)

Desire recovery same day of launch? ____ Yes __X__ No a.m. 25 July 78

Recovery of second stage? __X__ Yes ____ No

Recovery to be Class (1) 2 3 4 or 5. **Following personnel will accompany range recovery group and will need aural sound protectors, cradle, & tools:**

Need flight orders

If Flight Orders will be required (or changes to list needed), contact 678-5502, Room 76, Bldg. N-103 (Navy Headquarters).

Transponder or beacon used? __X__ Yes ____ No

Beacon on all the way? __X__ Yes ____ No

Optical? __X__ Yes ____ No

Telemetry? ____ Range ____ Project __X__ Both

Frequency? ____

Photographic requirements (NASA Standard)? ____ Yes ____ No

Build-up	6-20 views	1 set of color slides
Recovery	6-20 views	1 set of color slides
Motion of launch	2 cameras (1 remote at 1500 fps and 1 track at 400 fps)	
	EXPOSED FILM ONLY UNLESS A MALFUNCTION OCCURS	

Continued on reverse side

Other? _____ Yes _____ No

Horizontal	6 views	_____ slides	10 prints/negatives	color
Vertical	4 views	_____ slides	10 prints/negatives	"
Sequence launch	2 views	_____ slides	10 prints/negatives	"
Recovery	10 views	_____ slides	10 prints/negatives	"
Motion of launch	x original	_____ prints	x exposed film ONLY	

Standard meteorological support required? x Yes _____ No

Ionospheric data required? _____ Yes x No (Phone 678-3234/3909)

Using Tower "A" "B" L-455 L-462 L-479 L-536

Services required? No Nitrogen at Tower or Build-up
No Helium at Tower or Build-up
No Air at Tower or Build-up
No LN-2 at Tower or Buildup
No Other

How is material to be shipped back? Log Air Truck Van COD Mail Other

Project personnel to contact for: Telemetry Warren Donnell

Recovery Joe Geary Photography Joe Geary

TV coverage? _____ Yes x No _____ Ground _____ Rocket

Radioactive sources? ____ Yes x No. Sources being flown? ___ Yes ___ No

Altitude: 156 km

Booster 18 km

Weight measurement Friday-21 July

Tower installation Saturday or Sunday Day of servicing? Monday-July 24 after vert.

Hold criteria Nothing special

Back-up dates Tuesday-July 25, _____, _____

MFS close shut-off valves at 60 sec

Temperature in tower of rocket motor, payload 80 F Preferred 90 F max degrees

Local address & phone # of experimenter/project personnel _____

Thigpin (?) 678-5673
Briggs 523-4821

APPENDIX K

APPENDIX (K)

LASER ROCKET LAUNCH COUNTDOWN

COUNT TIME	~MDT	ACTION
T-3h	1900	All systems on external power (TM test)
T-2h, 56m, 30s	1902:30	Verify P/L status
T-2h, 55m, 30s	1904:30	Paper recorders on at 4 ips
		a. Paper recorders on at 8 ips b. Beacon, TM and Hskp on internal power c. Arm pyros
T-2h, 54m, 45s	1905:15	a. Experiment on internal b. Uncage gyro
T-2h, 54m, 30s	1905:30	All systems verify "go" status
		a. TM b. Hskp c. Experiment
T-2h, 54m, 20s	1905:40	a. Cage and uncage gyro b. All P/L systems to external
T-2h, 54m, 10s	1905:50	All P/L systems off
T-2h, 54m	1906	Radars off (end of TM test)
T-2h	2000	a. Missile flight safety check b. Photos c. Safety checks d. Beacon on external power
T-1, 57m	2003	Radar transponder checks
T-1, 30m	2030	a. Secure all rocket access doors b. Clean up tower A c. Open tower doors
T-1h, 20m	2040	Commence removing velostat from P/L
T-1h, 5m	2055	Velostat removal completed
T-60m	2100	All systems on external power (TM check)
T-56m, 30s	2103:30	Verify P/L status
T-55m, 30s	2104:30	Paper recorders on at 4 ips
T-55m	2105	a. Paper recorders to 8 ips b. Beacon, TM and hskp on internal power c. Arm pyros
T-54m, 45s	2105:15	a. Experiment on internal b. Uncage gyro

LASER ROCKET LAUNCH COUNTDOWN (CON'T)

COUNT TIME	~MDT	ACTION
T-54m, 30s	2105:30	All systems verify "go" status
		a. TM and beacon b. Hskp c. Experiment
T-54m, 20s	2105:40	a. Cage and uncage gyro b. All P/L systems to external
T-54m, 10s	2105:50	P/L systems off
T-54m	2106	Radars off - end of test
T-10m	2150	5m hold to meet 2205 T-0
T-10m	2155	Pick up count at T-10
T-6m	2159	All systems on external power
T-2m, 30s	2202:30	Verify P/L status
T-1m, 30s	2203:30	Recorders on. Paper at 4 ips
T-1m	2204	a. Paper recorders to 8 ips b. Beacon, TM and hskp to internal c. Arm pyros
T-45s	2204:15	a. Experiment on internal b. Uncage gyro
T-30s	2204:30	All systems verify "go" status
		a. TM and beacon b. Hskp c. Experiment
T-20s	2204:40	Cage and uncage gyro
T-15s	2204:45	Announce "go" or "no go" for P/L
T-0	2205	Lift off

APPENDIX L

ASSURANCE TECHNOLOGY CORPORATION

One River Road Carlisle MA 01741 Phone (617) 259-0120

DATE	FAILURE ANALYSIS REPORT	REPORT NO.
8/29/78		1019-01

CLIENT	CLIENT'S P.O.	DATE REC'D
VISIDYNE	EC 98080S	8/24/78

PART NAME	PART NUMBER	LOT # (LDC)
ZENER DIODE	1N751A	N/A

REPORTED FAILURE SYMPTOMS AND SPECIAL DIRECTIONS: SHORTED DIODE

Analyse diode to determine most probable cause of failure.

FAILURE ANALYSIS SUMMARY:

Device failed due to internal heating produced by excessive current for an extended period (minute or more). Available current was insufficient to melt the device but severe junction degradation was evident.

INDEX TO ANALYSIS DETAILS:

REPORTED BY: David Jones/k

1.0 EXTERNAL VISUAL EXAMINATION

The diode was inspected using a stereomicroscope at various magnifications with no visible evidence of damage being observed. Figure 1 shows the diode as received.

FIGURE 1: DIODE AS RECEIVED (4X)

The opaquing paint was removed from the glass body of the diode to reveal the inner construction. Figure 2 shows the diode with paint removed. An "S" strap maintains a compression contact with a silver plated button on the chip surface. The chip is soldered to a post and sealing of the glass brings the structure into compression.

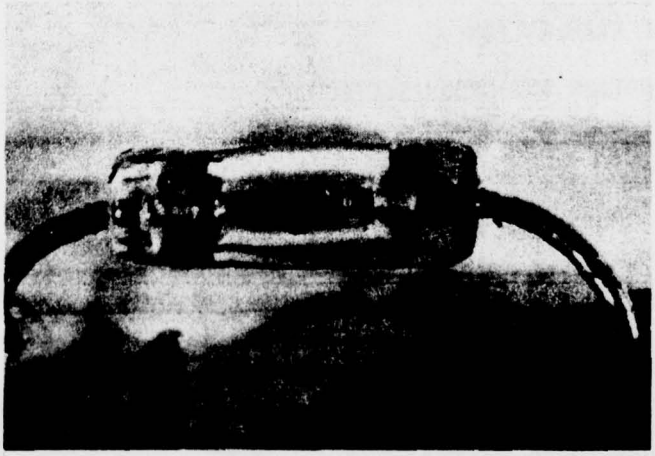

FIGURE 2: DIODE WITH PAINT REMOVED (10X)

No damage was evident at this junction.

2.0 ELECTRICAL TESTING

Using a Tektronix 576 Curve Tracer, the diode was tested to verify failure. This testing revealed a resistance short in both directions. Figure 3 shows the forward characteristics at 5 MA, 200 M V.

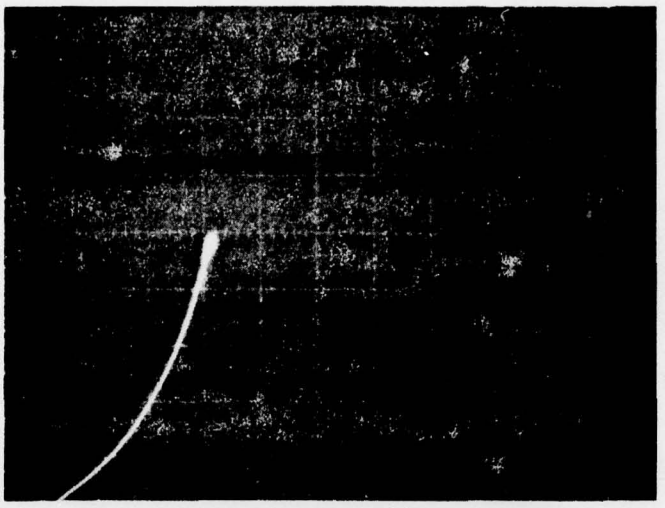

FIGURE 3: FORWARD OF DIODE

Figure 4 presents the reverse characteristics of the diode at 5 MA, 200 MV.

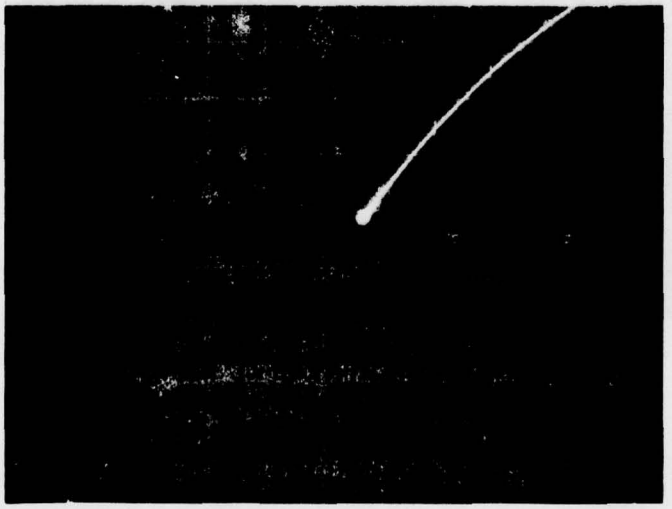

FIGURE 4: REVERSE OF THE DIODE

3.0 INTERNAL EXAMINATION AND CROSS-SECTION

The glass was scribed and broken to reveal the inner structure of the diode. Figure 5 presents the "S" strap end of the diode.

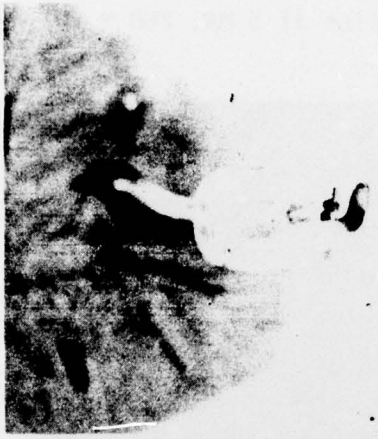

FIGURE 5: "S" STRAP OF THE DIODE (4X)

Figure 6 is a top view of the diode chip showing the silver button contact.

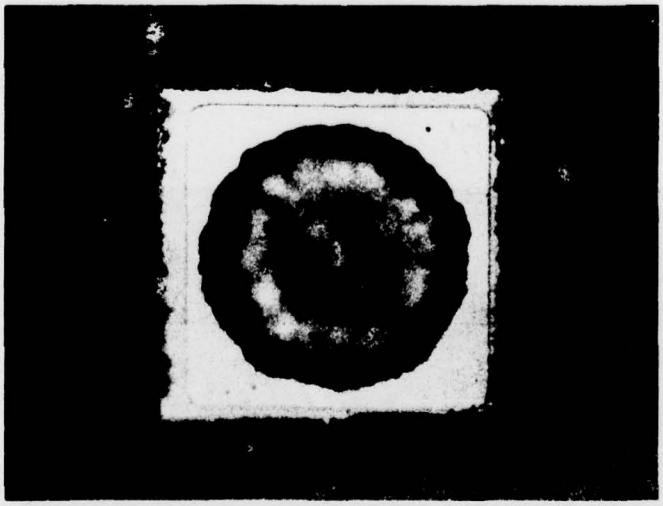

FIGURE 6: TOP VIEW OF THE DIODE WITH SILVER BUTTON CONTACT

The diode chip was probed at this point and short circuit was still present. The chip half of the diode was potted and cross-sectioned. Figure 7 is a cross-section showing the construction.

FIGURE 7: CROSS-SECTION OF DIODE (CENTRAL VIEW)

The oval shape at the top is the silver button contact, the parallelogram shape is the silicon chip which is soldered to the post. At higher magnifications the P/N junction is visible (arrows) after staining as in Figure 8.

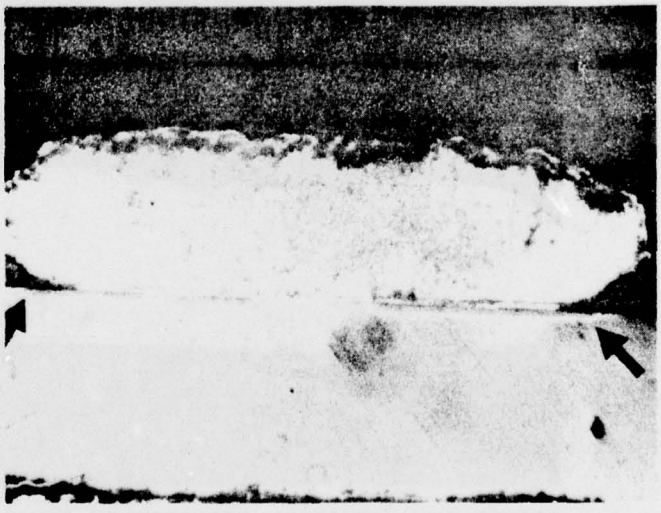

FIGURE 8: STAINED DIODE JUNCTION (300X)

Cross-sectioning was continued until damage at the periphery of the junction was located (Figure 9).

FIGURE 9: DAMAGE AT JUNCTION EDGE (800X)

The damage indicates a possible transient voltage overstress but would not explain the low resistance short that was previously measured. Cross-sectioning was continued until evidence of general junction degradation was seen as in Figure 10. At higher magnification (Figure 11) a moving diffusion is evident.

FIGURE 10: JUNCTION DEGRADATION REVEALED BY STAIN (300X)

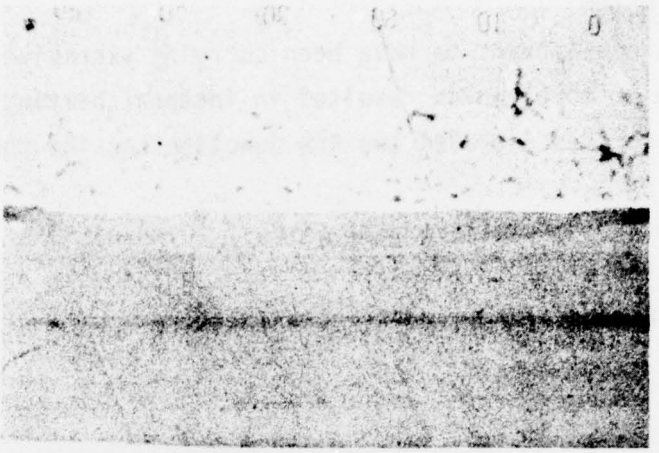

FIGURE 11: JUNCTION DEGRADATION BY DIFFUSION (600X)

When the center of the chip was reached a diffusion pattern was seen (Figure 12) which indicated that the diode saw long term overheating probably due to high current.

FIGURE 12: THERMALLY DEGRADED DIODE (400X)

4.0 CONCLUSION

The diode appears to have been carrying excessive current for a long term (minute or more) which resulted in internal heating to a degree the diffusion proccesses degraded the P/N junction causing the diode to appear as a resistive short.

Since the schematic of the circuit in which this diode is used was not available for this analysis, it is not possible to speculate on the cause of the apparent over-stress conditions.

APPENDIX M
SOLAR SCATTERING LIMB GEOMETRY

APPENDIX M
SOLAR SCATTERING LIMB GEOMETRY

We stated in Section 7.3 that the most likely source of the intense background signal is the scattered sunlight along the earth's limb. We also stated that because of the complexity of the atmospheric absorption, geography, and weather conditions, any comprehensive qualitative study is beyond the scope of the contract. Nevertheless, in this appendix we will make a simplistic estimate of the limb scattering signal. To do this we will neglect all signals which are generated by solar scattering when the total path, from the sun to the scattering point to the instrument, has an optical thickness greater than unity. The geometry is illustrated in Figure 1.

At 4580Å, the tangent optical air mass at sea level is approximately 38 and the vertical optical thickness is about .40 (Handbook of Geophysics and Space Environments, S.L. Valley, ed., AFCRL, 1965). Thus, the tangential optical thickness is about 15. We assume the optical thickness is proportional to the vertical number density, n, and therefore the altitude, h, at which the optical thickness along the total path is the altitude at which the density is

$$n_h = \frac{1}{4x15}\, n_{\text{sea level}} = \frac{1}{60}\ (2.7x10^{19}) = 4.5x10^{17}\ \text{cm}^{-3}$$

where the factor of 4 is from the total optical path as shown in Figure 1. From the 1976 U.S. Standard Atmosphere, we find that h is about 29 km. With minimum tangent heights of 29 km, we have calculated geometrically that the receiver line of sight and the direct solar rays will intersect at an altitude of about 54 km.

The signal at the receiver due to scattered solar radiation is approximately

$$S \simeq \frac{N_s\, \sigma\, n\, A\, \Omega\, L}{4\pi}\ \text{photons/sec}$$

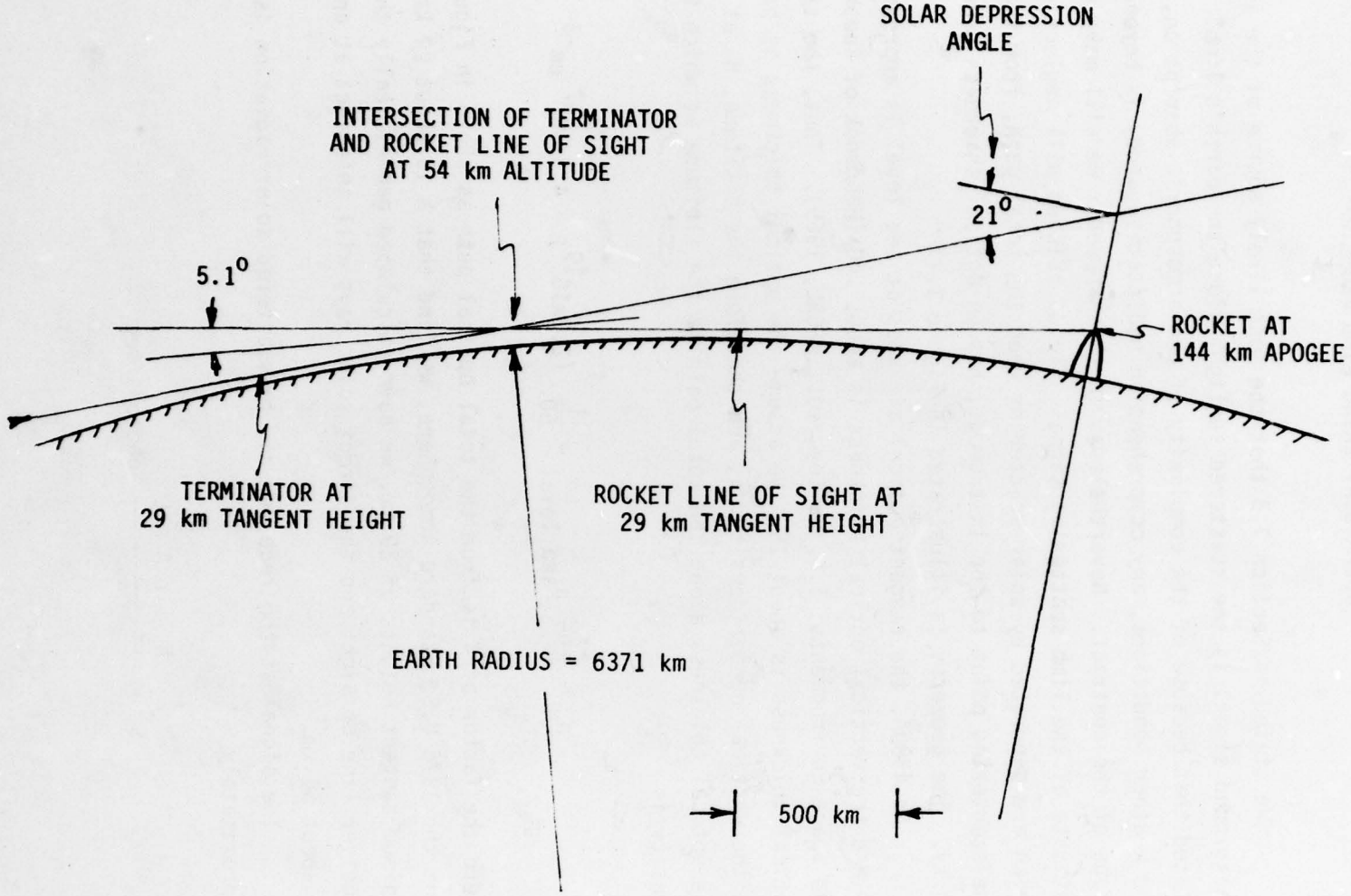

FIGURE 1 SOLAR LIMB SCATTERING GEOMETRY

where N_s is the solar flux at 4580Å for a 100Å bandpass (5.1×10^{15} photons/cm^2-sec)

σ is the Rayleigh scattering cross-section at 4580Å (9.6×10^{-27} cm^2)

n is the number density at the intersect altitude of 54 km (1.3×10^{16} molecules/cm^3)

A is the receiver optics collecting area (700 cm^2)

Ω is the steradiancy of the far field. We assume a scale height (7.5 km) in the vertical direction, or about 0.3^o, and the near field value in the horizontal direction, or 3^o. Thus $\Omega \simeq 3 \times 10^{-4}$ sr.

L is the path length through one scale height at the intersection. The instrument's line of sight makes an angle of 5.1^o with the horizontal. Thus L = (scale height)(csc 5.1^o) = (7.5×10^5) $(1.1 \times 10^1) = 8.4 \times 10^6$ cm.

Then,

$$S \simeq 8.9 \times 10^{10} \text{ photons/sec}$$

Since the integration time is 6.8×10^{-6} sec and the calibration factor is 2.5×10^6 photons/volt, the voltage signal for the scattered solar radiation at the earth's limb would be 2.4×10^{-1} for the medium gain channel. This is about an order of magnitude less than the background signals measured when the rocket payload was at apogee. For this simplified scattering model, one would not expect agreement to better than an order of magnitude. For instance, in this calculation we have neglected both the effects of attenuation and multiple scattering. Aerosol scattering at 50 kilometers has been assumed to be small compared to Rayleigh scattering. This estimated solar scattering is a factor of 40 brighter than Venus and a factor of 2×10^3 brighter than the night sky.

It should be mentioned that for the solar scattering to be in the field of view of the receiver, the attitude of the rocket would have to be abnormal from the experimental plan, which was for the receiver to be viewing well above the local horizontal at all times. As previously noted, confirmation of the rocket attitude will be made when the telemetry aspect data is reduced.